RAGE (RECEPTOR FOR ADVANCED GLYCATION END PRODUCTS) IN MELANOMA PROGRESSION

A Dissertation
Submitted to the Graduate Faculty
of the
North Dakota State University
of Agriculture and Applied Science

By

Varsha Meghnani

In Partial Fulfillment
for the Degree of
DOCTOR OF PHILOSOPHY

Major Department:
Pharmaceutical Sciences

May 2014

Fargo, North Dakota

North Dakota State University
Graduate School

Title

RAGE (RECEPTOR FOR ADVANCED GLYCATION END

PRODUCTS) IN MELANOMA PROGRESSION

By

VARSHA MEGHNANI

The Supervisory Committee certifies that this ***disquisition*** complies with North Dakota State University's regulations and meets the accepted standards for the degree of

DOCTOR OF PHILOSOPHY

SUPERVISORY COMMITTEE:

ESTELLE LECLERC
Chair

BIN GUO

STEPHEN O'ROURKE

JANE SCHUH

Approved:

5/22/2014
Date

JAGDISH SINGH
Department Chair

ABSTRACT

The Receptor for Advanced Glycation End Products (RAGE) and its ligands are expressed in multiple cancer types and are implicated in cancer progression. Our lab has previously reported higher transcript levels of RAGE and S100B in advanced staged melanoma patients. The contribution of RAGE in the pathophysiology of melanoma has not been well studied. Based on previous reports, we hypothesized that RAGE, when over-expressed in melanoma cells, promotes melanoma progression.

To study the pathogenic role of RAGE in melanoma, a primary melanoma cell line, WM115, was selected and stably transfected with full length RAGE (FL_RAGE) to generate a model cell line over-expressing RAGE (WM115_RAGE). WM266, a sister cell line of WM115, originated from a metastatic tumor of the same patient was used as a metastatic control cell line in the study. After assessing the expression levels of RAGE in the transfected cells, the influence of RAGE on their cellular properties was examined. An enhanced motility but suppressed proliferation of WM115 cells was found after RAGE over-expression, these properties could be reversed upon suppression of RAGE in these cells.

We next explored the mechanisms of RAGE induced changes in cell proliferation and migration in WM115_RAGE cells and found a significant upregulation in S100B protein in the WM115_RAGE melanoma cells compared to the MOCK cells. However, S100B suppression produced no effect on WM115_RAGE cells motility. Furthermore, expression of tumor suppressor p53 protein, which is one of the target proteins of S100B, was found to be significantly reduced in WM115 cells after RAGE over-expression.

We also investigated the effect of RAGE over-expression on melanoma tumor growth and deciphered the downstream signaling involved. We found a significantly larger tumor

growth rate of the WM115_RAGE cells compared to the control cells. S100B, S100A4, S100A6 and S100A10 proteins that are relevant in melanoma pathophysiology, were found to be upregulated in WM115_RAGE tumors compared to MOCK tumors. Moreover, enhanced AKT and ERK signal activation was observed in WM115_RAGE tumors as compared to MOCK tumors. Finally, anti-RAGE antibody treatment significantly suppressed tumor growth, which could be further enhanced by combining the antibody with the chemotherapeutic drug dacarbazine.

ACKNOWLEDGEMENTS

I sincerely thank my advisor Dr. Estelle Leclerc for guiding me throughout my doctoral studies. She is an excellent teacher, advisor and a nice human being. She always kept patient when things did not work for me. She discussed every single problem with me and came out with possible solution. Her critical comments for my presentations and seminars were always helpful for me. She also provided me career related guidance especially in the last year of my PhD when I was struggling for jobs. I also want to pay my gratitude to Dr. Stefan Vetter. His valuable suggestions were always helpful to me. I sincerely admire his teaching skills. He makes even complicate things easy to understand and grasp. I got to learn a lot from his critical thoughts and arguments in our lab journal club meetings.

I am also grateful to all my committee members Dr. Bin Guo, Dr. Stephen O' Rourke and Dr. Jane Schuh for their valuable comments during my preliminary defense. I am thankful to them for providing me career related guidance.

I want to pay my sincere gratitude to Dr. Jagdish Singh for allowing me to work in his department and providing all the instruments and facilities required for my research work.

I would like to thank ND-EPSCoR (Doctoral Dissertation Assistantship) and the College of Pharmacy, Nursing and Allied Sciences for funding my research work.

I am grateful to the departmental administrative staff Janet and Jean for always being so generous and always ready to help. I am also very thankful to my current and former lab members Mohit Koladia, Tayebeh Marzijarani, Venkata Indurthi and Faidat Jyoti for their cooperation in my research work and lab management. Finally and most importantly I would like to thank my husband Rahul Nahire and my parents and in laws for always being supportive and encouraging me in my tough times.

TABLE OF CONTENTS

LIST OF TABLES

LIST OF FIGURES

LIST OF ABBREVIATIONS

AB……..AlamarBlue®

ADC……...Antibody drug conjugate

ADCC…… ……Antibody dependent cell mediated cytotoxicity

AGE……..Advanced glycation end products

AJCC…… ……..American joint committee on cancer

AKT…….Protein kinase B

BCA…….. …….Bicinchoninic acid assay

BRAF……Rapidly accelerated fibrosarcoma homolog B

BSA……...Bovine serum albumin

C3a…….Complement component 3a

CD31…….Cluster of differentiation 31

CD44…… Cluster of differentiation 44

CDC…….. ……..Complement dependent cytotoxicity

Cdc-42……..Cell division control protein 42 homolog

CDK-2…… Cyclin-dependent kinase 2

cDNA……...complementary DNA

CHO……..Chinese hamster ovary cells

CTL-4…….Cytotoxic T-lymphocyte antigen 4

DAB……..……3,3'-Diaminobenzidine

DITC……..Dacarbazine

DNA……. Deoxyribonucleic acid

ECL……Enhanced chemiluminescence

EDTA……. Ethylenediaminetetraacetic acid

ELISA……Enzyme linked immunosorbent assay

EMT……Epithelial to mesenchymal transition

ERK……..…….Extracellular signal-regulated kinases

esRAGE……...Endogenous secretory receptor for advanced glycation end products

FACS……..Fluorescence-activated cell sorting

FBS……..….Fetal bovine serum

FDA……Food and drug administration

FITC……... Fluorescein isothiocyanate

FL_RAGE……..Full length receptor for advanced glycation end products

GAPDH…….……..Glyceraldehyde 3-phosphate dehydrogenase

GDP…….…….Guanosine diphosphate

GFP…….Green fluorescence protein

GPNMB……...Glycoprotein natural muscle binding

GST……..…….Glutathione S-transferase

GTP……. Guanosine-5'-triphosphate

HEK 293……...Human embryonic kidney 293 cells

HER 2……....Human epidermal growth factor receptor 2

HGPRT……...Hypoxanthine-guanine phosphoribosyltransferase

HMGB-1…….High-mobility group protein B1

Hox……...Homeobox

HRP…….…….Horseradish peroxidase

HUVEC……...Human umbilical vein endothelial cells

IACUC……..……..Institutional animal care and use committees

ICAM…….……...Intercellular adhesion molecule 1

IgG…….…….Immunoglobulin

IL-1…….……...Interleukin 1

IL-2……..……..Interleukin 2

IL-6…….....Interleukin 6

IL-8…….....Interleukin 8

IL-12…….……...Interleukin 12

IPTG……Isopropyl β-D-1-thiogalactopyranoside

JNK…….....c-Jun N-terminal kinases

LDH……..Lactate dehydrogenase

LLC PK-1…….LLC pig kidney-1 cells

Mac-1……. ……...Macrophage-1 antigen

MAPK……...Mitogen activated protein kinase

MCP-1…… Monocyte chemoattractant protein-1

MEKK…….……MAP kinase kinase kinase

MIA……..…...Melanoma inhibitory activity

MMP…….....Matrix metalloproteinases

MPTP……1-methyl-4-phenyl-1,2,3,6-tetrahydropyridine

Mts-1…….Metastasin

N2a……..Neuro-2a

NaN3……Sodium azide

NF-□B……Nuclear factor kappa-light-chain-enhancer of activated B

NHS……..n-Hydroxysuccinamide

NPP……p-Nitrophenyl phosphate

NRAS……..…….Neuroblastoma RAS

OCT…….…….Optimal cutting temperature

OPTIMEM……...OPTI Minimal Essential Medium

PAI-1……...…….Plasminogen activator inhibitor-1

PAK……...…….p21 activated kinase 1

PARIS……..……...Protein and RNA isolation system

PBS……...Phosphate buffer saline

PDB……...……p21 binding domain

PDGF-α.…….Platelet derived growth factor alpha

PDGF-β……...Platelet derived growth factor beta

PGK……Phosphoglycerate kinase

PI.……Propidium iodide

PML-RARα.……Promyelocytic leukemia protein retinoic acid receptor alpha

PMSF……...phenylmethanesulfonylfluoride

Rac-1…… Ras-related C3 botulinum toxin substrate 1

RAGE……...Receptor for advanced glycation end products

RNA……..…….Ribonucleic acid

ROS……Reactive oxygen species

RT_PCR……..Real time polymerase chain reaction

SAPK……...…….Stress-activated protein kinase

SCID……...…….Severe combined immunodeficiency

SDS PAGE……Sodium dodecyl sulfate Polyacrylamide gel electrophoresis

SPR…….Surface plasmon resonance

sRAGE……..Soluble receptor for advanced glycation end products

TBS…….Tris buffered saline

TBS-T……...……Tris buffered saline tween

TNF α……Tumor necrosis factor alpha

TNM……..Tumor node metastasis

tPA……..Tissue plasminogen activator

U87-MG……Human glioblastoma-astrocytoma, epithelial-like cell

VCAM-1……. ……..Vascular cell adhesion protein-1

VEGF-α……Vascular endothelial growth factor alpha

GENERAL INTRODUCTION

Melanoma

Epidemiology

Melanoma is the most lethal form of skin cancer [1]. It usually develops via transformation and uncontrolled proliferation of melanocytes [2, 3]. Melanocytes are the cells that reside at the basal layer of epidermis and produce the melanin pigment [4]. Melanocytic transformation is a consecutive series of certain genetic and epigenetic aberrations, which are not well understood [3]. In year 2009, the American Joint Committee on Cancer Staging System (AJCC) has published a revised staging system for melanoma progression [5]. Melanoma is classified on the basis of Breslow tumor thickness, the presence of ulceration, the number of lymph node metastasis and the presence of distant site metastasis [6]. Melanoma is associated with the highest number of skin cancer deaths [7]. Since 2010, a 10% increase in the number of melanoma associated deaths has been reported by the National Cancer Institute in the United States [8]. Primary melanoma is curable and has about 98% five year survival rate. As tumor spreads and enters into the lymph nodes the survival rates drops to 65%. Once melanoma metastasizes to other organs, the five year survival rate drops further to less than 20%, which poses major challenges in the therapeutic management of the disease [5, 8, 9].

Pathophysiology

The progression of melanoma is a complex series of sequential molecular and histopathological events which are not very well understood. Melanoma starts with a normal melanocytic nevus, which is a focal growth of normal cells. The melanocytic nevus becomes a dysplastic nevus and further progresses into a primary melanoma tumor. The primary melanoma tumor can easily metastasize to another part of the body [10]. In normal growth conditions the

melanocytes are in homeostasis with surrounding keratinocytes via E-cadherin [11]. Cadherins are Ca^{+2} dependent cell surface proteins involved in cell-cell adherence. E- and N- cadherins are two major subtypes of cadherins family [12]. Upon transformation the expression of E-cadherin is lost and the expression of N-cadherin enhances subsequently. Switching of E- to N- cadherin leads to uncoupling of melanocytes from keratinocytes and subsequent association with fibroblasts and vascular endothelial cells [12-14]. Dissociation of melanocytes and keratinocytes leads to uncontrolled migration and invasion of melanoma cells. E to N-Cadherin switching leads to cytoskeleton remodeling and epithelial to mesenchymal transition (EMT) of the cells [15, 16]. The transition of cancer cells from an epithelial to mesenchymal like morphology is an important event in melanoma metastasis and angiogenesis [17-19].

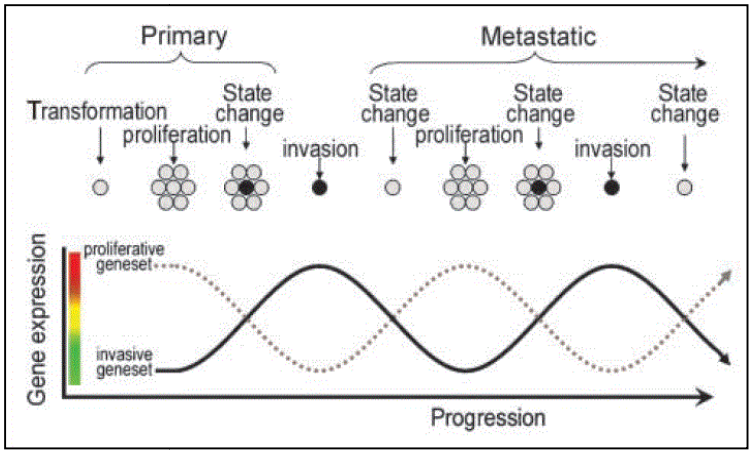

Figure 1: Two way switching model of melanoma progression. Primary melanoma cells switch from a proliferative state to a metastatic state. Once metastasized to a distant site, melanoma cells regain their proliferative state and again proliferate to form a new tumor at that site. The process of back and forth transition of the cells help propagation of melanoma. Taken from [20].

Recent studies have proposed a two-ways switching model between proliferative and invasive stages of melanoma (Figure 1). According to this model, a proliferative cell, upon an unknown stimulation, switches from a proliferative state to an invasive state. After invading to a distant location, the cell regains its proliferative trait and this cycle goes on. Back and forth

switching of cells between proliferative and invasive stages leads to heterogeneities in tumor cells [20, 21]. Advanced molecular profiling studies have revealed the expression of multiple genes specific for different cell phenotypes such as endothelial, epithelial, fibroblastic, hematopoietic, kidney, neuronal and muscle cells in different melanoma cells [22]. These findings suggest the presence of stem cell like pluripotent traits in melanoma cells [22, 23]. Recent findings have also shown the plasticity and vascular mimicry potentials of melanoma cells. Aggressive melanoma cells have been shown to acquire endothelial like genetic patterns and the abilities to undergo vasculogenesis [24]. Other reports have also demonstrated stem cell like characteristics of melanoma cells. Melanoma is considered to be a collection of heterogeneous cell population, which makes its diagnosis and treatment very challenging [21]. Failure of efficient and foolproof detection of melanoma at the early stage causes unimpeded progression of the disease and in turn leads to metastatic melanoma.

Biomarkers

Prognostic biomarkers are required for the timely detection of disease and to reduce the risk of disease progression. Biomarkers are measurable disease specific biological patterns (biochemical, genetic, or molecular) that are indicators of disease progression and patient outcomes [6, 25]. The National Institute of Health (NIH) has precisely defined biomarker as “a characteristic that is objectively measured and evaluated as an indicator of normal biological processes, pathogenic processes, or pharmacologic responses to a therapeutic intervention” [26]. Tumor specific biomarkers can predict the risk of cancer progression and are used in cancer staging systems. They can also indicate the therapeutic response and disease recurrence [6, 27]. Two important features that a biomarker must hold are the detection sensitivity and the specificity [28]. An ideal biomarker should also be inexpensive, fast and robust against any

method driven variability [27]. Several biomarkers with different sensitivities and specificities have been clinically used for melanoma prognosis and include tumor thickness, presence of ulceration, lactate dehydrogenase (LDH), S100B and melanoma inhibitory activity (MIA) (Table 1) [6]. Each biomarker has its own share of strengths and weaknesses in terms of specificity and selectivity.

Table 1: Clinically relevant melanoma biomarkers.

Biomarkers	**Type**	**Detection site**
LDH	enzyme	serum
S100B	protein	serum
MIA	protein	serum
BRAF mutation	mutation	DNA
Tumor thickness	tissue	tumor
Ulceration	tissue	tumor

S100B is a Ca^{+2} binding protein of the EF hand superfamily [29]. S100B protein was first found to be released from melanoma cells in 1980 [30]. Serum levels of S100B strongly correlate with melanoma progression and overall survival rates of patients [31]. A decrease in serum S100B concentration indicates a remission of the patient. Recent studies have shown that melanoma patients with a S100B protein concentration of less than 0.2 µg/l had a significantly longer overall survival rate ($P < 0.001$) than the patients with S100B levels of more than 0.2 µg/l, irrespective of the clinical stage of melanoma [6, 31]. Serum levels of S100B in stage III melanoma patients is a prognostic biomarker where its elevated levels are suggested to provide a prior indication of hematogenous dissemination of melanoma [32]. The determination of serum S100B levels in patients presenting tumors with > 1mm Breslow tumor thickness is

recommended every 3-6 months by the Swiss and German guidelines [33]. Since S100B is also a putative biomarker for brain injury and neurodegeneration, this hampers its specificity as melanoma biomarker [34]. S100B protein is one of the well characterized ligand of RAGE and binds to RAGE with nano molar affinity as shown by surface plasmon resonance [29]. Upon binding with cell surface RAGE, S100B triggers several RAGE dependent signaling pathways [29]. The strong correlation between the serum levels of S100B and melanoma progression indicates its potential role in melanoma pathophysiology.

LDH is another clinically used prognostic biomarker for metastatic melanoma [35]. It is an oxidative enzyme that plays a key role in the glycolytic pathway [36]. Glycolysis is the preferred mode of energy production in cancer cells due to impaired mitochondrial respiration and lack of oxygen. Enhanced anaerobic respiration of cancer cells is associated with the upregulation of LDH in these cells [37]. It was first detected in year 1954 in the serum of melanoma patients [38]. It is used as a prognostic biomarker for late stage melanoma patients and is a predictor of distant melanoma metastasis [31]. Although LDH has low detection sensitivities at early stage melanoma, it is widely used as prognostic marker at late stages of melanoma and has been included in the AJCC staging system of melanoma [5]. The melanoma inhibiting activity (MIA) protein was first detected in melanoma cells in 1990 [39, 40]. Enhanced serum concentration of MIA was found in 5.6%, 60%, 89.5% of melanoma patients in stage I/II, stage III and stage IV respectively [41].

Neither S100B nor LDH are appropriate biomarkers in stage I and II of melanoma growth [6]. However, S100B has been considered to be a more reliable marker than MIA and LDH in stage III and IV of melanoma due to its high detection sensitivity [42, 43].

New potential biomarkers have emerged in recent years and include mutation in the BRAF, KIT and NRAS genes [44-46]. Detection of BRAF V600E mutation has emerged as a new biomarker for melanoma after the approval of BRAF V600E inhibitor for the treatment of melanoma. Other melanoma biomarkers have been proposed on the basis of various epigenetic [47] and immunologic events associated with melanoma pathophysiology but their clinical relevance has yet to be defined.

Treatment of melanoma

Early detection and surgical removal of melanoma tumors from the site of origin is the most effective treatment option for melanoma patients [48]. Prior to surgery, the extent of tumor spread within the skin, and the presence of ulceration and lymph nodes metastasis are assessed by skin biopsy [49]. Melanoma lymphadenectomy is also a widely used clinical practice involved in surgical removal of melanoma affected lymph nodes. It may not only be curative but may also prevent further relapse at that site [48, 50]. Radiotherapy is another therapeutic module used for cancer treatment. However, primary cutaneous melanoma is shown to be radio resistant, and thus radiotherapy is not a prime treatment option for melanoma. Mostly, radiotherapy plays an important role in the palliation of many melanoma symptoms. However, the exact degree of the tumor response depends greatly on the tumor size, irradiation dose and time of irradiation [51]. For a long time, dacarbazine was considered to be the standard drug for the treatment of advanced melanoma. It was approved by the FDA in 1970 as a therapeutic agent against metastatic melanoma (Table 2) [52]. Dacarbazine is an alkylating agent. It acts by inserting alkyl group to the DNA which inhibits DNA replication and ultimately cause cell death. Dacarbazine alone has shown to produce only 19-25 % response rates in melanoma patients [48]. Therefore, numerous studies have been conducted to improve the over-all efficiency of dacarbazine by

combining it with other therapeutic agents. Dacarbazine has also been shown to upregulate vascular endothelial growth factor in melanoma cells, which may lead to increased angiogenesis and tumor growth [53]. Due to these limitations associated with dacarbazine, more effective therapies against melanoma need to be developed. Several immune modulating agents have been combined with dacarbazine in an attempt to improve its response rate and reduce its toxicity in melanoma [54]. Due to high levels of immunogenicity associated with melanoma several immune modulators have been developed in order to overcome immune system evasion by tumors. Cytotoxic T lymphocyte associate antigen 4 (CTL-4) has been targeted for the treatment of advanced melanoma [55, 56]. CTL-4 is a critical immunoregulatory molecule (expressed on activated T cells and a subset of regulatory T cells) capable of down-regulating T cell activation. T-cells are major components of the adaptive immunity. Blockade of CTLA-4 by anti-CTL-4 antibody leads to cytotoxic T cell stimulation and hence produce anticancer response [57, 58]. Three different monoclonal antibodies against CTL-4 have been developed: Tremelimumab (Pfizer) [59], Ipilimumab [60] and Urelumab (Bristol-Meyers Squibb) (Table 2) [61]. In March 2011, Ipilimumab was approved by the FDA for the treatment of metastatic melanoma patients that are not responding to chemotherapy [62]. Ipilimumab, a fully human IgG against CTL-4, has been shown to increase the circulating regulatory T cells and to improve the overall survival of melanoma patients (Table 2). Overall survival has been significantly improved in combination therapy of Ipilimumab and Dacarbazine in previously untreated metastatic melanoma patients [63]. Vemurafenib is another target specific drug for the treatment of metastatic melanoma approved in the same year [64]. Vemurafenib (PLX4032), a potent inhibitor of mutated BRAF V600E (substitution of Glutamic acid for Valine at 600 position) was developed by Genentech and received FDA approval in August 2011 (Table 2) [65, 66]. Approximately 40 to 60% of

cutaneous melanoma carry mutations in BRAF. A companion diagnostic test procedure was also approved by the FDA for assessing BRAF mutation in melanoma patients [67]. BRAF mutations lead to a constitutive activation of downstream signaling events through the MAPK pathway, a pathway that drives the growth of most cutaneous melanomas [68]. Moreover, the marked tumor regression and improved survival of late-stage BRAF-mutated melanoma patients in response to treatment with vemurafenib has demonstrated the essential role of oncogenic BRAF in melanoma maintenance. However, most patients relapse with drug-resistant disease, and therefore understanding and preventing the mechanism(s) of melanoma resistance are also critical to provide improved therapy.

Table 2: Examples of available therapies for melanoma treatment.

Melanoma therapy	**Approval year**	**Mechanism of action**
Dacarbazine	1970	Alkylating agent
Interleukin-α2b (high dose)	1995	T cell growth factor
IL-2 (Proleukin)	1998	T cell activator
Ipilimumab	2011	CTL-4 blocking antibody
Vemurafenib	2011	BRAF V600E inhibitor
Pegylated interferon	2011	T cell activator

Currently several antibody-drug conjugates (ADCs) are being developed for effective treatment of melanoma [69-71]. Antibody–drug conjugates are an improved way of targeting cytotoxic agents to the tumor by exploiting antibody's specificity and selectivity towards tumor cells [72]. The first approved antibody-drug conjugate (Brand name: Kadcyla, by Roche) consists of the monoclonal antibody trastuzumab (Herceptin) linked to the cytotoxic agent mertansine. It was approved by FDA in year 2013, for the treatment of Her-2 positive breast

cancer patients [73]. Auristatin (antineoplastic agent) conjugated with an anti-GPNMB antibody is another example of ADC which has been developed for the treatment of melanoma [71]. Despite the emergence of new therapies against melanoma, there has been no significant improvement in the overall survival of melanoma patients. Therefore a better understanding of the pathophysiology and the identification of new therapeutics targets are needed for developing effective new therapies against melanoma.

Receptor for Advanced Glycation End Products (RAGE)

Structure

RAGE is a cell surface receptor of the immunoglobin superfamily [74]. It is encoded by the class III major histocompatibility complex on chromosome 6 [75].

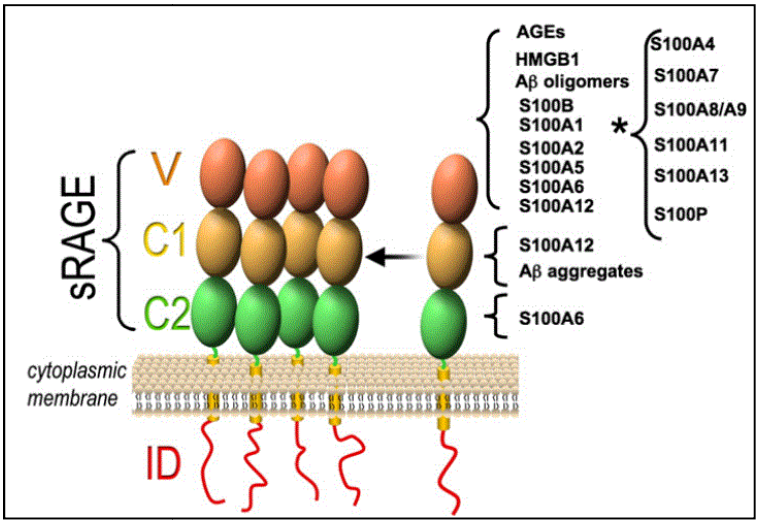

Figure 2: Schematic representation of RAGE and its various ligand binding domains. RAGE possesses three extracellular domains (V, C1 and C2), one transmembrane domain and one cytoplasmic domain. Different RAGE ligands (AGEs, HMGB-1, amyloid β oligomers or aggregates, S100 proteins) interact with different RAGE domains. Taken from [29].

RAGE consists of one extracellular domain, one small transmembrane domain and one cytosolic domain [76] (Figure 2). The extracellular domain consists of three immunoglobin like domains, a variable type “V” domain and two constant type “C1” and “C2” domains [29, 76]. The V-domain contains two N-terminal glycosylation sites [77]. The extracellular domain of

RAGE is responsible for ligand binding whereas the cytosolic domain helps in signal transduction within the cells [78]. The RAGE extracellular domain possesses two important features, which are crucial for ligand binding: a highly conserved hydrophobic patch and a large convex positive charged patch that assists RAGE in interacting with diverse ligands [79]. The interaction of RAGE cytosolic domain with formin homology domain of diaphanous-1 (dia-1) has been reported to be an important event in signal transduction [80] (Figure 3).

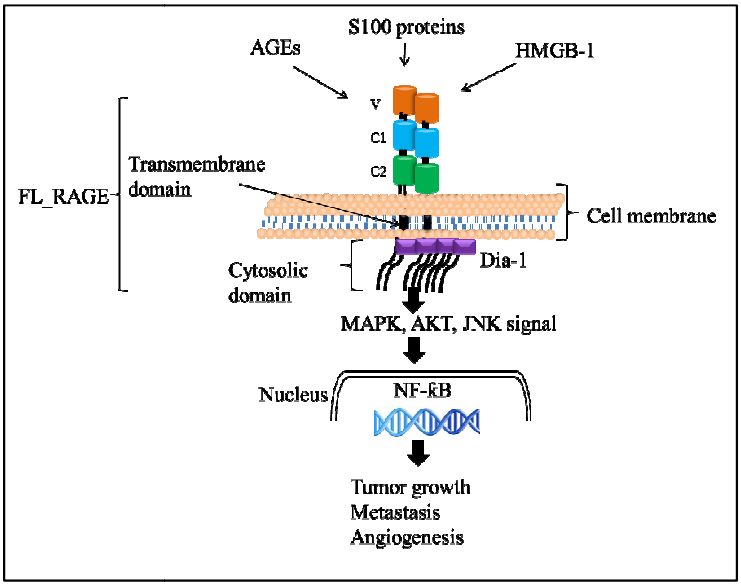

Figure 3: RAGE induced signal transduction pathways. Upon engagement with its ligands, RAGE stimulates the activation of a diverse array of signaling cascades, including mitogen activated protein kinases (MAPK), c-Jun N-terminal kinase (JNK), phosphoinositol 3-kinase (PI3K/AKT). RAGE also triggers activation of nuclear transcription factors, including nuclear factor NF-κB, and consequent target gene transcription.

RAGE exists in multiple isoforms: the full length RAGE (FL_RAGE), soluble RAGE (sRAGE), N-truncated form of RAGE (ΔN-RAGE) or the endogenous secretory RAGE (esRAGE/RAGE_v1) (Figure 4) [29]. Alternative splicing and proteolytic cleavage of the extracellular domain by ADAMs or γ- secretase are the two established mechanisms for the

generation of the different RAGE isoforms [81, 82]. Alternative splicing is a mechanism by which different forms of mature mRNAs (messengers RNAs) are generated from the same gene. It leads to functional complexity of the genome and hence plays an important role in development and disease [83]. RAGE_v1 (esRAGE) is the most common and well characterized splice variant of RAGE.

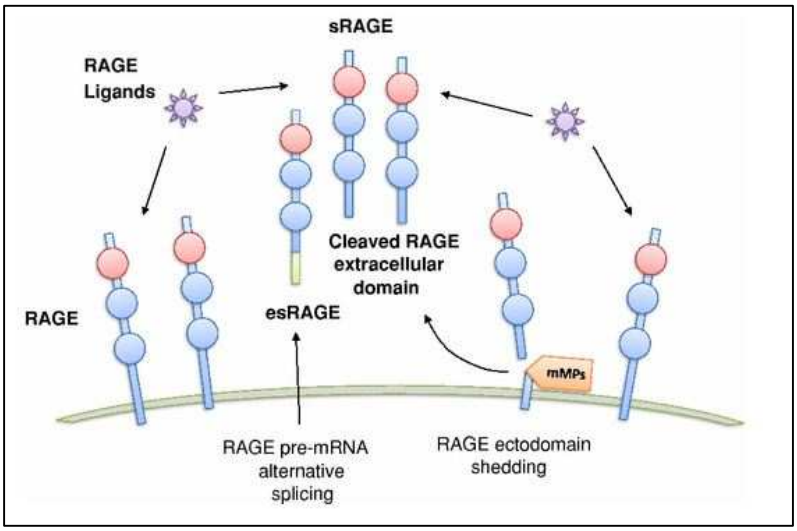

Figure 4: Generation and significance of soluble RAGE isoforms. The extracellular RAGE shedded form the cell-surface receptor by the action of membrane-associated metalloproteinases (mMPs), such as ADAM-10 and MMP-9 and esRAGE, arising from RAGE pre-mRNA alternative splicing. Spanning the ligand-binding domain, sRAGE probably acts as a decoy receptor for ligands. Taken from [84].

The proteolytic cleavage of the extracellular domain of RAGE by membrane associated metalloproteinases (ADAM10 and γ- secretase) is another mechanism for sRAGE formation [85]. The proteolytic cleavage of RAGE releases the corresponding intracellular domain of RAGE (RICD) into the cytosolic and nuclear space. This domain has been shown to promote cellular apoptosis [86]. RAGE isoforms lacking cytosolic domain (sRAGE and RAGE_v1) can only bind to the ligands and do not initiate any downstream signals. The ability of sRAGE to neutralize RAGE mediated adverse effects has made it an attractive therapeutic candidate against

RAGE induced pathologies [84]. RAGE_v1 variant could block RAGE/S100B mediated signaling in glioma and thus suppress glioma tumor growth [87]. Soluble isoforms of RAGE have been shown to be down regulated in certain cancer types such as lung [87], breast [88] prostate [87], melanoma [89] and brain tumors [87] as compared to their corresponding normal tissues. Also, the plasma concentration of sRAGE has been shown to correlate with the therapeutic response of certain cancer types [88]. The significance of serum sRAGE as a cancer biomarker for monitoring therapeutic response has been discussed in previous reports [84, 90]. However, its clinical utility as a cancer biomarker has not been established yet. Our lab has recently shown a significant down regulation in sRAGE isoforms in advanced stages of melanoma as compared to non-melanoma tissue suggesting the contribution of RAGE in melanoma pathophysiology [89]. RAGE is expressed differentially in different tissues depending upon the type, physiological state and development stage of the tissue [91]. This suggests a tight cell and tissue specific regulation of RAGE expression. RAGE is highly expressed in the brain during early development and promotes neurogenesis [92]. RAGE is expressed in neurons, microglia, and endothelial cells and is essential for neuronal development and neuron outgrowth [92, 93]. Neuronal RAGE has also been suggested to contribute to S100B mediated synaptic functions [94]. Previous studies have also reported that deletion of RAGE significantly reduced neointimal expansion upon arterial injury [95]. This suggests that RAGE is important for regulating smooth muscle cells function in stress conditions. In healthy adults, RAGE is downregulated in all tissues except the lungs, suggesting that RAGE is involved in pulmonary physiology [96]. RAGE and its ligands are expressed in significant abundance in healthy lungs but their precise role in pulmonary physiology is not known. RAGE null mice have been reported to be more susceptible to develop pulmonary fibrosis than control mice [97].

Furthermore, downregulation of RAGE is associated with human non small cell lung carcinoma progression [98]. These reports strongly support the significance of RAGE in lung physiology.

Ligands

RAGE interacts with several structurally and functionally diverse ligands such as Advanced Glycation End Products (AGE) [76, 99], S100 proteins [100], transthyretin [101] HMGB-1 [93], Amyloid β peptide [102], mac-1 [103], phophatidyl serine [104] and C3a [105]. Despite of structural variations, RAGE ligands share some common features, explaining their affinity towards RAGE [106]. First, most of the RAGE ligands tend to oligomerize and form multimers. Secondly, most of the RAGE ligands possess a net negative charge at the physiological pH [106, 107]. The presence of a positively charged patch on the extracellular domain of RAGE provides a binding force for some of the negatively charged ligands (AGE, phophatidyl serine) [79]. Binding of S100 proteins to RAGE is also mediated via hydrophobic interaction which is modulated by intracellular Ca^{+2} [79]. Consequences of RAGE-ligands interactions are different depending upon ligand type [108], ligand concentration [109], tissue type and physiological state of the tissue [109]. RAGE either alone or after ligand stimulation has been shown to play significant roles in many pathological conditions such as cancer [110], Alzheimer's disease [102], cardiovascular disorders [111], diabetes [112], pulmonary disorders [113] and several neurological disorders [114]. RAGE upon engagement with its ligands initiates several signaling pathways that involve mitogen activated protein kinase (MAPK) [78], Rho-GTPase (Rac-1 and Cdc42) [115], NF-□B [116] and SAPK/JNK [87].

NF-□B is a transcription factor that binds to DNA and regulates gene transcription. It plays a central role in immune response and inflammatory reactions [117]. The presence of a NF-□B binding site at the promoter region of RAGE gene stipulates NF-□B as a key signaling

molecule for RAGE [118]. AGE-RAGE mediated activation of NF-□B signaling has been implicated in diabetes and aging [119]. Also, in familial amyloidotic polyneuropathy, interaction of RAGE with transthyretin fibrils has been shown to activate NF-□B signaling and subsequent neurodegeneration [101].

ERK, JNK and p38 are the three major components of the MAP kinase (serine/threonine/tyrosine specific protein kinase) pathway [120]. RAGE mediated activation of MAPK pathway is involved in many pathologies including cancer. For example, S100A8/A9, a heterodimeric complex of S100A8 and S100A9, has been shown to induce the MAPK pathway via RAGE in human prostate cancer cells [121]. The AGE ligand has also been shown to induce the MAPK signaling that plays a role in diabetes and other inflammatory disorders [122]. In glioma, S100B activates JNK signaling through RAGE and enhances glioma tumor growth [87]. The Rho family of GTPases is a family of small signaling G proteins. Three members of the family have been studied in detail: Cdc42, Rac1, and RhoA [123]. AGE has been shown to induce Rho signaling in human vascular endothelial cells through RAGE, which led to cytoskeleton remodeling and vascular hyper-permeability [115], and was implicated in diabetic vasculopathy [124]. Ligand binding induces oligomerization of RAGE on the cell surface, which is critical for the initiation of RAGE mediated downstream signaling [79, 125]. RAGE can dimerize in the absence of ligands and ligand binding can further amplify the oligomerization process [125]. The precise mechanism by which RAGE oligomerizes on the cell surface and activates downstream signal is not clear yet. All the three domains of RAGE (V, C1 and C2) have been reported to be involved in RAGE oligomerization. A group of researcher reported that intermolecular disulfide bonds between C2 domains of RAGE contribute in the oligomerization process [126]. Other groups showed the involvement of V, C1 as well as transmembrane

domains in the RAGE oligomerization process [125] [107] [127]. These data suggest a complex mechanism of RAGE oligomerization and downstream signal activation that needs to be understood. Soluble RAGE can competitively inhibits cell surface dimerization of RAGE and hence inhibit the downstream signal activation [125]. RAGE dimerization/oligomerization and its significance in cellular activation is currently a hot topic for research. The precise mechanism of RAGE mediated signal activation is not known. Association of RAGE molecules on the cell surface might alter the orientation of corresponding cytosolic domains and might also affect their interaction with the intracellular binding partners [125]. Binding of RAGE ligands also leads to receptor internalization, but very little is known about intracellular trafficking of RAGE. Advanced glycation end products induce RAGE internalization in CHO and N2a cells, which has been shown to be an important event in signal activation [128]. In schwan cells, RAGE has been shown to internalize within endocytic compartment and to recycle back to the cell surface upon S100B stimulation [129].

RAGE-ligand mediated signaling can be suppressed by blocking RAGE-ligand interaction using either anti-RAGE antibodies or sRAGE [78]. RAGE blocking antibodies have been demonstrated to suppress many RAGE induced pathologies [130-132]. For example in a xenograft rat model of glioma, blocking RAGE with either anti-RAGE antibody or soluble RAGE led to significant suppression in tumor growth [78]. In the same cells over-expressing an alternative splice variant of RAGE (RAGEv1) (lacking the transmembrane and intracellular domain of RAGE) has been shown to significantly reduce tumor growth compared to control [87]. Anti-RAGE antibodies have also been shown to inhibit AGE-RAGE mediated melanoma cell migration and melanoma tumor growth [133]. However, therapeutic utility of anti-RAGE antibodies has never been tested clinically. Besides anti-RAGE antibodies, small RAGE

antagonistic peptides have also been designed to block RAGE-ligand interaction [134]. Moreover, other drugs have also been tested for their potential to inhibit RAGE-ligand interaction. For example, anti-allergic drug Cromolyn inhibits RAGE-S100P interaction and in turn suppresses pancreatic cancer growth and metastasis [135].

In depth knowledge of RAGE, its ligands, their binding affinities and their functional roles in cancer progression is crucial for developing new therapies targeting RAGE. In the next paragraph, RAGE ligands that are associated with cancer pathogenesis have been described in detail.

Advanced Glycation End Products (AGE)

AGEs were the first known ligands of RAGE. They are non-enzymatic adducts of proteins with reducing sugars. They can be generated within the body or outside the body. The process of AGE formation is known as Maillard reaction, which leads to the formation of a broad range of heterogeneous compounds [136]. Certain food processing events such as broiling, grilling and roasting lead to excessive formation of AGEs [137, 138]. Glycation of proteins leads to structural and functional alterations causing pathogenic consequences [139]. Initially, RAGE was identified as a scavenger receptor for AGEs but later it was established that RAGE was also a signal transducer for AGEs [100]. AGEs upon interaction with RAGE, triggers oxidative stress and inflammatory reactions [140, 141]. AGE-RAGE interaction has been shown to activate AKT [142], NF-□B [143], Ras and MAPK [144] signaling pathways and hence to contribute to various diseases such as cancer [145], diabetes [146], and other inflammatory disorders [141]. The contribution of AGE-RAGE mediated signaling in diabetes complication has been studied in detail. Accumulation of AGEs in diabetic blood leads to AGE-RAGE mediated activation of pro-inflammatory signals which are implicated in diabetic vasculopathy [147]. Tissue accumulation

of RAGE ligands can lead to enhanced RAGE expression to amplify and sustain overall signal [110]. AGEs can upregulate RAGE expression in human vascular endothelial cells via NF-□B dependent signaling [148]. High glucose consumption of cancer cells leads to accumulation of AGE products within tumor microenvironment, which might upregulate RAGE expression in the tumors [149]. AGE/RAGE axis has also been shown to enhance melanoma cell proliferation and migration, which suggests its active contribution in promoting melanoma growth [133].

Table 3: Roles of RAGE and its ligands in cancer progression and their potential inhibitors.

RAGE ligands	**Role in cancer**	**Inhibitors**
HMGB-1	Glioma [78] Prostate cancer [150]	Anti-RAGE antibody, Amphoterin binding peptide, soluble RAGE [78] Not known
S100P	Pancreatic cancer [135]	Cromolyn [135]
S100B	Melanoma [151] Glioma [87]	Small molecule inhibitors of S100B-p53 binding [151] Soluble RAGE [87]
AGE	Melanoma [133]	Anti-RAGE antibody [133]
S100A4	Prostate cancer [152] Colon cancer [153] Melanoma [154]	Not known Not known Not known
S100A6	Pancreatic cancer [155]	Not known

HMGB-1 (High mobility group box-1)

HMGB-1 protein also known as amphoterin, is a small basic nuclear protein implicated in chromatin remodeling [156]. HMGB-1 protein consists of two HMGB-1 box domains connected with a short linker followed by a negative C terminal tail. The two box domains of HMGB-1 are

important for DNA binding [157]. Not much has been studied regarding the acidic C-terminal tail of HMGB-1. HMGB-1 is a non-histone protein that interacts with chromatin and assists in nucleoprotein complex formation. It is a highly ubiquitous and conserved protein abundantly present in most mammalian cells suggesting its important physiological role [158, 159]. Knockdown of HMGB-1 gene in mice leads to lethal consequences and eventually death [160]. Inside the cell, HMGB-1 resides in the nuclear compartment where it interacts with its targets (DNA, RNA and nucleosomes) and subsequently regulates several cellular functions. HMGB-1 binds to the minor groove of DNA and increases the binding affinities of several transcriptional factors [161] such as Hox, Pou proteins, p53 [162] and TBP [157, 163]. Thereby, HMGB-1 regulates the transcriptional activities of certain genes. HMGB-1 has also been suggested to be an architectural protein within the cells which might trigger local deformation of DNA and facilitate recruitment of other DNA binding partners [164].

Despite its intracellular functions, HMGB-1 has also shown to be released from the cells. It can be released actively from live cancer cells or passively from dead cells [157]. Passive release of HMGB-1 protein has been demonstrated from necrotic cells but not from apoptotic cells due to its tight interaction with DNA [165]. HMGB-1 can also be released actively from the cells via vesicle mediated active secretion pathway upon activation by various stimuli [166]. Post-translational modification (methylation, acetylation) of HMGB-1 is important for its active secretion, target binding and pro-inflammatory activity [167-169]. In melanoma, HMGB-1 is released from cells upon induction with tumor-specific cytolytic T lymphocytes [170]. Upon release, HMGB-1 acts as a cytokine and triggers immune responses and inflammatory reactions in other cancer cells but its role in melanoma is not defined [157]. Being a pro-inflammatory mediator, HMGB-1 induces the secretion of several cytokines (TNF-α, IL-1, IL-6, IL-8 and IL-

12) and adhesion molecules (ICAM, VCAM). Adhesion molecules assist in macrophage and neutrophil recruitment at the site of inflammation and cytokines released from these cells further amplify the overall inflammatory signal [167]. HMGB-1 interacts with several cell surface molecules such as heparin [171], proteoglycans, sulfoglycolipids and phospholipids [172]. RAGE is one of the extracellular targets of HMGB-1. RAGE and HMGB-1 have been reported to co-localize in certain cancer cells. Once released, HMGB-1 interacts with RAGE and activates several pro-inflammatory signaling pathways [167]. Major downstream signaling cascades activated by HMGB-1 and RAGE are Erk-1/2 [167], JNK [78], p38 [78] and Nf-□B [157]. The contribution of HMGB-1 in cancer progression is quite complex. HMGB-1 contributes in tumor growth, angiogenesis, metastasis and invasion through multiple mechanisms. By modulating extracellular matrix environment, HMGB-1 promotes tumor metastasis and invasion. HMGB-1 has been shown to activate plasminogen activation system and matrix metalloproteases activities which in turn facilitate tumor cell invasion [167]. HMGB-1 also promotes angiogenesis by inducing vascular endothelial cells growth and activities [173]. Enhanced expression of HMGB-1 protein has been detected in melanoma [78, 170, 174, 175]. In melanoma, HMGB-1 induces Melanoma Inhibitory Activity (MIA) protein via NF-□B signaling [176]. MIA is a fibronectin and integrin binding protein which modulates cell-matrix interaction and enhances tumor cell migration and invasion [177]. Anti-HMGB-1 antibody treatment has been shown to suppress Lewis Lung tumor growth and metastasis [178]. Suppression of glioma tumor growth after blocking RAGE-HMGB-1 interaction with anti-RAGE antibody has also been reported [78]. Other strategies to inhibit HMGB-1 and RAGE mediated signaling such as antibody against HMGB-1, soluble RAGE (sRAGE) [78], ethyl pyruvate [179], quercetin [180] and platinum [181] have been developed and tested for cancer therapy.

S100 proteins

S100 proteins are Ca^{+2} binding proteins of the EF hand superfamily. These proteins are exclusively expressed in vertebrates. They are small (≈10 KDa) acidic proteins and some are soluble in 100% saturated ammonium sulfate, therefore they were named S100 [29, 182, 183]. A total of 24 S100 members, that include $S100A_{1-16}$, S100B, S100P, S100Z and S100G have been described [29]. Most of the S100 protein genes are clustered on human chromosome 1q21 [182] except for S100B, S100P, S100Z, S100G proteins. These later genes are found to be located at chromosomal loci 21q22 (S100B), 4p16 (S100P), 5q14 (S100Z) and Xp22 (S100G) [184, 185]. This unusual chromosomal pattern of different S100 proteins has some implications for their biological significance. Human chromosome 1q21 is highly susceptible to chromosomal rearrangements and genes on this chromosome are associated with cancer. Chromosome 21q22.3 dysfunction is associated with Down syndrome, Alzheimer's disease and other neurodegenerative disorders that indicates the functional roles of S100B in brain development [186]. S100 protein members are localized in different cellular compartments [109]. Some of the S100 proteins preferably localize in the nucleus (S100A2) whereas others are associated with either the cytoplasm (S100A4, S100A6, S100B) or the cell membrane (S100A10) [187, 188]. S100 proteins can also be released in the extracellular space [189, 190]. The mechanism behind S100 protein secretion is not clear yet. Some reports suggest passive release of S100 proteins from apoptotic or necrotic cells, whereas some propose an active secretion pathway for S100 proteins [191, 192].

S100 proteins are Ca^{+2} sensor proteins which consist of two Ca^{+2} binding domains of the EF-hand type (helix-loop-helix). The C-terminal domain contains a canonical EF hand domain which has a 100-times higher affinity for Ca^{+2} than the N terminal domain. The EF hand in the

C-terminal domain consists of 12 amino acids and is common to all EF hand proteins. The N-terminal domain is different and described as pseudo domain. It consists of 14 amino acids and is specific to each S100 protein [182,188, 193]. The two EF hands domains are interconnected by a the hinge region [182]. Upon Ca^{+2} binding, a conformational change is induced in the S100 protein structure that leads to the exposure of hydrophobic regions in the protein. The hydrophobic regions assist in interacting with their target proteins [109, 194]. In resting conditions the intracellular Ca^{+2} concentration is low and keeps the S100 proteins in their inactive (apo) conformation. Upon activation by either internal or external signal, intracellular Ca^{+2} concentration increases and is sensed by S100 proteins and hence triggers their interaction with the target proteins [109]. Several Ca^{+2} independent interactions of S100 proteins have also been described [195]. Besides Ca^{+2}, S100 proteins have also been reported to interact with Zn^{+2} and Cu^{+2} [196]. Due to structural homologies, S100 proteins share similar target proteins. Most of the S100 proteins tend to dimerize by hydrophobic interaction which is facilitated by Ca^{+2} binding [194]. S100G is an exception and remains as a monomer [29, 197]. Some of the S100 proteins such as S100A8 and S100AA9 can also form heterodimers (S100A8/9) [198]. Oligomerization of S100 proteins leads to improve target binding. For example, tetrameric S100B has been shown to have higher affinity towards RAGE than dimeric S100B [29, 109]. Similarly, hexameric S100A12 has been shown to induce tetramerization in RAGE that in turn increase overall affinity [199, 200]. S100 proteins have both intracellular and extracellular functions. Within the cell, S100 proteins interact with cytoskeleton elements, various metabolic enzymes, cell cycle regulating proteins and Ca^{+2}. They regulate cell homeostasis, cell growth, cell differentiation, cell motility, cell energy metabolism, cytoskeleton dynamics and Ca^{+2} homeostasis [109].

S100 proteins have also been shown to be actively secreted from astrocytes [189], neurons [201], microglia [201], glioblastoma [202], schwann cells [129] and melanoma [6]. Secreted S100 proteins can exert cytokine or chemokine like extracellular activities by interacting with the Receptor for Advanced Glycation End Products (RAGE), in either a paracrine or autocrine manner [203]. Dysregualtion of S100 mediated signaling contribute to many pathologies such as cancer [204], Down syndrome [186], Alzheimer's [205], neurodegeneration [206], cardiomyopathy [207] and other inflammatory disorders [208].

Apart from the S100 proteins that will be described here in detail, other S100 proteins like S100P [135, 209, 210], S100A8/9 [211], S100A12 [212], S100A16 [213] are also known to be involved in cancer pathogenesis via multiple mechanisms. S100P protein has been shown to promote pancreatic cancer progression, via RAGE mediated signaling [135]. S100A8/9 heterodimer protein is known to interact with RAGE and trigger inflammatory reactions in the tumors [211]. S100A12 is also expressed in certain cancer types and is used as a marker for inflammatory reactions [212]. S100A16 is expressed in cancer cells and its expression is regulated by S100A14, another member of S100 protein superfamily [214].

In the next section we will describe some of the S100 proteins that are known to be associated with melanoma pathogenesis. Following are the descriptions of S100B, S100A2, S100A4, S100A6, S100A10 and S100A11 proteins and their roles in melanoma progression.

S100B: S100B protein is the best studied member of the S100 protein superfamily. As mentioned previously, S100B gene is located on chromosome 21q22.3 [109]. S100B is mainly expressed in the neurological system and in certain cancer types. Expression of S100B protein by astrocytes, oligodendrocytes, neural progenitor cells, pituicytes, ependymocytes, chondrocytes, suggest a cell specific distribution of the protein [29, 109]. S100B expression increases in certain

cancer types including melanoma [6]. Inside the cells, S100B protein is localized in the cytoplasm either as a free form or associated with centrosomes, microtubules and/or type III intermediate filaments [183]. Like other S100 proteins, intracellular S100B protein interacts with Ca^{+2} and acts as a Ca^{+2} buffering agent. Upon Ca^{+2} binding, a conformational change is induced in S100B protein that leads to exposure of a hydrophobic cleft through which S100B interacts with its target proteins [109]. Several cell specific intracellular target proteins for S100B have been reported. In astrocytoma cell lines, S100B interacts with IQGAP1 protein, which is an effector of small GTPase Rac1 and Cdc42 signaling and thereby regulates astrocytes cell migration [215, 216]. S100B also interacts with the tumor suppressor, p53 protein in a Ca^{+2}-dependent manner [217]. Upon interaction, S100B inhibits the phosphorylation and transcriptional activities of p53 protein in melanoma cells [218]. S100B mediated p53 inhibition leads to increased melanoma cell survival [219]. Besides being a binding partner of p53, S100B also inhibits p53 expression in melanoma cells. Previous studies have reported a negative correlation between S100B and p53 protein expressions in melanoma cells [217]. Small molecule inhibitors of S100B-p53 interaction have been identified and evaluated for anti-proliferative activities in melanoma cells [151, 220]. The anti-protozoal drug pentamidine has been identified as an potent inhibitor that disrupts S100B-p53 interaction and suppresses melanoma cell proliferation [221]. Pentamidine is currently in clinical trials for treating relapsed melanoma. Several other inhibitors of S100B-p53 interaction have also been identified and screened for their anti-proliferative activities in melanoma cells. S100B protein is also released from a variety of cells through different mechanisms. It is actively released from astrocytes [189], adipocytes [222] and other cells [202, 223]. On the contrary S100B has been shown to passively leak from damaged melanoma tumor cells [224, 225], injured brain [226] [227] and

ischemic heart [228, 229]. Upon release, S100B interacts with its extracellular target proteins either in a paracrine, autocrine or endocrine manner and triggers downstream signaling cascades [109]. RAGE is the only well described extracellular target for S100B protein. In nanomolar concentration S100B stimulates neurite outgrowth and enhances survival of neurons during development through RAGE [230-232]. In contrast, in micromolar concentrations, S100B induces inflammatory reactions and neuronal death in a RAGE dependent manner [92, 233]. The dual effect of S100B on neurons is mediated by RAGE [109]. S100B is known to play important roles in several neurodegenerative and psychiatric disorders such as Down syndrome [234], Parkinson's disease [235], Alzheimer's disease [236], Epilepsy [237], Schizophrenia [238] and bipolar disorder [239, 240]. The elevated serum levels of S100B protein in the neurodegenerative disorders is being used as a prognostic marker to evaluate extent of neuronal damage [206, 241]. S100B expression also increases in melanoma [224]. Besides its intracellular roles in melanoma cells, S100B protein is also released from melanoma cells and tumors [6, 224]. Serum concentration of S100B protein correlates with melanoma tumor burden/progression and with the chemotherapeutic remission of melanoma tumor. Hence serum S100B protein has become a very useful prognostic biomarker for melanoma [242-245]. Both RAGE and S100B are expressed in melanoma tumors and their expression correlates with tumor progression [89]. However, the contribution of RAGE/S100B interaction in melanoma has not been discussed yet. The goal of this study was to investigate the contribution of RAGE in regulating S100B expression in melanoma and to decipher the downstream signaling events involved.

S100A2: S100A2 is encoded by a gene located on chromosome 1q21 which is highly prone to mutations, suggesting its important role in cancer pathogenesis [246, 247]. It is widely expressed in different body tissues and is found at high levels in lungs and kidneys [248] and at

low levels in liver, cardiac cells and skeleton muscle cells [249]. Unlike other S100 proteins, S100A2 protein is mostly located in the nuclear compartment and very diffusely expressed in the cytoplasm [188]. It interacts with many intracellular target proteins such as tropomyosin [250], p53 [251], p63 [252] and p73 [253] in a Ca^{+2} dependent manner. S100A2 interacts with recombinant tropomyosin and can also co-localize with tropomyosin in LCC-PK1 cells, suggesting its possible role in cytoskeleton remodeling [250]. S100A2 also interacts with p53 but unlike S100B protein, it enhances transcriptional activities of p53 protein presumably to induce p53 mediated apoptosis of cancer cells [251]. Our lab showed that recombinant S100A2 protein can interact with RAGE with micromolar affinity in a Ca^{+2} dependent manner [29]. S100A2 expression has been found to be reduced in advanced stage of certain cancer tissues (breast [254], lung [255], oral [256], melanoma [257], prostate [258]) as compared to benign and non-cancer tissues, and to play the role of tumor suppressor [259]. On the contrary, it was found upregulated in other cancers (ovarian [260], gastric [261], non-small cell lung carcinoma [262] and esophageal squamous carcinoma [263], suggesting a complex role of S100A2 in cancer progression [264]. For example, in human head and neck squamous carcinoma S100A2 protein has been shown to inhibit cell migration which might be mediated via RAGE. Contrary to this, it promotes metastasis in non small cell lung cancer [265]. Further studies are required to resolve these conflicting findings regarding its role in cancer progression. Our lab has previously reported a significant reduction in S100A2 transcript level in stage III/IV melanoma patients as compared to early stage melanoma [89]. In melanoma cells, treatment with rexinoid and thiazolidinedione resulted in increased S100A2 expression and simultaneous decrease in cell proliferation. Moreover, over-expression of S100A2 in melanoma cells has been shown to

enhance the anti-proliferative potential of rexinoid based hormone therapy [266]. In the present study, our goal was to investigate the role of S100A2 and RAGE in melanoma progression.

S100A4: S100A4 protein is also known as Metastasin (Mts-1), because of its potential to promote cancer metastasis [267]. Like most of the other S100 proteins, the gene encoding S100A4 is also located in 1q21 chromosome [268]. Within the cell S100A4 can exist as either homo- or hetero-dimers with S100A1 protein [269]. It has been found in the cell cytoplasm, nucleus and also in the extracellular milieu [270]. Many cells have demonstrated to express S100A4. These cells include macrophages, lymphocytes, fibroblasts, endothelial cells, smooth muscle cells, suggesting a wide spread expression of the protein in the body [270, 271]. S100A4 has numerous intracellular and extracellular binding partners that include actin, p53, myosin IIA/IIB, tropomyosin and methionine aminopeptidase 2 [270, 272]. S100A1 is another member of S100 protein superfamily that shows strong affinity for intracellular S100A4 [269]. The interaction of S100A4 with cytoskeleton elements helps modulate cytoskeleton assembly and hence enhance cell motility [273]. Like other S100 proteins, S100A4 also interacts with p53 and inhibits its DNA binding activities [274]. Upon release into the extracellular space S100A4 has been shown to interact with RAGE [29], annexin II [275] and heparan sulfate proteoglycan [276]. Our lab has previously reported micromolar affinity of S100A4 towards GST tagged RAGE by surface plasmon resonance (SPR) [29]. Depending upon the cell types, S100A4 can elicit both RAGE dependent and independent effects. S100A4 has been shown to trigger RAGE dependent signaling in osteoarthritic cartilage [277] and pulmonary artery smooth muscle cells [278] but in neurons S100A4 induce neurite outgrowth independent of RAGE activation [276]. These data suggests complex roles of S100A4 protein depending upon the type and physiological state of the tissue.

S100A4's association with cancer metastasis was first described in 1989 where a strong correlation between S100A4 expression and metastatic potential of the cancer cells was found [279]. In another study, highly metastatic mouse mammary carcinoma did not generate metastasis in S100A4 knock-out mice whereas many metastases were found in the control animals [280]. S100A4 enhances cell motility and tumor metastasis via different mechanisms. It promotes myosin IIA assembly which results in enhanced cell migration and in turn cancer metastasis [273]. S100A4 has also been shown to induce epithelial to mesenchymal transition (EMT) in cancer cells, which is a crucial event in cancer metastasis [270, 281]. EMT is a process that leads to phenotypic and genotypic changes in the cell and is involved in embryogenesis, wound healing and cancer metastasis [282]. Treatment with recombinant S100A4 has also been shown to enhance MMP activities, which helps cancer cells to invade the extracellular matrix [283] and to stimulate angiogenesis [275, 284]. Transgenic mice over-expressing S100A4 have been shown to develop more hemangiomas in liver as compared to control animals [270].

The role of S100A4 in melanoma has not been clearly established yet. An earlier study demonstrated no significant change in S100A4 mRNAs between melanoma samples and benign nevi [257]. Our recent analysis of 40 samples of stage III and stage IV melanoma tissues showed a significantly reduction of S100A4 mRNA in stage IV tissue samples compared to control samples [89]. A positive correlation between the level of S100A4 and primary nodular melanoma tumor growth has also been reported [154]. To summarize, there are contradictory reports on S100A4 expression in melanoma, suggesting a complex role of S100A4 in melanoma progression. Therapies targeting S100A4 might be an effective strategy to treat cancer. The goal of the present study is to define S100A4 and RAGE contribution in melanoma progression.

S100A6: S100A6, also known as Calcyclin, is another member of the S100 protein superfamily [285]. Like other S100 proteins of the "A" series, S100A6 is encoded by a gene located at chromosome 1q21 suggesting its implication in cancer [246]. At the opposite of S100B, S100A6 is widely expressed in a variety of tissues, organs and cells such as stomach, skeletal muscle, heart, lung, kidney and spleen [286]. A wide range of cell types such as fibroblasts, epithelial cells, neurons, glial cells, cardiac myocytes, platelets and smooth muscle cells are known to express S100A6 protein [287]. S100A6 is mainly located in the cytoplasm but it has also been found to be associated with the cell membrane and nucleus upon Ca^{+2} stimulation [288].

Numerous factors have been shown to regulate S100A6 protein expression [287]. Stress [289], injury [290] and ischemic conditions [291] can lead to upregulation of S100A6. Other factors such as growth factors (platelet derived growth factor, epidermal growth factor) [292], tumor necrosis factor [293], estrogen [294], palmitate [295], vasopressin [296] and gastrin [297] can also promote its expression. Several transcription factors regulating the expression of S100A6 have been described. For example, Nf-□B has been shown to activate S100A6 gene [298] whereas p53 has been shown to suppress its gene expression [299]. DNA methylation and histone modification have also been reported to regulate S100A6 expression [300, 301]. The tight regulation of S100A6 expression by multiple elements implicates its important physiological and pathophysiological roles.

S100A6 interacts with multiple target proteins in Ca^{+2} dependent manners. Examples of the targets at protein levels are glyceraldehyde-3-phosphate dehydrogenase, annexin II, annexin VI, annexin XI and the prolactin receptor [302]. Calcyclin binding protein (CacyBP) is another target for S100A6 that suppresses cancer cell proliferation and motility by regulating β-catenin

ubiquitination and ERK signaling pathway [303]. Like S100B, S100A2 and S100A4 proteins, S100A6 can also interact with p53 but its interaction results in the absence of effect on the interaction of p53 with the DNA [304]. However, S100A6 interaction enhances the nuclear accumulation of p53 which might modulate p53 tumor suppressor activities [302]. S100A6 has also been shown to be released from cancer cells. S100A6 has been detected in the breast cancer extracellular medium [108] and pancreatic cancer patient's serum [155]. S100A6 has also been shown to be released from human U87-MG glioblastoma cells in response to increased Ca^{+2} concentrations [108]. RAGE is considered to be one of the target proteins for extracellular S100A6 protein. S100A6 interacts sRAGE with micromolar affinities as determined by surface plasmon resonance [29]. S100A6 mostly interacts with the V and C2 domains of RAGE [108]. High expression of S100A6 protein has been associated with several cancers such as colorectal cancer [305], pancreatic [155], hepato-cellular carcinoma [306], melanoma [307], lung cancer [308] and gastric cancer [309]. The role of S100A6 in cancer progression is complex. In some instances S100A6 has been shown to promote cell apoptosis whereas in other cancer types it promotes cell proliferation. S100A6/RAGE interaction has been shown to trigger apoptosis in SHSY5Y neuroblastoma cells by inducing reactive oxygen species formation which then stimulates JNK signaling [108]. On the contrary, high protein levels of S100A6 has been associated with poor patient outcomes in pancreatic cancer [155]. In pancreatic cancer cells, S100A6 protein has been shown to interact with annexin 2 and to assist in its recruitment to the cell membrane. Thereby, S100A6 protein promotes pancreatic cancer cells motility [310]. These data suggest an active role of S100A6 protein in pancreatic cancer progression. There are currently very few reports on the role of S100A6 in melanoma. A significant correlation was found between the expression of S100A6 in melanoma metastases and the survival time of

patients. Melanoma patients with thick primary lesion and short survival time have been shown to express significantly higher S100A6 mRNA levels as compared to patients with thin lesions and longer survival time [257]. We quantitatively analyzed S100A6 mRNA expression in 40 melanoma tumor samples by Real Time PCR. This study found that 43% of stage III melanoma tissue samples have significant over-expression of S100A6 mRNA [89]. In the current study we have further investigated the association of RAGE with S100A6 in melanoma.

S100A10: S100A10 is another member of the S100 protein superfamily. The gene encoding this protein is located on chromosome 1q21 [246]. S100A10 is also referred as p11, 42C, calpactin I light chain or annexin II light chain [185]. Like other S100 proteins, S100A10 also possesses two EF hand domains but one exceptional feature of this protein is its inability to interact with Ca^{+2}. Deletion and substitution of certain amino acids critical for Ca^{+2} binding renders its EF hands incapable of binding Ca^{+2}. Unlike other S100 proteins, S100A10 possesses a permanent active conformation and remains active without interacting with Ca^{+2} [194, 311].

The expression of S100A10 is induced by interferon, glucocorticoid, transforming growth factor-β, gonadotrophin, epidermal growth factor, basic fibroblast growth factor and interleukin 1β [185, 312]. Promoter hypermethylation can also regulate S100A10 gene expression [313]. S100A10 protein is found in the cytosol and is also expressed on the cells surface in complex with annexin A2 [314]. Annexin A2 plays important roles in regulating S100A10 expression at both mRNA and protein levels [315, 316]. Loss of annexin A2 leads to a reduced S100A10 protein expression at transcript levels [316]. Annexin A2 also stabilize S100A10 and protects it from ubiquitin proteasome degradation pathway [315]. The transport of S100A10 on the cell surface is mediated by annexin A2 through exosomal secretion pathway [317]. The hetero-tetramer complex of S100A10 with annexin A2 is called AIIt, which consists of two molecules

of annexin A2 in complex with homodimer of S100A10 [314]. S100A10 anchored with annexin A2 on the cell surface acts as a plasminogen receptor [314] and interacts with plasminogen, plasmin and tPA (tissue plasminogen activator). Upon binding with S100A10, plasminogen gets cleaved to its activated form plasmin, which leads to proteolytic cleavage of extracellular matrix [318, 319]. By activating plasminogen to plasmin S100A10 contributes in extracellular matrix degradation that assists cancer cells to invade the matrix and enter into the circulation to metastasize to other parts of the body [319]. The presence of excess fibrin clots deposited in S100A10 null mice suggests an important contribution of S100A10 in fibrinolysis [320]. A defective vascularization observed in S100A10 null mice also suggests its role in promoting angiogenesis [320]. Besides this, S100A10 has also been demonstrated to induce macrophage recruitment at the tumor site, that creates an inflammatory microenvironment within the tumor [321]. Inflammatory reactions can further stimulate tumor progression via activating multiple signaling pathways. S100A10 has been shown to contribute in cancer pathogenesis. For example S100A10 knockout mice showed slower tumor growth rate in lewis lung carcinoma as compared to control mice [322]. The regulation of S100A10 protein expression by oncogenes such as PML-RARα [323] and K-Ras [312] further implicates its role in cancer progression. The contribution of S100A10 protein in melanoma progression is not known yet. A recent report by our lab has demonstrated a significant decrease in S100A10 mRNA expression in 58% of stage IV melanoma tumors [89]. The association of S100A10 protein with RAGE has not been reported yet. It is very essential to investigate its association with RAGE in melanoma and the functional significance of S100A10/RAGE in melanoma pathogenesis.

S100A11: S100A11 is another member of the S100 protein superfamily (also known as S100C or calgizzarin) and is encoded by a gene located on 1q21 chromosome [246]. It is

expressed in a wide range of cell types and tissues but is expressed at the highest levels in the skin [324, 325]. Other tissues reported to express S100A11 are placenta, liver, spleen, lung, kidney, heart [326]. It is also expressed in the colon, skeleton muscle, thymus and brain at low levels [327]. Within the cell S100A11 is found both in cytoplasm and nucleus depending upon the cell type and cell environment [325]. S100A11 has also been detected in the extracellular space of normal human keratinocytes [327]. At the molecular level, S100A11 interacts with a number of targets.

Annexin A1 and A2 are the two important binding targets for S100A11 [328]. Translocation of S100A11 from the cytoplasm to the nucleus is important for controlling cell proliferation in response to DNA damage [329]. Over-expression of S100A11 was detected in malignant uveal melanoma [330], but its precise role in melanoma is not clear yet. In the present study we have studied the role of RAGE and its association with S100A11 protein in melanoma progression

To summarize, RAGE and its ligands are associated with various cancer types. In melanoma, co-expression of RAGE and its different ligands implicates their significant contribution in melanoma pathogenesis. To the best of our knowledge there is no scientific report demonstrating the precise role of RAGE and its ligands in melanoma progression. There is a need to understand how RAGE together with its ligands influence melanoma tumor growth. In the present study we have investigated their contribution in melanoma and also explored the downstream signaling involved.

HYPOTHESIS, APPROACH AND RESEARCH OBJECTIVES

The goal of this study was to investigate the role of the RAGE in melanoma progression. Previous literature has suggested an active contribution of RAGE and its ligands in melanoma pathophysiology [133, 219]. Tissue microarrays of human melanoma tumor samples demonstrated strong positive signal for RAGE protein expression in 10% of the tumors tested [331]. Another study reported that AGE-RAGE mediated enhanced melanoma cell proliferation and migration. This study also showed a significant reduction in tumor growth and lung metastasis in a xenograft mouse model of melanoma upon treatment with RAGE blocking antibody [133]. In 2009, our lab reported highly variable transcript levels of RAGE in different melanoma patient tissue samples. This study showed a significant increase in RAGE mRNA expressions in stage IV melanoma patients compared to stage III melanoma patients [89]. All together these reports suggested a possible contribution of RAGE and its ligands in melanoma progression. However, the precise role of RAGE in melanoma progression has not been well defined. In the present study we have asked the following questions:

Does RAGE contribute to melanoma pathogenesis? If yes, what is the mechanism behind it? How S100 proteins contribute to RAGE mediated melanoma progression? If they do play a role, can we suppress melanoma tumor growth mediated via RAGE and S100 proteins?
Based on the previous reports, we hypothesized that RAGE, when overexpressed in melanoma cells, triggers melanoma progression.

To test our hypothesis we have selected two melanoma cell lines (WM115, WM266), that were established from the same patient. The WM115 cell line was established from a primary melanoma tumor in vertical growth phase, whereas the WM266 cell line was established from a metastatic tumor. In order to study the contribution of RAGE, we have over-expressed RAGE in

WM115 cells with two different expression levels (10x and 100X). As a control, we have transfected these cells with noncoding empty plasmid to generate WM115_MOCK cells. Simultaneously, WM266 cells were also transfected with the empty vector in order to comparatively analyze the functional properties of WM115_MOCK, WM115_RAGE and WM266_MOCK cells. This approach has provided us a platform where we can simultaneously study the role of RAGE at different phases of melanoma progression. Using this approach, we have tested our proposed hypothesis by defining specific research objectives.

In Chapter 1 our objective was to generate RAGE over-expressing WM115 melanoma cell lines and characterize them for the presence of RAGE. For this purpose, WM115 cells were stably transfected with either empty or RAGE encoded pcDNA3 plasmid to generate WM115_MOCK, WM115_RAGE-I (intermediate) and WM115_RAGE cells. The metastatic melanoma cell line, WM266, was also transfected with the empty pcDNA3 in the similar way to generate WM266_MOCK cells. The expression of RAGE in WM115_MOCK, WM115_RAGE-I, WM115_RAGE and WM266_MOCK cells was determined by Real Time PCR and ELISA. Using flow cytometry and immunofluorescence we have confirmed the cell surface expression of RAGE in the transfected WM115 cells. As a part of the characterization, we have also assessed the influence of RAGE over-expression on WM115 cells morphology and compared it between WM115_MOCK and WM266_MOCK cells.

In Chapter 2, we aimed to study the effect of RAGE over-expression on the tumorigenic properties of the WM115 cells. To meet our research objective we have performed several cell based assays that reflect the tumorigenic potential of the cells. Proliferation, migration and anchorage independent growth potentials of the cells were assessed and compared by performing AlamarBlue® assay, Boyden chamber assay and soft agar colony formation assay respectively.

To assess whether ligand stimulation could further activate the proliferation and migration properties of these cells, we have also performed the similar assays in the presence of two RAGE ligands (S100B and ribose BSA).

The research objective of Chapter 3 was to decipher RAGE induced downstream molecular mechanisms involved in melanoma progression. First, to confirm that the changes observed in the cellular properties of WM115 cells after RAGE over-expression (Chapter 2) were RAGE dependent, we suppressed RAGE expression in WM115_RAGE cells by transiently transfecting these cells with RAGE specific siRNA. The extent of RAGE suppression was assessed by Real Time PCR and ELISA. The effect of RAGE suppression on WM115_RAGE cells proliferation and migration was assessed using AlamarBlue® and the Boyden chamber assay. Our next goal was to determine the role of S100B, which is one of the ligand for RAGE, in RAGE mediated melanoma progression. For that purpose, we determined and compared the expression levels of S100B protein in WM115_MOCK, WM115_RAGE and WM266_MOCK cells at transcript and protein levels by Real Time PCR and ELISA. Furthermore, expression of S100B protein was suppressed in WM115_RAGE cells by transiently transfecting these cells with S100B specific siRNA. After confirming the suppression of S100B in the siRNA transfected WM115_RAGE cells by Real Time PCR and ELISA, we have performed the AlamarBlue® and Boyden chamber assays to assess their proliferation and migration potentials. Next, expression of the S100B binding partner and tumor suppressor p53 protein was determined in WM115_MOCK and WM115_RAGE cells by Real Time PCR and Western blot. We have also assessed cyclin E protein expression, which is another molecule involved in cancer progression, in the transfected WM115 cells by Western blot and flow cytometry. To investigate the downstream signaling pathways induced by RAGE in melanoma progression we have

assessed AKT, MAPK and JNK activities in WM115_MOCK and WM115_RAGE tumors by Western blot. NF-κB signaling activity in WM115_MOCK and WM115_RAGE was also determined by performing NF-κB luciferase assay. Furthermore, to determine the effect of RAGE over-expression on the expression of cancer associated genes we have performed a cancer pathway finder PCR array on the transfected WM115 cells. The PCR array we used in the study included 84 genes representative of six biological pathways involved in transformation and tumorigenesis.

The major objective in Chapter 4 was to assess the role of RAGE in melanoma tumor growth and to decipher the downstream signaling involved. To meet this objective we have generated a xenograft mouse model of melanoma tumor using the WM115_MOCK and WM115_RAGE cells. The tumorigenic growth potential of these cells was assessed and compared. We have confirmed the expression of RAGE in WM115_MOCK and WM115_RAGE tumors by Real Time PCR, ELISA and immunohistochemistry. We aimed to determine how RAGE overexpression in WM115 melanoma tumors affected S100 proteins expression. For that purpose, expression of S100 proteins (S100B, S100A2S100A4, S100A6 and S100A10) relevant in melanoma pathogenesis were assessed in WM115_MOCK and WM115_RAGE tumors by Real Time PCR and Western blot. Furthermore, genotypic changes in WM115_MOCK and WM115_RAGE tumors were deciphered by performing the same cancer pathway finder PCR array that we used for the transfected WM115 cells.

Next to test the therapeutic potential of anti-RAGE antibody in melanoma tumor growth we have treated WM115_RAGE tumor bearing mice with anti-RAGE antibody. We also assessed the distribution pattern of Cy5.5 conjugated anti-RAGE antibody in mice body by whole animal imaging. To test whether anti-RAGE antibody when given in combination with

chemotherapeutic drug, dacarbazine produce synergistic tumor suppressive effects on melanoma tumors, we have treated WM115_RAGE tumor bearing mice anti-RAGE antibody and dacarbazine.

CHAPTER 1. GENERATION AND CHARACTERIZATION OF RAGE OVER-EXPRESSING MELANOMA CELL LINES

Abstract

The objective of this chapter was to generate melanoma cell lines overexpressing different levels of RAGE and characterize them for the presence of RAGE. For that purpose, we selected two different melanoma cell lines (WM115, WM266) originated from two different stages of tumors of a same melanoma patient. We have stably transfected the WM115 cells with FL_RAGE encoding pcDNA3 plasmid. We also transfected both WM115 and WM266 cells with noncoding pcDNA3 plasmid to generate the control cell lines WM115_MOCK and WM266_MOCK cells respectively. RAGE transcript levels were assessed and compared by Real Time PCR in the transfected cells. RAGE protein levels in the cells were quantified by ELISA. We obtained two clones of WM115_RAGE (WM115_RAGE-I and WM115_RAGE) cells with different expression levels of RAGE. Expression of RAGE was found to be ≈100 and ≈10 fold higher in WM115_RAGE and in WM115_RAGE-I cells respectively than in WM115_MOCK cells. Also, the expression of RAGE in WM266_MOCK cells was found to be ≈2.4 fold higher than in WM115_MOCK cells. Using flow cytometry and immunofluorescence, we demonstrated that RAGE was expressed on the cell surface. Furthermore, to demonstrate the influence of RAGE over-expression on WM115 cells morphologies, we stained the WM115_MOCK and WM115_RAGE cells with FITC conjugated CD44. We observed differences in the morphology of the WM115 cells after RAGE over-expression. The WM115 cells, originally with polygonal morphology, acquired an elongated mesenchymal like morphology after RAGE over-expression. To test the effect of RAGE over-expression on the cytoskeleton organization, we stained the cells with rhodamine conjugated phalloidin that

specifically binds to filamentous actin. Our results demonstrated that WM115_MOCK cells with short thick actin filaments switched to elongated parallel bundles of actin filaments, after RAGE over-expression.

We have successfully generated a model of melanoma cell line over-expressing RAGE. These cells were characterized in terms of expression and subcellular localization of RAGE. Furthermore, the influence of RAGE on the cell morphology and cytoskeleton assembly was also assessed.

Introduction

One of the biggest threats associated with any cancer is the metastatic dissemination of cancer cells throughout the body. Understanding the molecular switch between the proliferative and metastatic states of cancer cells is extremely challenging. A better elucidation of this mechanism could help the development of appropriate therapies against cancer. Transition of tumor cells from epithelial to mesenchymal phenotype, also known as EMT, is one of the crucial events in tumor metastasis [332, 333]. Multiple distinct molecular changes are associated with the EMT process such as activation of transcription factors, expression of specific cell-surface proteins, reorganization of cytoskeletal proteins and production of extracellular matrix degrading enzymes [333].

RAGE is a cell surface receptor of the immunoglobin superfamily. Previous studies have shown an important role of RAGE in modulating cancer cells properties and therefore in cancer progression [78, 133, 135, 210]. RAGE and its ligands (S100B, AGEs, HMGB-1) have been reported to be expressed in significantly higher levels in melanoma tissues as compared to the normal skin tissues [89, 170, 331]. Moreover, AGEs have been shown to enhance melanoma cell

proliferation and migration through RAGE. However, the precise role of RAGE in melanoma pathophysiology is not well defined yet.

Here, our goal was to assess the influence of RAGE over-expression on a primary melanoma cell line. To study the role of RAGE in melanoma progression, we have selected two sister melanoma cell lines (WM115 and WM266) originated from the same patient but from different stages of melanoma progression. The WM115 cell line was obtained from a primary melanoma tumor in vertical growth phase, whereas the WM266 cell line was obtained from a metastatic melanoma tumor of the same patient. We investigated the influence of RAGE on the cellular behavior of WM115 cells and compared it with that of WM266 cells. Understanding the influence of RAGE over-expression on the cellular properties of WM115 cells will help to determine the contribution of RAGE in melanoma progression.

Material and Methods

Cell lines and stable transfection

Two different melanoma cell lines, WM115 and WM266 were obtained from ATCC (Manassas, VA). The cells were maintained in OPTIMEM media (Life Technologies, Grand Island, NY) with 4% FBS, 1% penicillin and streptomycin at 37 °C and 5% CO_2. The cells were stably transfected with FL_RAGE using the pcDNA3 plasmid and Satisfection reagent (Agilent Technologies, Santa Clara, CA) as per manufacturer's instruction. The pcDNA3 plasmid encoding RAGE was kindly provided by Prof. Heizmann, University of Zurich, Switzerland. The empty pcDNA3 plasmid was used to generate the control WM115_MOCK and WM266_MOCK cell lines. The plasmids were digested and linearized with Mfel (New England Biolabs, Ipswich, MA). The transfected clones were then selected with different concentration of G418 sulfate (CellGro). The WM115_RAGE cells were maintained in OPTIMEM with 4% FBS, 1%

Penicillin/Streptomycin and in the presence of 1 mg/ml G418 sulfate, whereas the WM115_MOCK and WM266_MOCK cells were maintained in the same media in the presence of 0.5 mg/ml of G418.

Real Time PCR

Total RNAs were extracted from all the transfected cell lines using the Ambion RNA extraction kit according to the manufacturer's instructions. 200ng of each RNA was reverse transcribed using the Reverse Transcription System (Promega, WI) according to the manufacturer's instructions. The cDNA products were run on a Mx3000 Stratagene RT_PCR system using Brilliant II Ultra fast SYBER Green QPCR Master mix (Agilent Technologies, CA) and appropriate primers (Table 7). The RT_PCR Thermal cycle program comprised an initial denaturation step at 95°C for 10 secs, followed by 40 cycles of denaturation at 95°C for 30 sec, then annealing at 58°C for 30 sec and extension at 72°C for 60 sec. The point at which the fluorescence signal crosses the set threshold is known as Ct value. Ct values of RAGE from WM115_MOCK and WM115_RAGE cells were compared to the corresponding Ct values of actin in both the cell lines. The fold of change of RAGE mRNA expression in WM115_RAGE cells compared to WM115_MOCK cells was calculated using the double delta Ct method [334]. Briefly, Ct values for RAGE gene from both WM115_RAGE and WM115_MOCK cells were normalized with their corresponding Ct values for β-actin gene. The obtained delta Ct value of WM115_RAGE cells was further normalized with the delta Ct value of WM115_MOCK cells. The fold of change was calculated from the double delta Ct value using the following equation.

$$\text{Fold change} = 2^{\Delta\Delta Ct}$$

Where $\Delta\Delta Ct = [Ct\ (RAGE) - Ct\ (\beta\text{-actin})]_{WM115\_MOCK} - [Ct\ (RAGE) - Ct\ (\beta\text{-actin})]_{WM115\_RAGE}$

We have also determined RAGE expression in the transfected WM115 cells by regular PCR using the same set of RAGE primers. The amplified PCR products obtained from the WM115_MOCK and the WM115_RAGE cells were run on a 1% agarose gel (0.01% ethidium bromide) with 100 bp DNA ladder (New England Biolabs, MA).

Human RAGE immunoassay

Protein extracts were prepared form the cells using the PARIS kit (Life Technologies). The concentration of RAGE protein in the cell lysates was quantified using the Quantikine Human RAGE Immunoassay sandwich ELISA system (R & D System, Minneapolis) as per manufacturer's directions. The soluble form of RAGE in the cell condition media of the transfected cells was also quantified using the same immunoassay.

Flow cytometry

A Flow cytometric titration was performed to detect cell surface expression of RAGE on the transfected cells. In brief, both MOCK and RAGE transfected cells were grown to 70-80% confluence. Cells were harvested by scrapping using sterile cell scrappers and incubated with serial dilution of a mouse antibody against human RAGE (R & D System) in 1% FBS / PBS on ice for 1 hour. After washing with 1% FBS in PBS, the cells were further incubated with a FITC conjugated anti mouse IgG $F(ab)'_2$ (Jackson Immunoresearch) antibody (1/100 dilution) on ice for 20 minutes. After a final wash, the fluorescence intensity (Ex: 495nm; Em: 519 nm) was measured on a C6 Accuri Flow Cytometer (Core Biology Facility, NDSU). A total of 5000 events were recorded. The results are shown as the mean fluorescence in arbitrary units.

Immunofluorescence

Cells were grown on sterile glass slides to 60-70% confluence. The attached cells were washed thrice with PBS and were incubated with 100nM of monoclonal human anti-RAGE antibody (R & D System) followed by a FITC conjugated anti-mouse IgG $F(ab)_2$' (Jackson Immunoresearch) (1/100 dilution) in 1% BSA/ PBS containing 0.01% NaN3 on ice for 30 mins. Using a similar procedure, the transfected WM115 cells were stained with a FITC conjugated anti-CD44 antibody (BioLegend, San Diego, CA). The nuclei were stained with the Hoechst dye (Life Technologies). After a final washing step, the cells were imaged using an Olympus Fluoview FV1000 fluorescence microscope at 20x magnification.

To stain the actin filaments, WM115_MOCK and WM115_RAGE cells were first fixed with 4% paraformaldehyde and permeabilized with 0.5% triton X-100. After blocking with 5% BSA/PBS for 1 hour, the cells were incubated with rhodamine conjugated phalloidin (Biotium Inc. Hayward, CA) for 20 mins. The cells were counter stained with the Hoechst dye as mentioned previously. The cells were then imaged using a Zeiss AxioObserver Z1 inverted microscope with LSM700 laser scanning head attachment at 60x magnification.

To compare the cell morphologies of WM115_MOCK, WM115_RAGE-I, WM115_RAGE and WM266_MOCK cells, bright field images of these cells were taken using an Olympus Fluoview FV1000 fluorescence microscope at 20x magnification. The extent of cells' ellipticity was determined by calculating the ratio of cell length over cell width using the CellSens software (Olympus, USA). An average length to width ratio of more than 30 cells from different fields were calculated for each cell type and compared.

Results

Generation of the WM115 cell line model over-expressing RAGE

WM115 cells were stably transfected with a plasmid encoding FL_RAGE. WM115 and WM266 cells were transfected with an empty (MOCK) plasmid and served as controls. We generated three transfected clones of WM115 cells: WM115_MOCK, WM115_RAGE-I and WM115_RAGE. RAGE protein was quantified in the transfected cells by using a commercial sandwich ELISA. WM115_MOCK, WM115_RAGE-I and WM115_RAGE cells expressed 11.5 ± 0.1, 81.0 ± 7.2 and 1081 ± 53 pg of RAGE protein per mg of total protein, respectively (Table 4). WM266_MOCK cells expressed 24.5 ± 6.5 pg of RAGE per mg of total protein. Our results demonstrated 7 fold and 94 fold higher transcript levels of RAGE in WM115_RAGE-I and WM115_RAGE cells respectively than in WM115_MOCK cells. WM266_MOCK cells express 2.4 fold higher RAGE than WM115_MOCK cells (Table 4). We also quantified the soluble form of RAGE released in the culture media of the WM115_MOCK and WM115_RAGE cell lines. We obtained 422 ± 50 pg of RAGE in per ml of culture media of WM115_RAGE cells. In our experimental conditions we couldn't detect any soluble RAGE in WM115_MOCK cells culture media (Table 5).

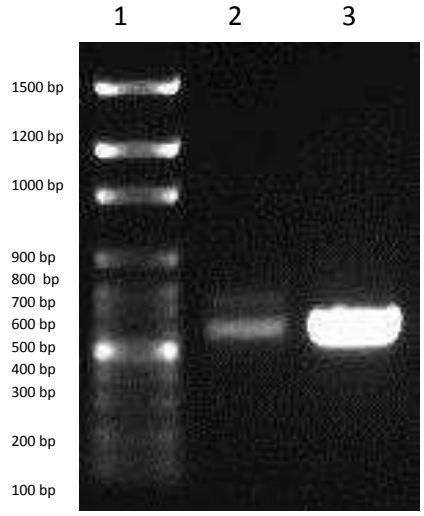

Figure 5: Representative agarose gel demonstrating PCR products of transfected WM115 cells Lane 1. 100 bp DNA ladder, Lane 2. WM115_MOCK and Lane 3. WM115_RAGE. Real Time PCR experiment was performed in the transfected WM115 cells in triplicate on at least three independent sets of cDNAs using primer pairs specific for FL_RAGE.

Table 4: Quantification of RAGE in WM115 cell lysates by ELISA.

Cell lysates	**RAGE (pg/mg of total protein)**
WM115_MOCK	11.5 ± 0.1
WM115_RAGE-I	81.0 ± 7.2
WM115_RAGE	1081 ± 53
WM266_MOCK	24.5 ± 6.5

Table 5: Quantification of soluble form of RAGE in WM115 cell supernatants by ELISA.

Cell supernatant	**RAGE (pg/ml of cell supernatant)**
WM115_MOCK	≤ 10
WM115_RAGE	422 ± 50

RAGE was detected on the cell surface of WM115_RAGE and WM266_RAGE cells

The flow cytometric experiment data showed a higher level of RAGE in the WM115_RAGE cells than in the MOCK control cells (Figure 6). In our experimental conditions, the cells were not permeabilized prior to the incubation with the antibody which restricted the antibody to binding to cell surface RAGE. Our results suggest that RAGE was accessible to the antibody and hence it is probably located on the cell surface. Flu_{max} of WM115_RAGE cells was found to be 4.1 $*10^5$ A.U. whereas the mean fluorescence from WM115_MOCK cells remained in the baseline levels. We also detected RAGE in the transfected cells by immunofluorescence (Figure 7). RAGE was found both on the cell surface and in the cytoplasm of WM115_RAGE cells (Figure 7B). RAGE could not be detected in WM115_MOCK cells in our experimental conditions (Figure 7A).

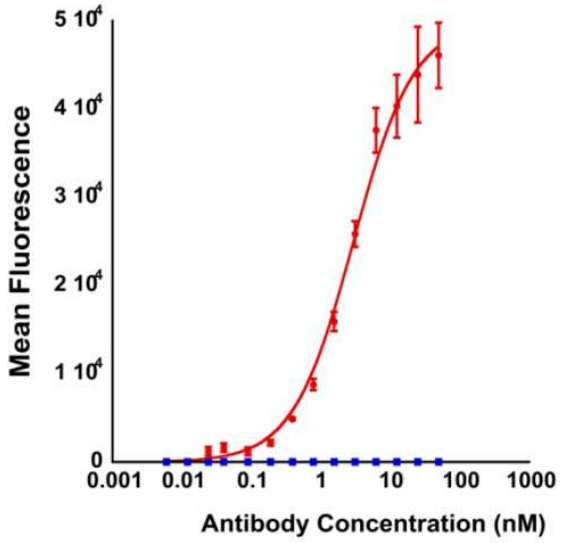

Figure 6: Detection of RAGE protein on the cell surface of WM115 cells by flow cytometry. Expression of RAGE was assessed in WM115_RAGE (red circles) and WM115_MOCK (blue squares) cells by flow cytometry using increasing concentration of anti-RAGE antibody. The experiment was performed in triplicate for two independent times. (n = 3).

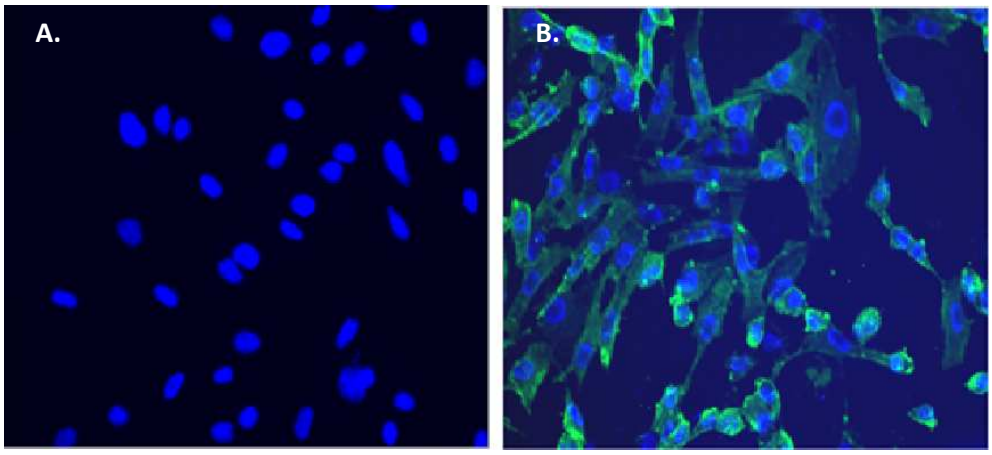

Figure 7: RAGE detection on the cell surface of WM115 cells by the immunofluorescence. Merged images of WM115_MOCK (A.) and WM115_RAGE (B.) cells stained with Hoechst dye (blue) and anti-RAGE antibody with FITC conjugated secondary antibody (green). Magnification 20X.

RAGE over-expression triggers a phenotypic change and filamentous actin remodeling in WM115 cells

In order to assess the effect of RAGE over-expression on WM115 cell morphology, we stained the cells with FITC conjugated anti-CD44 antibody. CD44 is a cell surface glycoprotein expressed in most melanoma cells including WM115 cells [335]. The microscopic images demonstrated a morphological switch from a polygonal morphology in the WM115_MOCK cells to an elongated mesenchymal like morphology in the WM115_RAGE cells (Figure 8). We have also quantified the ellipticity of the transfected cells by calculating the ratio of the cell length over the cell width (R_{cell}). We found that the ratio was significantly higher in the WM115_RAGE cells ($R_{cell} = 9.8 \pm 3.8$) than in the WM115_MOCK cells ($R_{cell} = 1.8 \pm 0.7$). The ellipticity of the WM266_MOCK cells ($R_{cell} = 10.8 \pm 4.0$) was equivalent to that of the WM115_RAGE cells. We have also calculated length to width ratio ($R_{nucleus}$) of transfected WM115 cells' nuclei. Our results demonstrated a significant increase in $R_{nucleus}$ in WM115_RAGE (1.8 ± 0.5) cells as compared to WM115_MOCK (1.3 ± 0.2) cells ($p < 0.05$).

To further assess the effect of RAGE over-expression on the filamentous actin arrangement in WM115 cells, we stained the cells with rhodamine conjugated phalloidin. Phalloidin is a fungal toxin that binds to and stabilizes filamentous actin by preventing its depolymerization. We observed short thick bundles of filamentous actin in WM115_MOCK cells which remodeled to long parallel bundles of actin after RAGE over-expression (Figure 9). WM115_RAGE-I (WM115_RAGE-10x) demonstrated intermediate level of filamentous actin remodeling (Figure 40). We also compared the cellular morphologies of the transfected WM115 cells with that of WM266_MOCK cells by bright field microscopy. We showed that WM115 cells acquired an elongated morphology after RAGE over-expression which is equivalent to the morphology of metastatic melanoma cell line WM266_MOCK (Figure 10). These data suggest a RAGE dependent modulation in cells morphology and cytoskeleton remodeling induced in WM115 cells upon RAGE over-expression.

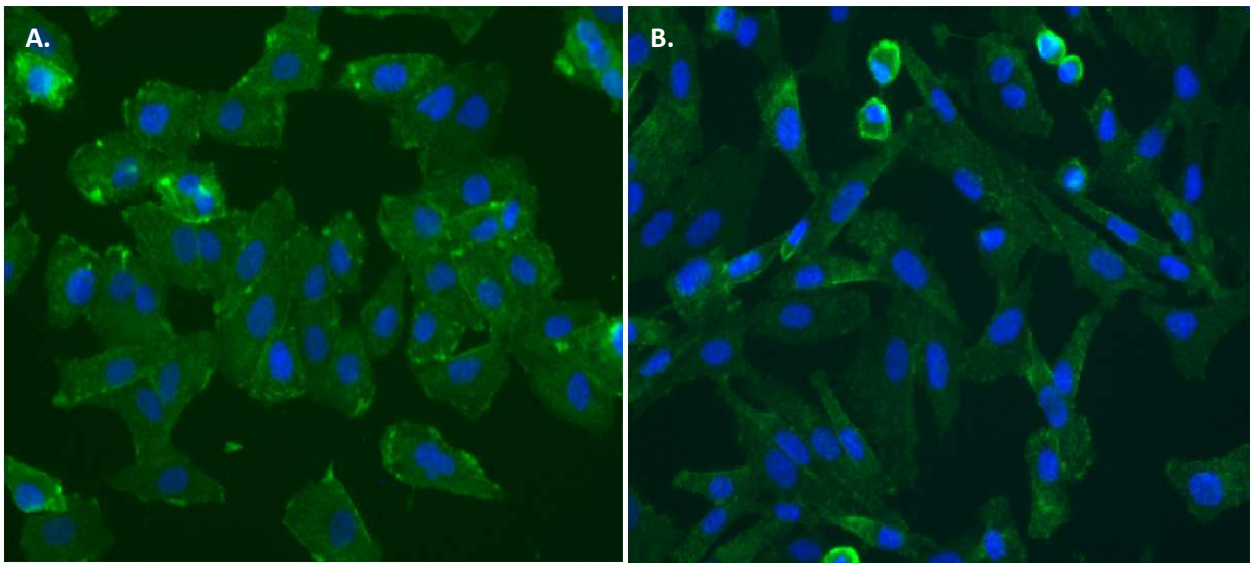

Figure 8: CD44 staining in the transfected WM115 cells. WM115_MOCK (A.) and WM115_RAGE (B.) cells were stained using a FITC conjugated CD44 antibody. Cells' nuclei were stained with the Hoechst dye. Merged images with 20X magnification.

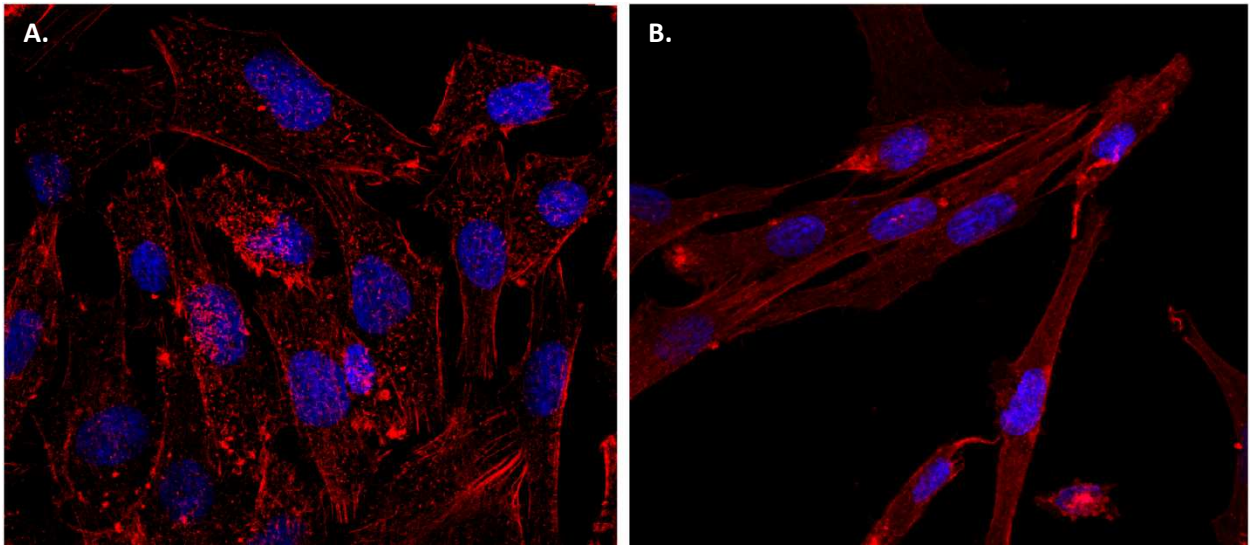

Figure 9: Filamentous actin staining in the transfected WM115 cells. Actin filaments were stained in WM115_MOCK (A.) and WM115_RAGE (B.) cells using rhodamine conjugated phalloidin. Cells' nuclei were stained with the Hoechst dye. Merged images with 60X magnification.

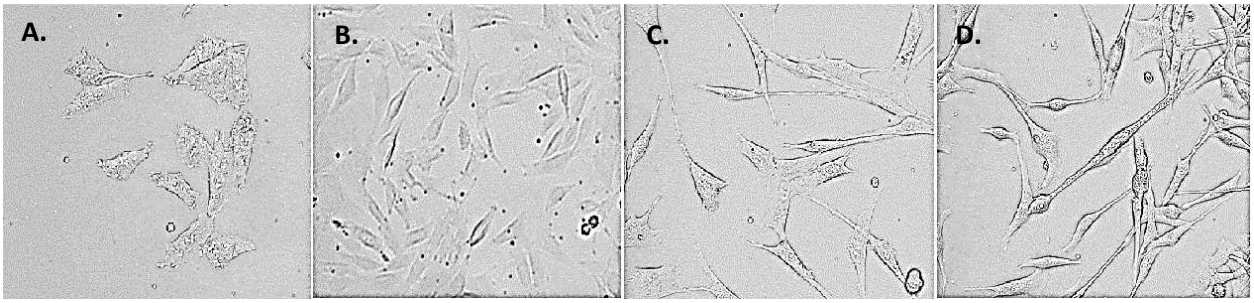

Figure 10: Bright field images of transfected WM115 and WM266 cells. Image showing morphologies of WM115_MOCK (A.), WM115_RAGE-I (B.), WM115_RAGE (C.) and WM266_MOCK (D.) cells. Magnification 20X.

Discussion

We have successfully generated two new melanoma cell lines overexpressing ≈10 and ≈100 fold higher RAGE compared to the MOCK control cells. We hypothesized that RAGE, when over-expressed in melanoma cells, plays a role in melanoma progression. To simulate the pathological conditions, we generated WM115 cells that over-expressed 10-100 fold higher RAGE as compared to their MOCK counterparts. Flow cytometry (Figure 6) and immunofluorescence (Figure 7) results show that RAGE was not only expressed on the cell surface but also present in the cytoplasm. Our data are in agreement with previous reports. Indeed several reports have demonstrated intracellular location of RAGE previously. RAGE has been shown to be present on the cell surface as well as in the cytoplasm of G361 malignant melanoma cells, which upon activation with AGE enhances cell proliferation and migration [133]. RAGE has also been reported to internalize from the cell membrane and be transported in the cytoplasm upon engagement with either its ligand (AGE and S100B) or anti-RAGE antibody [336]. Internalization of RAGE upon stimulation with Advanced Glycation End Products has been shown to be an important event for downstream signaling in CHO cells [128]. In Schwan cells, S100B stimulation led to internalization of RAGE, which was shown to recycle back to the cell surface by Src mediated signaling. Recycling of RAGE induced S100B secretion and morphological changes in the cells [129].

We could also detect higher levels of soluble RAGE in WM115_RAGE cell supernatants as compared to MOCK cells supernatants. These data suggest a shedding of membrane bound RAGE into its soluble form via proteolytic cleavage. Shedding of membrane bound RAGE by metalloprotease ADAM10 has been reported previously [81]. Soluble form of RAGE has been suggested to act as a decoy receptor that can counteract RAGE mediated signaling [337]. At this

point, we don't know the role of soluble RAGE on the cellular properties of WM115 cells. Soluble form of RAGE released from WM115_RAGE cells might counteract RAGE mediated signaling in WM115 cells by interacting with the RAGE ligands. However, it might just be a mechanism to shed the excess of RAGE proteins to maintain a constant number of RAGE molecules on the cell surface.

Cells were stained with the cell surface biomarker CD44 in order to observe possible phenotypic changes induced in WM115 cells upon RAGE over-expression (Figure 8). CD44 is a cell surface receptor for hyaluronan, it is implicated in cell proliferation, cell migration, cell-cell adhesion and cell-matrix adhesion [338-341]. CD44 is expressed in many cancer cell types including melanoma [335]. We showed an enhanced ellipticity in the WM115_RAGE cells and their corresponding nuclei compared to the MOCK control cells. Induction of elongated mesenchymal like morphology is one of the mechanism by which cancer cells acquire migration potential. Elongated mesenchymal morphology is one of the characteristics of metastatic cells [342]. RAGE induced altered cell morphology might affect cells migration and invasion potentials. An altered nuclear structure is also one of the hallmark of cancer and is used in disease diagnosis [343].

Next, in order to assess the effect of RAGE on cytoskeleton remodeling, we stained filamentous actin with rhodamine conjugated Phalloidin (Figure 9). The images showed a significant actin remodeling induced in WM115 cells upon RAGE over-expression. The short thick actin filaments in WM115_MOCK cells, remodeled into long thin parallel filaments after RAGE over-expression. The cytoskeleton plays a central role in modulating cell morphology. Polymerized actin constitutes a major part of the cell cytoskeleton and provides a mechanical support to the cells. Polymerization and depolymerization of actin filaments modulate the cells

morphology and provide propulsive forces for cell movement [344, 345]. RAGE has been previously shown to alter actin assembly in different cell types. Over-expression of RAGE in Human Umbilical Vein Endothelial Cells (HUVEC) has been shown to trigger actin filament remodeling [346].

In summary, we have demonstrated that RAGE over-expression induced morphological changes to the WM115 cells from an epithelial like morphology to a mesenchymal like morphology. Our data suggest an enhanced WM115 cell motility upon RAGE over-expression. In the next chapter we will test the effect of RAGE over-expression on the cellular behavior of WM115 cells.

CHAPTER 2. EFFECT OF RAGE OVER-EXPRESSION ON MELANOMA CELL PROLIFERATION, MIGRATION AND INVASION

Abstract

In order to decipher the role of RAGE in melanoma progression, we have generated and characterized new melanoma cell lines over-expressing RAGE (described in Chapter 1). In this chapter, the effect of RAGE over-expression on cell proliferation, migration and invasion with and without ligand activation was assessed and compared. We found a reduced cell proliferation in the WM115_RAGE cells as compared to their MOCK counterparts in normal growth conditions. Contrary to this, we showed that the WM115_RAGE cells had increased their anchorage independent growth potential compared to the MOCK control cells as shown by soft agar colony formation assay. The WM115 cells appeared to have acquired a migratory like and invasive like phenotype after RAGE over-expression as shown by the wound healing and Boyden chamber assays. We showed that after transfection with RAGE, the WM115 melanoma cells exhibited similar migration potentials than those of the WM266 cells, the sister metastatic cell line of WM115.

We next investigated the influence of RAGE ligand (S100B, ribose BSA) on the migration of the WM115_MOCK and WM115_RAGE cells. Treatment with 1mg/ml of 500nM ribose BSA led to two fold increase in WM115_MOCK cells' migration but no effect was found on the WM115_RAGE cells. Recombinant S100B protein treatment didn't alter the migration of either cell lines. Treatment with an anti-RAGE antibody could not suppress the migration of the WM115_RAGE cells nor the AGE induced migration of the WM115_MOCK cells.

Introduction

Melanoma is the most lethal form of skin cancer [347]. Melanoma cells are highly heterogenous in terms of cell morphology, genetic pattern and sensitivity towards chemotherapy [348-350]. Melanoma cells undergo reversible changes in phenotypes and genotypes which provide diversity in the tumor cell population. The heterogeneous population of melanoma cells has the ability to respond differently to chemotherapy. For example, some cells acquire chemoresistance, that makes melanoma difficult to treat [20]. In the present study we used two melanoma cell lines WM115 and WM266. As mentioned previously the WM115 melanoma cell line was obtained from a primary melanoma tumor and WM266 was established from a metastatic melanoma tumor from the same patient. Both cells consist of phenotypically and genotypically diverse traits [351, 352]. Understanding the influence of a particular target in melanoma cells is necessary in order to develop an effective therapy against melanoma. Recent studies have suggested the involvement of RAGE and its ligands in cancer progression [110]. S100B protein, one of the best known ligand of RAGE, promotes melanoma progression by inhibiting tumor suppressor p53 protein [219]. Serum concentration of S100B protein correlates with melanoma progression, therefore its concentration is used as a prognostic biomarker for melanoma [353]. Advanced glycation end products (AGEs) form another group of RAGE ligands and have been shown to increase melanoma cell proliferation and migration in RAGE dependent manner [133]. The co-localization of RAGE and its different ligands in melanoma tumors suggest their important role in melanoma pathophysiology [133]. Understanding the role of RAGE in melanoma pathophysiology may lead to the discovery of new therapeutic approaches against melanoma. In this chapter we have investigated the influence of RAGE over-expression on the cellular behavior of WM115 cells and compared it with those of WM266, a

metastatic melanoma cell line. We have also tested whether RAGE ligands (AGE and S100B) can further modulate cellular properties of the transfected WM115 cells.

Materials and Methods

Expression and purification of recombinant S100B protein

Bacterial cells were transformed with a pGEMEX® plasmid encoding for S100B gene. After transformation, the cells were grown over night and subcultured until the optical density (OD) reached 0.7. The expression of S100B was then induced with 0.8 mM of IPTG for the next three hours. Subsequently, the cells were pelleted and sonicated in the presence of 1/1000 dilution of phenyl methyl sulfonyl fluoride (PMSF). The supernatant was treated with 85% of $(NH_4)_2SO_4$ solution for 30 mins at 4°C which resulted in the precipitation of other proteins except S100B. After centrifugation the supernatant containing S100B was further processed by adjusting the pH to 4 using 10% phosphoric acid. In these conditions, S100B protein precipitated. After centrifugation the pellet was dissolved in 50mM Tris buffer containing 2mM of $CaCl_2$ at pH 7.4. Further purification was performed by affinity chromatography using phenyl sepharose column on an AKTA Prime system (Amersham Biosciences). Bound S100B was eluted by the presence of 2mM of EDTA. Purified S100B was quantified by measuring its absorbance at 280nm (Extinction coefficient 1490 M^{-1} cm^{-1}). To remove possible endotoxin contaminants, the S100B containing solution was passed on a polymyxin B column (Sigma Aldrich, USA) (Figure 11).

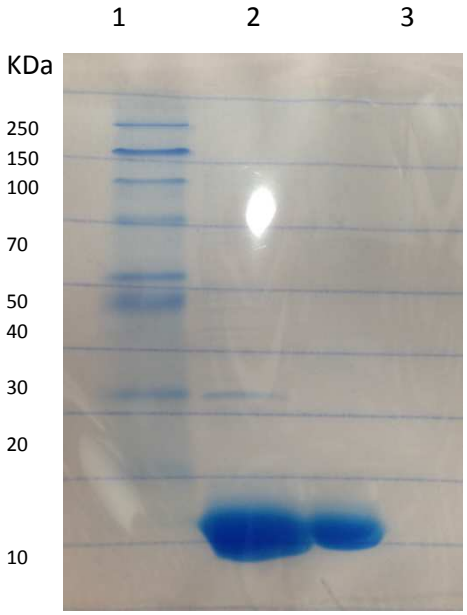

Figure 11: Representative SDS PAGE gel image showing the purity of S100B protein after purification. Recombinant S100B protein was run on 15% SDS PAGE gel. Lane 1. Protein ladder, Lane 2. S100B protein before phenyl sepharose chromatography. Lane 3. Purified S100B after phenyl sepharose chromatography.

Advanced Glycation End Products

500mM of ribose BSA (bovine serum albumin) was prepared and characterized in our lab by Venkata under the supervision of Dr. Stefan Vetter [354]. Briefly, 20mg/ml of BSA solubilized in sodium phosphate buffer with 1 mM EDTA and 1mM sodium azide (pH 8) was mixed with 500mM of ribose and incubated at 37°C for 21 days. After the incubation period, the samples were dialyzed twice against 200 volumes of PBS at 4 °C. Upon characterization, we found 96% and 15% modification of BSA protein at lysine and arginine residues respectively.

Anti-RAGE antibody purification

Briefly, Balb/CByj mice were immunized with the extracellular part of human RAGE protein, which was expressed and purified in yeast cells. Mice with the highest titer of anti-RAGE antibodies in their serum were euthanized and their spleens were isolated. B-lymphocytes from the spleens were subsequently fused with mouse myeloma cells in the presence of 50%

polyethylene glycol (PEG). Hybridomas were then selected to remove any unfused or improperly fused cells. Antibodies secreted in the hybridoma culture supernatants were purified by affinity chromatography using a G-sepharose column. The bound antibodies were eluted with 20mM glycine (pH 2.2). The final pH of the antibody solution was neutralized to 7.4 using 200mM of dibasic sodium phosphate buffer. The eluted antibody fractions were sterile filtered using 0.2 micron pore sized filters. The purity of the antibody was determined by coomassie blue stained SDS PAGE and was estimated to be greater than 95%.

Anti-RAGE antibody characterization

A particular anti-RAGE antibody producing clone of hybridoma (2A11), was used for all the studies. The affinity of this antibody towards different RAGE domains was determined by ELISA and surface plasmon resonance (SPR). The ability of this antibody to interact with cell surface RAGE was determined by flow cytometry and immunofluorescence.

Proliferation assay

The proliferations of MOCK and RAGE transfected WM115 cells were assessed and compared using the AlamarBlue® (AbD Serotek, Raleigh, NC) redox indicator dye. In this assay, an equal number of both MOCK and RAGE transfected cells were seeded in their corresponding growth media (described in Chapter 1) in the wells of 96 well plates. After 24 hours, 10% v/v of AlamarBlue® (AB) was added to each well. The fluorescence intensities (Ex: 540nm; Em: 590nm) of the wells were measured after 4 hours incubation. To assess ligand dependent effect on cell proliferation, the melanoma cells were seeded either with 1mg/ml of AGE or 100nM of S100B. After 24 hours of incubation the cell proliferation was assessed as mentioned above.

Soft agar assay

In this assay, 1% agar (DIFCO BD, France) solution was prepared in OPTIMEM containing 4% FBS. This solution was plated in the wells of 6 well plates and allowed to solidify. A 0.7% agarose (Invitrogen, CA) solution in OPTIMEM/4%FBS was prepared by mixing equal volume of 1.4% of autoclaved agarose in OPTIMEM/8% FBS. The solution was allowed to cool down to 37°C. The soft agar assay was performed on four types of cells: WM115_MOCK, WM115_RAGE, Hek 293 and Hek_RAGE. Hek_RAGE cells were a generous gift from Prof. Heizmann (University of Zürich, Zurich, Switzerland). An equal number of WM115_MOCK, WM115_RAGE, Hek 293 and Hek_RAGE cells were mixed in the 0.7% agarose solution and $1*10^4$ cells were seeded in each well on top of the solidified 1% agar solution layer. The plates were incubated at 37°C for 4 to 5 weeks. The media was replenished every 3-4 days. Colonies were stained with crystal violet and imaged with an Olympus Fluoview FV1000 microscope connected to a camera. Ten independent fields in each well were imaged and the experiment was repeated for three independent times.

Wound healing assay

In order to determine the migration potential of the transfected cells we performed a wound healing assay. Both MOCK and RAGE transfected cells were grown to confluence in the wells of a 24 well plate. A uniform wound was created on the surface of the confluent cells using a sterile 10µl pipette tip. The wound healing was followed over the period of 24 hours. Cells were imaged immediately after the wound formation, 14 hours later and then 24 hours later using an Olympus Fluoview FV1000 microscope. Wound widths were measured at different time

points The percentage of wound closure after 14 hours and after 24 hours was calculated in both the types of cells as following:

Percentage of wound closure = [(Wound width after 0 hour)-(Wound width after 14 or 24 hours) / (Wound width after 0 hour)]*100

Migration and Invasion assay

The migration potential of the cells was also determined by using the Boyden chamber assay. In this assay $4 * 10^4$ of both MOCK and RAGE transfected WM115 cells in serum free media were seeded on a 8 micron pore sized cell culture insert. Serum containing media (4% serum) was added to the bottom chamber and the cells were allowed to migrate across the filter for 24 hours. Equal numbers of cells were also seeded without filter directly to the bottom chamber as a control. At the end of the incubation period, non-migrated cells were gently removed from inside the filter using sterile cotton swab. After placing the filters back into their corresponding wells, 10% v/v of AlamarBlue® was added to the bottom chamber. The percentage of migrated cells was calculated as following:

Percentage of migrated cells = (AB fluorescence with filter / AB fluorescence without filter)*100

To assess the effect of RAGE ligands (S100B, AGE products) on cell migration, both WM115_MOCK and WM115_RAGE cells were seeded on the culture inserts in the presence of either 100nM of S100B or with 1mg/ml of AGE. After 24 hours of incubation, the cell migration potential was assessed as described above.

To determine the invasion potential of the transfected cells, culture inserts were coated with bovine collagen I (Santa Cruz Biotechnology) prior to seed cells. Briefly, a 0.02 mg/ml

solution of bovine collagen I was prepared in 70% ethanol. Each filter was coated with 4µg of collagen I and air dried under the laminar flow hood. Transfected cells were seeded on to the coated filters as described previously. The percentage of cells that had invaded across the coated filter were determined using the same equation.

Statistical Analysis

Data are shown either as Mean ± SD. Comparative analysis between two groups was made by one tail two sample (unpaired) Student's t-test and $p < 0.05$ was considered as significant.

Results

RAGE over-expression leads to reduced proliferation but increased anchorage independent growth of WM115 cells

We observed that WM115_RAGE cells were significantly ($p < 0.05$) less proliferative than WM115_MOCK cells in 2D cell culture conditions (Figure 12). The influence of RAGE over-expression on the anchorage independent growth potential of WM115 cells was assessed using the soft agar colony formation assay. Interestingly, the WM115_RAGE cells formed about 4 times more colonies compared to the WM115_MOCK cells when grown in anchorage independent conditions. We observed that the colonies obtained from the WM115_RAGE cells were larger in size than those formed from the WM115_MOCK cells (Figure 13). On the contrary, the Hek 293 and Hek_RAGE cells were unable to develop colonies in anchorage independent conditions (Figure 14).

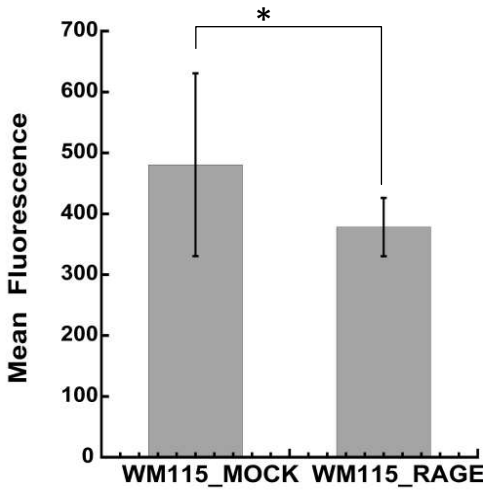

Figure 12: AlamarBlue® assay in transfected WM115 cells. Cell proliferation of WM115_MOCK and WM115_RAGE cells was assessed using the AlamarBlue® redox indicator reagent. Experiment was performed in triplicate three independent times. Data are shown as mean ± SD. (n=3; *p < 0.05)

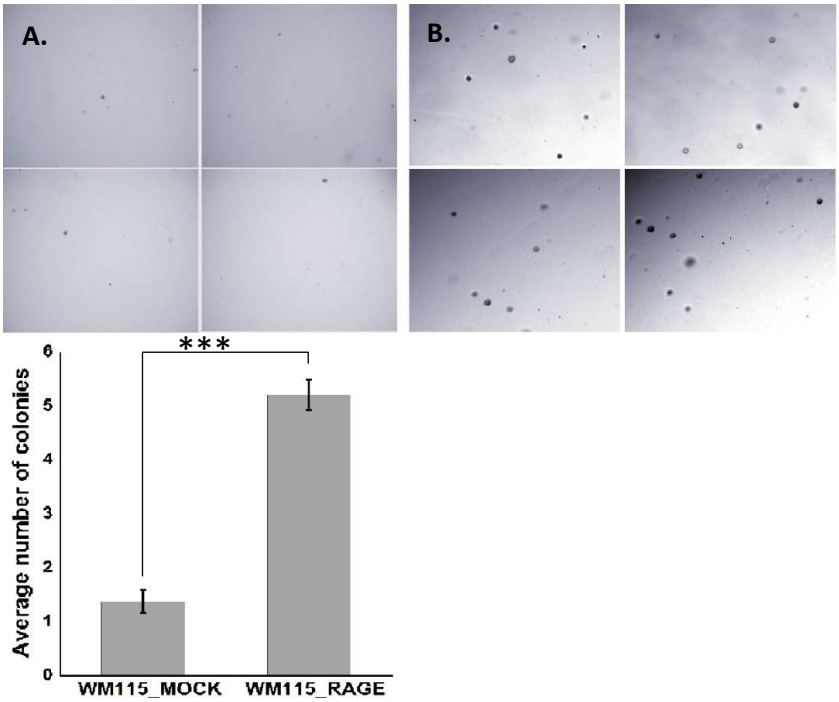

Figure 13: Soft agar colony formation assay with transfected WM115 cells. Anchorage independent growth of WM115_MOCK (A.) and WM115_RAGE (B.) cells was assessed by embedding the cells in agar and allowed them to grow for 4 weeks. Ten independent fields were imaged and only four are shown here. Experiments were performed in triplicates. Magnification 20X. Graph shows average number of colonies formed in both cell types. Data are shown as mean ± SD. (n= 3; ***p < 0.001).

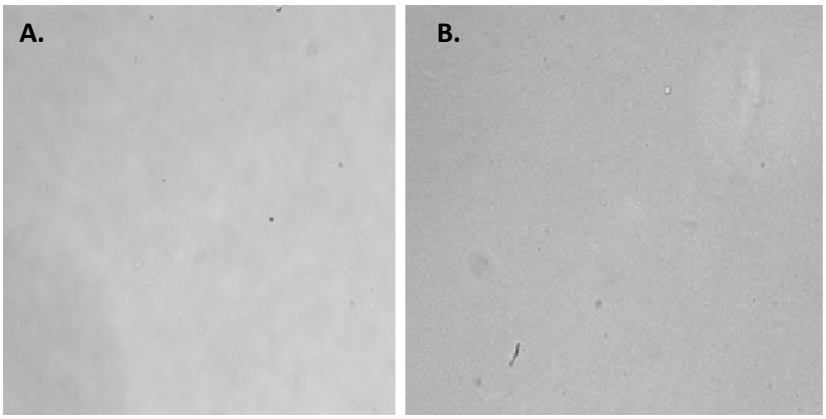

Figure 14: Soft agar colony formation assay in transfected Hek cells. Anchorage independent growth potential of Hek293 (A.) and Hek_RAGE (B.) cells. Cells were embedded in agar and were grown in anchorage independent condition for 4 weeks. Non tumor cells were unable to from colonies in anchorage independent condition.

RAGE over-expression in WM115 cells increases the cell motility to a level that is comparable to that of WM266_MOCK cells

The effect of RAGE over-expression on the migration potential of the WM115 melanoma cells was assessed by the wound healing assay. The results showed a faster wound healing in the WM115 cells after RAGE over-expression. After 24 hours, the WM115_RAGE cells could close 100% of the wound whereas the WM115_MOCK cells could close less than 50% of the wound (Figure 15). We next compared the migration levels of the WM115_MOCK cells with those of WM115_RAGE-I (10x higher RAGE), WM115_RAGE (100x higher RAGE) and WM266_MOCK cells. Both RAGE transfected WM115 cell lines expressed different levels of RAGE (described in Chapter 1). We observed a ≈2 fold increase in the percentage of cells migrated in the WM115_RAGE-I cells as compared to the WM115_MOCK cells. The migration potential of the WM115_RAGE cells was found to be ≈3 fold higher than that of WM115_MOCK cells (Figure 16A). Moreover, WM266_MOCK cells migrated to a level that was similar to that of the WM115_RAGE cells (Figure 16A). We have also assessed the invasion

potential of the WM115 cells on collagen I coated filters. We found a 6 fold higher invasion of the WM115_RAGE cells compared to the MOCK control cells (Figure 16B).

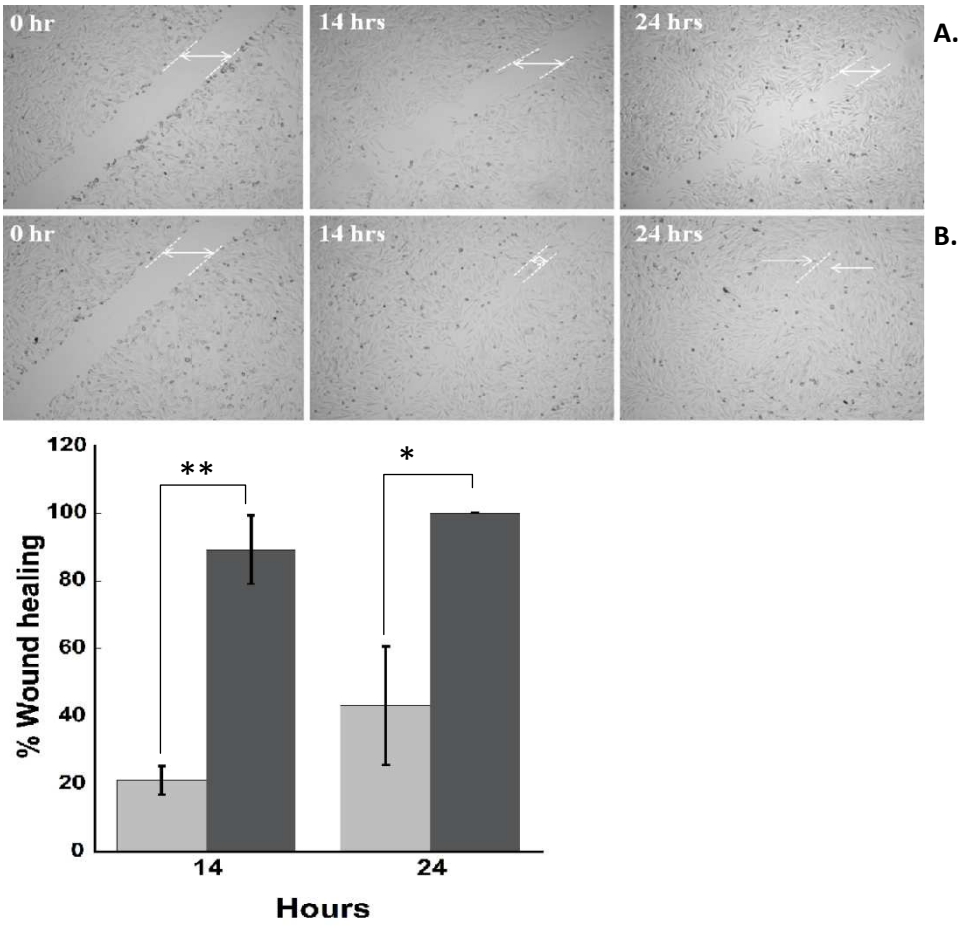

Figure 15: Migration potentials of the transfected WM115 cells by wound healing assay. After formation of a uniform wound on the confluent cell surface, WM115_MOCK (A.) and WM115_RAGE (B.) cells were imaged at 0 hour and after 14 and 24 hours. The graph represents the percentage of estimated surface covered by WM115_MOCK (light grey) and WM115_RAGE (dark grey) cells at different times. The experiments were performed three independent times in triplicate. Data are shown as mean ± SD. (n=3; *$p < 0.05$; **$p < 0.01$).

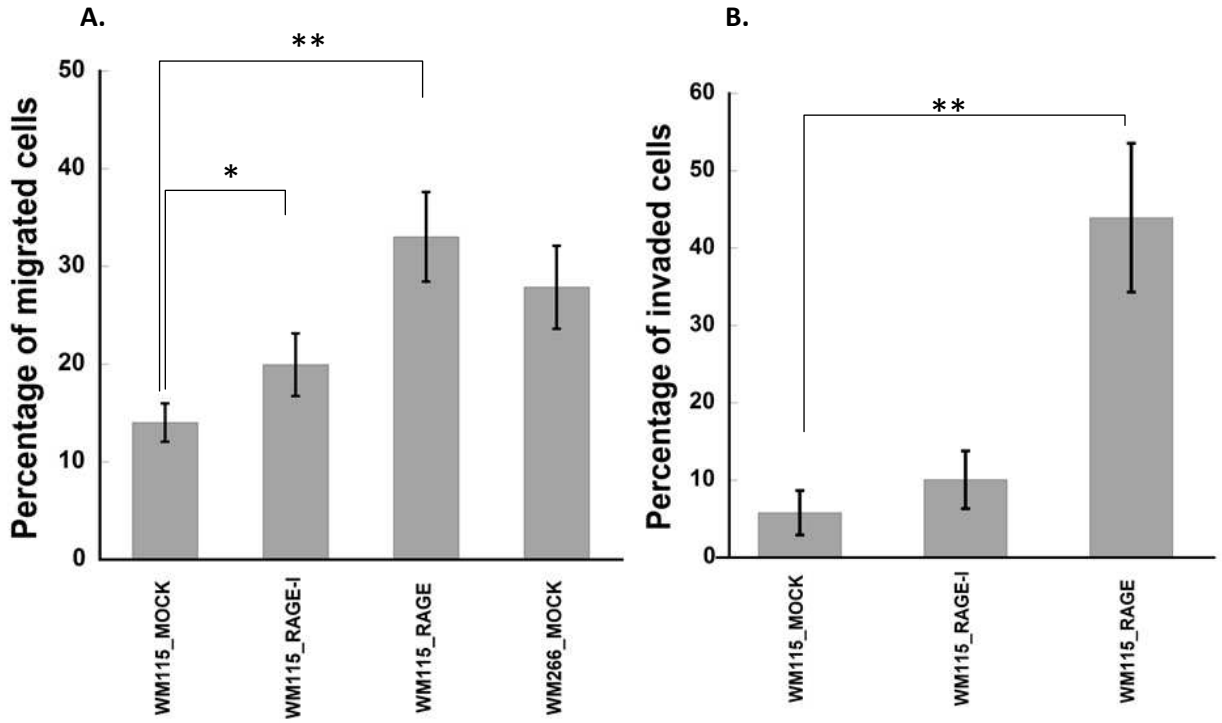

Figure 16: Migration and invasion potentials of the transfected WM115 cells. A. Migration potential of WM115_MOCK, WM115_RAGE-I, WM115_RAGE and WM266_MOCK cells as measured by Boyden chamber assay. B. Invasion potential of WM115_MOCK, WM115_RAGE-I and WM115_RAGE cells by Boyden chamber assay. Experiments were performed in triplicate three independent times. Data are shown as mean ± SD. (n = 3; *$p < 0.05$; **$p < 0.01$).

IgG 2A11 could interact with V domain, VC1C2 domain and sRAGE

Our lab has shown previously that IgG 2A11 could interact with RAGE V domain. The experimental details and the data obtained will not be shown here but the results of the experiments are summarized below. ELISA results showed a nanomolar affinity of IgG 2A11 towards RAGE V domain (K_D = 7.0 ± 0.4 nM) and VC1C2 domain (K_D = 3.6 ± 0.1 nM) of RAGE respectively. Our results from SPR experiments demonstrated a K_D value of $3.8 * 10^{-10}$ M of IgG 2A11 for V domain of RAGE. IgG 2A11 can also interact with RAGE expressed on the cell surface of Hek 293 cells as determined by flow cytometry and immunofluorescence. We

have also tested the ability of IgG 2A11 to displace S100B from RAGE binding sites by performing a competition ELISA (data not shown).

Ribose BSA but not S100B induces WM115 cell proliferation and migration in the WM115_MOCK cells

The stimulation of the WM115_MOCK cells with 500nM ribose BSA resulted in a dose dependent increase in the cell migration. On the contrary, the WM115_RAGE cells didn't respond to ribose BSA activation. Treatment with recombinant S100B had no effect on the migration potential of either cell type (Figure 17A). Furthermore, blocking RAGE with anti-RAGE antibodies could not suppress WM115_RAGE cells migration. Ribose BSA induced cell proliferation and migration was also not affected by anti-RAGE antibody treatment (Figure 17B).

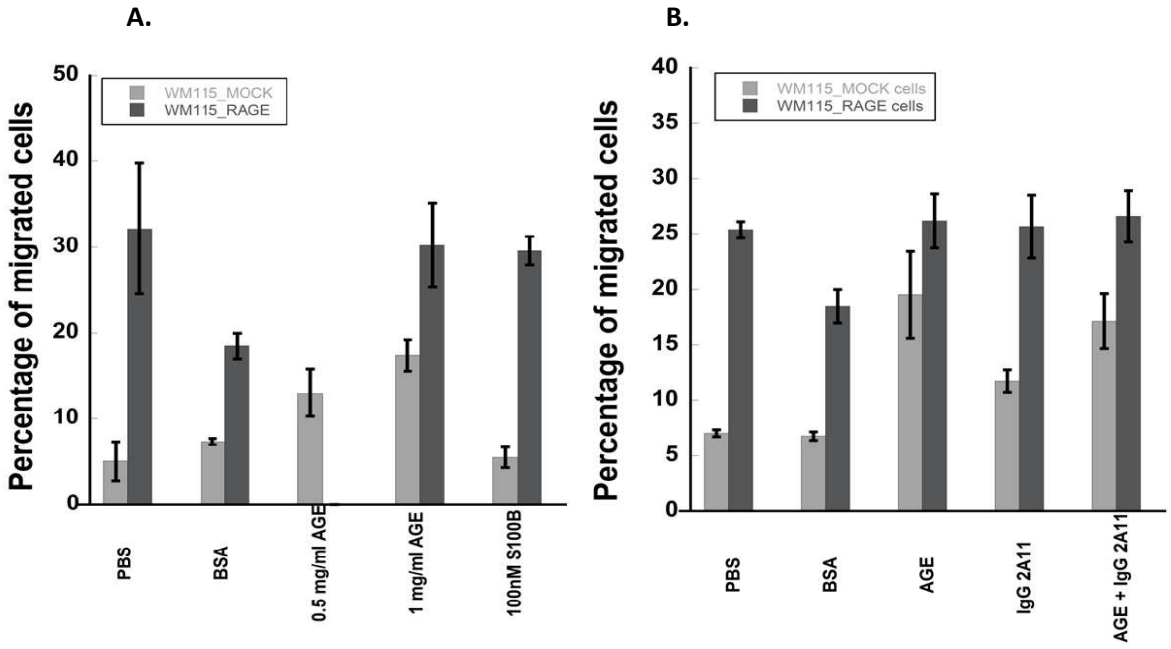

Figure 17: Percentage migration of transfected WM115 cells after ligand (A.) and IgG2A11 (B.) treatment. PBS and BSA were used as controls. Experiment was performed in triplicate three independent times. Data are shown as average percent migration ±SD. ($n = 3$; $p < 0.05$).

Discussion

In Chapter 1 we demonstrated the induction of a phenotypic change in WM115 cells upon RAGE over-expression. WM115 cells acquired a mesenchymal like morphology after RAGE over-expression, which was analogous to the morphology of the WM266_MOCK cells. The epithelial to mesenchymal transition in cells leads to a loss of contact inhibition between the cells and hence enhances anchorage independent growth and motility of the cells [355, 356]. We proposed that the WM115 cells attained migratory features like those of WM266 cells after RAGE over-expression. The WM266 cell line was established from the same patient than the WM115 cell line, but derived from a metastatic tumor. Our results suggest a RAGE dependent increase in cell migration in the WM115 cells (Figure 16). The enhanced motility of the WM115_RAGE cells was demonstrated by both the wound healing assay (Figure 15) and the Boyden chamber assay (Figure 16). The presentations of the cells in the wound healing assay and in the Boyden chamber assay are quite different. In the wound healing assay, the cells crawl on the surface whereas in the Boyden chamber assay, the cells have to migrate through the pores of the filter in order to get access to the other side of the filter [357]. These two assays represent different mechanisms of cell migration in tumors. In primary tumors, cancer cells migrate linearly while still associated with basement membrane but in order for cancer cells to reach the blood vessels, they need to squeeze through the endothelial cell barrier and enter into the blood stream in order to metastasize to the distant organs [358]. Our results demonstrate that RAGE can not only enhance the crawling movement of WM115 cells but also enhance their motility across the barriers.

Our results also demonstrate a significant reduction in cell proliferation in the WM115_RAGE cells as compared to their MOCK counterparts in cell culture conditions (Figure

12). These data suggest that RAGE might act as a metastatic switch in melanoma cells. WM115, a primary melanoma cell line from vertical growth phase can switch to a less proliferative and more migratory phenotype upon RAGE over-expression. This switch might assist in metastatic spread of the cells. A state switching model for melanoma progression has been reported recently [20]. According to this model, melanoma cells can switch to a metastatic program and hence lose their proliferative features. After migration to a different location these cells switch back to their proliferative traits allowing the growth of the metastatic tumor. Back and forth switching of cells leads to a large heterogeneity in the melanoma cell population [20]. Here, RAGE seems to be one of the players in metastatic switching of melanoma cells. We have also shown an enhanced anchorage independent growth in the WM115 cells after RAGE over-expression suggesting a role of RAGE in melanoma tumor growth (Figure 13). The ability of cells to grow in a non-adherent environment correlates with their tumorigenic potential. Normal (non-cancerous) cells need a substrate to adhere, spread and grow. These cells are required to be attached to the tissue through cytoskeleton and extracellular matrix anchoring. These cells cannot survive in non-adherent conditions and undergo cell detachment induced apoptosis. This apoptotic phenomenon is a self-defense mechanism called anoikis. As shown in Figure 14 non-cancerous Hek 293 cells and their RAGE over-expressing counterparts could not develop colonies in anchorage independent conditions and eventually died. Tumor cells use different strategies to acquire anchorage independent proliferation potential [359, 360]. Epithelial–Mesenchymal transition (EMT) is one of the strategies for the cells to circumvent anoikis process [361, 362]. Our data show that RAGE enhances anchorage independent growth potential of WM115 cells which might translate into enhanced tumor growth potential of these cells.

In the next set of study, we demonstrated the effect of RAGE and its ligands (S100B and ribose-BSA AGE products) in melanoma cells migration. Our data from the migration assay show a dose dependent increase in the migration of WM115_MOCK cells after stimulation with AGE products. However, WM115_RAGE cells didn't respond to AGE stimulation. Our data suggest that RAGE has already been activated to its full capacity in the WM115_RAGE cells therefore, AGEs have no possibility to further activate these cells. AGE induced melanoma cell migration are in the agreement with previous study from another research group [133]. Contrary to this, stimulation with recombinant S100B had produced no effect on cell migration in both types of cells (Figure 17A). We suggest that S100B released from the transfected WM115 cells can activate RAGE, hence addition of recombinant S100B cannot further stimulate the cells. Another possibility is that extracellular S100B does not activate RAGE in melanoma cells. Moreover, IgG 2A11 could not suppress cell migration of either WM115_RAGE cells or AGE induced WM115_MOCK cells (Figure 17B). At this point, we do not know the precise mechanism of RAGE activation in WM115 cells.

Our results from this chapter suggest that RAGE, when over-expressed, triggers a metastatic like switch in the WM115 melanoma cell line. Furthermore, WM115_MOCK cells, with baseline levels of RAGE could be activated upon AGEs activation. However, WM115_RAGE cells with 100 fold higher levels of RAGE were constitutively activated and were insensitive towards AGEs activation. In the next chapter, we will decipher the RAGE induced mechanisms that are involved in melanoma progression.

CHAPTER 3. RAGE INDUCED MOLECULAR MECHANISMS INVOLVED IN MELANOMA CELL PROLIFERATION AND MIGRATION

Abstract

In Chapter 2 we showed an increase in WM115 cell migration/invasion and simultaneous decrease in WM115 cell proliferation after RAGE over-expression. In this chapter we have assessed RAGE mediated downstream signaling mechanisms involved in the switching process. Expression of RAGE ligands (S100A2, S100A4, S100A6, S100A10 and S100B) that are relevant in melanoma pathophysiology were assessed in the transfected melanoma cells. S100B was found to be upregulated in WM115 cells after RAGE over-expression. Also, higher levels of S100B protein were found in WM115_RAGE cells supernatant compared to its MOCK counterpart. S100A6 and S100A10 proteins were found unchanged in the WM115 cells after RAGE over-expression. S100A2 and S100A4 proteins were detected neither in WM115_MOCK cells nor in WM115_RAGE cells. Furthermore, we observed the downregulation of one of the S100B target protein (p53) in the WM115_RAGE cells compared to the WM115_MOCK cells. We used a gene array to identify genes that were up- or down regulated in WM115 cells upon RAGE over-expression. We observed a downregulation in cyclin E transcripts in WM115_RAGE cells. Downregulation of cyclin E protein in the transfected WM115 cells was confirmed by Western blot and flow cytometry. We assessed the expression of cyclin E in different phases of the cell cycle. Cyclin E expression was significantly reduced in all the cell cycle stages of WM115_RAGE cells compared to MOCK control cells. However, no difference in the percentage of cells in each cell cycle stage was found between WM115_MOCK and WM115_RAGE cells. To decipher the downstream mechanisms of RAGE involved in melanoma progression we have studied three major signaling pathways that were previously shown to be

activated by RAGE. We assessed AKT, ERK and NF-□B signaling activities in the WM115_MOCK and WM115_RAGE cells. We found a reduced NF-□B activity in the WM115_RAGE cells compared to MOCK cells. Also, a reduced phosphorylated level of ERK was also found in the WM115_RAGE cells as compared to their MOCK counterparts. Phosphorylated AKT was not affected by RAGE over-expression.

Introduction

RAGE triggers a wide range of signaling pathways depending upon the type of cell and the ligands involved. RAGE interacts with different structurally and functionally diverse ligands, which is one of the unique features of RAGE [79]. S100B is one of the best characterized ligands of RAGE, and has been suggested to be an important player in melanoma pathogenesis. S100B is small Ca^{+2} binding protein of the EF hand superfamily that resides in the cytoplasm and can also be released in the extracellular milieu [109]. Within the cell, S100B protein interacts with multiple target proteins and can regulate cell morphology, motility, proliferation, metabolism and certain signaling cascades [109]. The tumor suppressor p53 protein is one of the intracellular target proteins of S100B protein in melanoma cells. Interaction of S100B with p53 inhibits oligomerization and phosphorylation of p53 which is important for its transcriptional and tumor suppressive activities. S100B can also downregulate p53 protein in melanoma cells [217-219]. Inhibitors for S100B–p53 interaction have shown their therapeutic potentials in melanoma treatment in several murine models of melanoma [220]. S100B protein is also released from melanoma cells and tumors. Serum concentration of S100B increases during melanoma progression and is used as a prognostic biomarker for melanoma [6]. Upon release S100B protein could interact with extracellular domain of RAGE and initiate downstream signaling cascades [109]. Engagement of RAGE with its ligands has been shown to activate several

signaling pathways such as the JNK/SAPK [87], MAPK [121], cdc42/rac, $P21^{ras}$ [144] and NF-□B [121] pathways and to modulate diverse cellular functions. RAGE induced signaling can be suppressed by blocking RAGE-ligand interaction with anti-RAGE antibody [133]. In this chapter, we have investigated RAGE induced signaling mechanisms involved in melanoma progression.

Materials and Methods

Ligand gene array

RNAs from transfected WM115 and WM266 cells were extracted using the commercially available PARIS kit (Ambion Life Sciences, USA). Extracted RNAs were quantified by measuring their absorbance at 260nm. Furthermore, RNA quality was assessed by running them on 1% agarose gel. RNAs with two intact bands corresponding to 28S and 18S of ribosomal RNA, were used for further studies. The RNAs were reverse transcribed (200ng of RNA) using the reverse transcription system (Promega, WI) as per manufacturer's instructions. The cDNAs were run on a Mx3000 Stratagene thermocycler using Brilliant II Ultra fast SYBER Green QPCR Master mix and the appropriate primer pairs for each gene. The list of primers used is given in Table 6. We used four housekeeping genes (β actin, Glyceraldehyde 3-phosphate dehydrogenase, Phospho glycerate kinase and S18) in the array. Proteins encoded by these genes are relatively stable and are constitutively expressed in high levels in most cells and tissues. These are the most important characteristics of housekeeping genes. Glyceraldehyde 3-phosphate dehydrogenase and Phospho glycerate kinase are the enzymes involved in the glycolysis process within the cell. The β actin is a cell structural protein and is one of the major constituents of the contractile apparatus and cytoskeleton. S18 is a ribosomal protein and one of the core components of the small subunit of eukaryotic RNA. Each RT_PCR experiment was repeated

with three independent sets of RNAs. In order to study the molecular mechanisms of RAGE in melanoma progression we have assessed the transcript levels of 84 genes involved in tumorigenesis in WM115_MOCK and WM115_RAGE cells.

Table 6: Primers used in all the RT_PCR experiments.

Gene	Primer sequence	Gene Bank accession number
Rev_β-Actin	CTCCTTAATGTCACGCACGAT	NM_001101
Fwd_ β-Actin	CATGTACGTTGCTATCCAGGC	NM_001101
Fwd_S100A1	GACCCTCATCAACGTGTTCCA	NM_006271
Rev_S100A1	CCACAAGCACCACATACTCCT	NM_006271
Fwd_S100A2	CACTACCTTCCACAAGTACT	NM_005978
Rev_S100A2	GAAGTCATTGCACATGAC	NM_005978
Fwd_S100A3	GCAGGCGGTAGCTGCCATC	NM_002960
Rev_S100A3	TTGAAGTACTCGTGGCAGTAG	NM_002960
Fwd_S100A4	CAAGTACTCGGGCAAAGAGG	NM_002961
Rev_S100A4	CTTCCTGGGCTGCTTATCTG	NM_002961
Fwd_S100A5	CACTATGGTGACCACGTTTCA	NM_014624
Rev_S100A5	TCCCCAAGACACAGCTCTTTC	NM_014624
Fwd_S100A6	GGACCGCTATAAGGCCAGTC	NM_014624
Rev_S100A6	GGTCCAAGTCTTCCATCAGC	NM_014624
Fwd_S100A7	ACGTGATGACAAGATTGACAAGC	NM_002963
Rev_S100A7	GCGAGGTAATTTGTGCCCTTT	NM_002963
Fwd_S100A8	TGATAAAGGGGAATTTCCATGCC	NM_002964
Rev_S100A8	ACACTCGGTCTCTAGCAATTTCT	NM_002964
Fwd_S100A9	GGTCATAGAACACATCATGGAGG	NM_002965
Rev_S100A9	GGCCTGGGCTTATGGTGGTG	NM_002965
Fwd_S100A10	AAAGACCCTCTGGCTGTGG	NM_002966
Rev_S100A10	AATCCTTCTATGGGGGAAGC	NM_002966
Fwd_S100A11	CTGAGCGGTGCATCGAGTC	NM_005620
Rev_S100A11	TGTGAAGGCAGCTAGTTCTGTA	NM_005620
Fwd_S100A12	AGCATCTGGAGGGAATTGTCA	NM_005621
Rev_S100A12	GCAATGGCTACCAGGGATATGAA	NM_005621
Fwd_S100A13	ACCACCTTCTTCACCTTTGC	NM_005979
Rev_S100A13	AGGCGGCTTTACTTCTTCCT	NM_005979
Fwd_S100A14	CATGAGCCATCAGCTCCTCT	NM_020672
Rev_S100A14	TTCTCTTCCAGGCCACAGTT	NM_020672
Fwd_S100A16	ATGTCAGACTGCTACACGGAG	NM_080388
Rev_S100A16	TTCTGGATGAGCTTATCCGCA	NM_080388

Table 6: Primers used in all the RT_PCR experiments (continued).

Fwd_S100B	TGGCCCTCATCGACGTTTTG	NM_006272
Rev_S100B	CAGTGTTTCCATGACTTTGTCCA	NM_006272
Fwd_S100P	ATGACGGAACTAGAGACAGCC	NM_005980
Rev_S100P	AGGAAGCCTGGTAGCTCCTT	NM_005980
Fwd_S100Z	TGGAGTGGTCAGTTCTGCTG	NM_130772
Rev_S100Z	CATCCAGGTCCTGCACTATCTTA	NM_130772
Fwd_S100G	CTATTGGGCAACCAGACACC	NM_004057
Rev_S100G	TCTCCATCTCCATTCTTGTCC	NM_004057
Fwd_HMGB-1	GGTGCATTGGGATCCTTGAA	NM_002128.4
Rev_HMGB-1	GCTCAGAGAGGTGGAAGACCA	NM_002128.4
Rev_RAGE	TGTGTGGCCACCCATTCCAG	NM_001136
Fwd_RAGE	GCCCTCCAGTACTACTCTCG	NM_001136
Rev_TNF	GAGGACCTGGGAGTAGATGAG	NM_000594
Fwd_TNF	CCTCTCTCTAATCAGCCCTCTG	NM_000594
Rev_VEGFa	AGGGTCTCGATTGGATGGCA	NM001204384
Fwd_VEGFa	AGGGCAGAATCATCACGAAGT	NM001204384
Rev_TSP-1	TCACCACGTTGTTGTCAAGGG	NM_0032446
Fwd_TSP-1	AGACTCCGCATCGCAAAGG	NM_0032446
Rev_TGF-β	GCACATACAAACGGCCTATCTC	NM_004612
Fwd_TGF-β	ACGGCGTTACAGTGTTTCTG	NM_004612
Rev_Tek	GGGGCACTGAATGGATGAAG	NM_000549
Fwd_Tek	CAGGATACGAACCATGAAGATGC	NM_000549
Rev_PDGF-β	CGTTGGTGCGGTCTATGAG	NM_002608
Fwd_ PDGF-β	CTCGATCCGCTCCTTTGATGA	NM_002608
Rev_PDGF-α	GGCACTTGACACTGCTCGT	NM_002607
Fwd_PDGF-α	GCAAGACCAGGACGGTCATTT	NM_002607
Rev_IL-8	AACCCTCTGCACCCAGTTTTC	NM_000584
Fwd_IL-8	TTTTGCCAAGGAGTGCTAAAGA	NM_000584
Rev_IGFR	GAACTGAAGAGCATCCACCA	NM_000618
Fwd_IGFR	ATGTCCTCCTCGCATCTCTT	NM_000618
Rev_INF-α	CTGTGGGTCTCAGGGAGATCA	NM_024013
Fwd_INF-α	GCCTCGCCCTTTGCTTTACT	NM_024013
Rev_INF-β	ATAGATGGTCAATGCGGCGTC	NM_002176
Fwd_INF-β	GCTTGGATTCCTACAAAGAAGCA	NM_002176
Rev_FGFR	AGATGGGACCACACTTTCCATA	NM_023029
Fwd_FGFR	GGTGGCTGAAAAACGGGATG	NM_023029
Rev_Cola	CCCATCTGAGTCATCGCCTT	NM_009929
Fwd_Cola	GTTCCAGAGAATGCCGCTTG	NM_009929
Rev_Angp1	TCTCCGACTTCATGTTTTCCAC	NM_001146
Fwd_Angp1	TCGTGAGAGTACGACAGACCA	NM_001146
Rev_Angp2	CGAGTCATCGTATTCGAGCGG	NM_001147
Fwd_Angp2	AACTTTCGGAAGAGCATGGAC	NM_001147

A commercially available gene array including 84 genes representative of the six biological pathways of tumorigenesis, five housekeeping genes (Beta-2-microglobulin, Hypoxanthine phosphoribosyltransferase 1, Ribosomal protein L13a, Glyceraldehyde-3-phosphate dehydrogenase, beta Actin) and negative/positive controls were used in the study. The expression of the genes were assessed using Brilliant II Ultra-fast SYBER Green QPCR Master mix (Agilent Technologies) on a Mx3000 Stratagene RT_PCR system as described in Chapter 1. Since we did not observe any differences in the different housekeeping genes' expression levels, the data obtained were analyzed with respect to β actin only. The melting curves were recorded for each gene in order to determine the quality of the amplified product and the specificity of the amplification. The cancer pathway array was performed with only one set of WM115_MOCK and WM115_RAGE cells cDNAs. Later, we have repeated the array with 15 genes associated with angiogenesis process using primers specific for those genes, obtained from the primer bank.

Western blot analysis

Cell Protein lysates were prepared using the PARIS kit (Ambion Life Sciences, USA) as per manufacturer's instructions. 40µg to 100µg of proteins were resolved on 12% to 15% SDS gels and blotted onto nitrocellulose membranes. After overnight blocking with 4% BSA/TBS at 4°C, the blotted membranes were incubated with specific antibodies (Table 7) diluted in 1% BSA/TBS/0.1% tween for 1 hour at room temperature. The blots were developed using a chemoluminescent substrate (ThermoScientific, IL, USA). The data obtained were analyzed by densiometric analysis using the Image-J software. The Western blot experiments were performed three independent times.

Table 7: Specifications of all antibodies used in the study.

Antibodies	Source	Catalog No.	Concentration
Mouse monoclonal anti β actin	Sigma	A2228	1:1000
Rabbit polyclonal anti S100B	Dako	N1573	1:1000
Mouse monoclonal anti-S100B	R & D Sys	MAB1820	1:100
Rabbit serum anti S100A1	Dako	-	1:1000
Rabbit serum anti S100A2	Dako	-	1:1000
Rabbit serum anti S100A4	Dako	-	1:1000
Rabbit serum anti S100A6	Dako	-	1:1000
Mouse monoclonal anti S100A10	Cell Signaling Technologies	4E7E10	1:1000
Mouse monoclonal anti S100A11	Abcam	H00006282-M01	1:1000
Mouse monoclonal anti S100A8	Abnova	H00006279-AP51	1:250
Mouse monoclonal anti S100A9	Abnova	H00006280-AP11	1:250
Mouse monoclonal anti S100A13	Abnova	H00006284-M01	1:250
Mouse monoclonal anti S100A16	Abnova	ab130419	1:250
Mouse monoclonal anti HMGB-1	Abnova	H00003146-M01	1:250
Rabbit monoclonal anti-AKT	Cell Signaling Technologies	C67E7	1:1000
Rabbit monoclonal anti-p-AKT	Cell Signaling Technologies	C31E5E	1:1000
Rabbit monoclonal anti-JNK/SAPK	Cell Signaling Technologies	56G8	1:1000
Rabbit monoclonal anti-p-JNK/SAPK	Cell Signaling Technologies	81E11	1:1000

Table 7: Specifications of all antibodies used in the study (continued).

Rabbit monoclonal anti-MAPK	Cell Signaling Technologies	137F5	1:1000
Rabbit monoclonal anti-p-MAPK	Cell Signaling Technologies		1:1000
Goat polyclonal anti p53	Santa Cruz	Sc-7997	1: 200
Mouse monoclonal anti cyclin E	Santa Cruz	Sc-247	1: 200
Alkaline phosphatase conjugated goat anti mouse F $(ab)_2'$	Jackson ImmunoResearch	115-055-072	1:1000
HRP conjugated donkey anti rabbit IgG	Jackson ImmunoResearch	711-035-152	1:1000
HRP conjugated goat anti mouse IgG	Jackson ImmunoResearch	115-035-174	1:1000
HRP conjugated horse anti goat IgG	Vector labs	PI-9500	1:500

Table 8: Cancer pathway gene array in WM115_MOCK and WM115_RAGE cells. Data were analyzed using β-actin as housekeeping gene. (n=1).

No.	**Genes**	**Fold change**	**Functional role**
1.	Integrin, alpha 1	-2.4	Cell Adhesion
2.	Integrin, alpha 2 (CD49B, alpha 2 subunit of VLA-2 receptor)	1.6	
3.	Integrin, alpha 3 (antigen CD49C, alpha 3 subunit of VLA-3 receptor)	3.1	

Table 8: Cancer pathway gene array in WM115_MOCK and WM115_RAGE cells. Data were analyzed using β-actin as housekeeping gene. (n=1) (continued).

4.	Integrin, alpha 4 (antigen CD49D, alpha 4 subunit of VLA-4 receptor)	-2.5	
5.	Integrin, alpha V (vitronectin receptor, alpha polypeptide, antigen CD51)	2.9	
6.	Integrin, beta 1 (fibronectin receptor, beta polypeptide, antigen CD29 includes MDF2, MSK12	1.4	
7.	Integrin, beta 3 (platelet glycoprotein IIIa, antigen CD61)	1.2	
8.	Integrin, beta 5	-2	
9.	Melanoma cell adhesion molecule	-1.9	
10.	Metastasis suppressor 1	-2.1	
11.	Pinin, desmosome associated protein	1.2	
12.	Synuclein, gamma (breast cancer-specific protein 1)		
13.	Angiopoietin 1	1.6	Angiogenesis
14.	Angiopoietin 2	1.3	
15.	Collagen, type XVIII, alpha 1	1.8	
16.	Fibroblast growth factor receptor 2	-4.3	
17.	Interferon, alpha 1	-1.3	
18.	Interferon, beta 1, fibroblast	1.1	
19.	Insulin-like growth factor 1 (somatomedin C)	1.1	
20.	Interleukin 8	-2.1	
21.	Platelet-derived growth factor alpha polypeptide	1.4	

Table 8: Cancer pathway gene array in WM115_MOCK and WM115_RAGE cells. Data were analyzed using β-actin as housekeeping gene. (n=1) (continued).

22.	Platelet-derived growth factor beta polypeptide	8.4	
23.	TEK tyrosine kinase, endothelial	1.5	
24.	Transforming growth factor, beta 1	1.1	
25.	Transforming growth factor, beta receptor 1	-1.5	
26.	Thrombospondin 1	-1.3	
27.	Tumor necrosis factor	-2.8	
28.	Vascular endothelial growth factor A	-1.1	
29.	Met proto-oncogene (hepatocyte growth factor receptor)	-2.4	Invasion and Metastasis
30.	Matrix metallopeptidase 1 (interstitial collagenase)	1.3	
31.	Matrix metallopeptidase 2 (gelatinase A, 72kDa gelatinase, 72kDa type IV collagenase)	1.4	
32.	Matrix metallopeptidase 9 (gelatinase B, 92kDa gelatinase, 92kDa type IV collagenase)	1.1	
33.	Metastasis associated 1	-2.4	
34.	Metastasis associated 1 family, member 2	-1.2	
35.	Non-metastatic cells 1, protein (NM23A) expressed in	1.2	
36.	Non-metastatic cells 4, protein expressed in	1.1	
37.	Plasminogen activator, urokinase	1.2	
38.	Plasminogen activator, urokinase receptor	-1.3	
39.	S100 calcium binding protein A4	1.6	

Table 8: Cancer pathway gene array in WM115_MOCK and WM115_RAGE cells. Data were analyzed using β-actin as housekeeping gene. (n=1) (continued).

40.	Serpin peptidase inhibitor, clade B (ovalbumin), member 5	-1.1	
41.	Serpin peptidase inhibitor, clade E (nexin, plasminogen activator inhibitor type 1), member 1	-3.4	
42.	TIMP metallopeptidase inhibitor 1	-1.1	
43.	TIMP metallopeptidase inhibitor 3	1.1	
44.	Twist homolog 1 (Drosophila)	-1.1	
45.	Apoptotic peptidase activating factor 1	-1.3	Apoptosis and Cell Senescence
46.	BCL2-associated agonist of cell death	1.3	
47.	BCL2-associated X protein	-1.3	
48.	B-cell CLL/lymphoma 2	-4.2	
49.	BCL2-like 1	-1.1	
50.	Caspase 8, apoptosis-related cysteine peptidase	1.5	
51.	CASP8 and FADD-like apoptosis regulator	1.1	
52.	Fas (TNF receptor superfamily, member 6)	1.5	
53.	Granzyme A (granzyme 1, cytotoxic T-lymphocyte-associated serine esterase 3	-1.5	
54.	HIV-1 Tat interactive protein 2, 30kDa	-1.5	
55.	Telomerase reverse transcriptase	-1.6	
56.	Tumor necrosis factor receptor superfamily, member 1A	1.3	
57.	Tumor necrosis factor receptor superfamily, member 25	-1.4	
58.	Tumor necrosis factor receptor superfamily, member 10b	-1.3	

Table 8: Cancer pathway gene array in WM115_MOCK and WM115_RAGE cells. Data were analyzed using β-actin as housekeeping gene. (n=1) (continued).

59.	Ataxia telangiectasia mutated	-2.2	Cell Cycle Control & DNA Damage Repair
60.	Breast cancer 1, early onset	-1.4	
61.	Cyclin E1	2.1	
62.	Cell division cycle 25 homolog A (S. pombe)	-1.4	
63.	Cyclin-dependent kinase 2	1.2	
64.	Cyclin-dependent kinase 4	-1.4	
65.	Cyclin-dependent kinase inhibitor 1A (p21, Cip1)	-1.0	
66.	Cyclin-dependent kinase inhibitor 2A (melanoma, p16, inhibits CDK4)	1.7	
67.	CHK2 checkpoint homolog (S. pombe)	-1.1	
68.	E2F transcription factor 1	-1.3	
69.	Mdm2 p53 binding protein homolog (mouse)	-1.8	
70.	Retinoblastoma 1	-1.1	
71.	S100 calcium binding protein A4	1.6	
72.	Tumor protein p53	-2.4	
73.	V-AKT murine thymoma viral oncogene homolog 1	-2.6	Signal Transduction Molecules and Transcription Factors
74.	V-erb-b2 erythroblastic leukemia viral oncogene homolog 2, neuro/glioblastoma derived oncogene homolog (avian)	-1.2	
75.	V-Ets erythroblastosis virus E26 oncogene homolog 2 (avian)	-3.8	

Table 8: Cancer pathway gene array in WM115_MOCK and WM115_RAGE cells. Data were analyzed using β-actin as housekeeping gene. (n=1) (continued).

76.	FBJ murine osteosarcoma viral oncogene homolog	-1.4	
77.	Jun proto-oncogene	-1.2	
78.	Mitogen-activated protein kinase kinase 1	-1.8	
79.	V-myc myelocytomatosis viral oncogene homolog (avian)	-1.3	
80.	Nuclear factor of kappa light polypeptide gene enhancer in B-cells 1	0	
81.	Nuclear factor of kappa light polypeptide gene enhancer in B-cells inhibitor, alpha	-3.8	
82.	Phosphoinositide-3-kinase, regulatory subunit 1 (alpha)	1.9	
83.	V-raf-1 murine leukemia viral oncogene homolog 1	1.4	
84.	Synuclein, gamma (breast cancer-specific protein 1)	-1.2	

Table 9: PCR gene array with angiogenesis associated genes in the transfected WM115 cells. Expression of fifteen selective genes associated with angiogenesis were assessed using appropriate primer pairs and WM115_MOCK and WM115_RAGE cells' cDNAs as templates. Experiment was performed at least three times with three independent sets of cDNAs. Data are shown as Mean ± SD (n = 3; **p < 0.01; *p < 0.05).

Number	Genes	Average fold change ± SD
1.	Angiopoietin 1	2.0 ± 0.3
2.	Angiopoietin 2	2.6 ± 0.4
3.	Collagen, type XVIII, alpha 1	0.4 ± 2.1
4.	Fibroblast growth factor receptor 2	0
5.	Interferon, alpha 1	-0.2 ± 2.5
6.	Interferon, beta 1, fibroblast	1.3 ± 2.9
7.	Insulin-like growth factor 1 (somatomedin C)	-2.3 ± 0.7
8.	Interleukin 8	-2.5 ± 0.5
9.	Platelet-derived growth factor alpha polypeptide	1.3 ± 0.1
10.	Platelet-derived growth factor beta polypeptide	4.2 ± 0.4*
11.	TEK tyrosine kinase, endothelial	-2.2 ± 0.9
12.	Transforming growth factor, beta 1	0.7 ± 2.0
13.	Vascular endothelial growth factor A	0.8 ± 1.7
14.	Tumor necrosis factor	-2.1 ± 0.7
15.	Thrombospondin 1	1.1 ± 0.1

Detection of S100B by ELISA

Equal numbers of both MOCK and RAGE transfected WM115 cells were seeded into the wells of six well plates with constant volume of media. After 3 days of incubation, the cell supernatants were collected and concentrated to $1/10^{th}$ of their initial volumes using Nanosep centrifugal devices with 3000 molecular weight cutoff filter (Pall Corporation, Washington, NY). The corresponding cells were lysed as described in the Western blot analysis section. For the

ELISA, 1/1000 dilution of polyclonal anti-S100B antibody (Dako, Agilent Technologies) was coated on ELISA plates overnight at 4°C. Subsequently, the plates were blocked with 3% BSA/TBS for 1 hour at room temperature. As a standard, a serial dilution of recombinant S100B was prepared in TBS. In the next step, 50µl of standard S100B dilutions, cell lysates and cell supernatants were added in their respective wells and incubated for 1 hour. Next, the wells were incubated with 1/100 dilution of monoclonal anti-S100B (R& D system) antibody for 1 hour. After three times washing with TBS-tween, the wells were incubated with AP conjugated secondary antibody (Jackson ImmunoReserach) for 30 mins. In the final step, 1 mg/ml of the AP substrate (4-Nitrophenyl Phosphate) (Gold Biotechnologies) was added in each well and the absorbance was measured at 405nm.

NF-□B Luciferase assay

In this assay, we transiently transfected WM115_MOCK and WM115_RAGE cells with a NF-□B responsive luciferase construct that encoded the firefly luciferase reporter gene under the control of a NF-κB transcriptional response element. MAP kinase kinase kinase (MEKK), an upstream signaling molecule of NF-□B that hyperactivates NF-□B signaling [363] was co-transfected and used as a positive control. Transfection of the plasmid encoding the Green Fluorescence Protein (GFP) was used to determine the transfection efficiency. Ten different fields of GFP transfected cells were imaged and manually counted in order to estimate the percentage of transfection. Following the transfection, the cells were lysed with a reporter lysis buffer (Promega, WI, USA). The luciferase activity in the cell lysates was quantified by mixing 100µl Luciferin substrate (Promega, USA) with 10µlof cell lysates and the generated luminescence was measured immediately on a Quick Pak luminometer.

siRNA transfection

siRNA against RAGE and S100B were obtained from Santa Cruz, USA. WM115_RAGE cells were seeded in the wells of 6 well plates and incubated until they reached 60-70% confluency. The cells were transiently transfected with siRNA against either S100B or RAGE as per manufacturer's instructions. As a control, cells were transfected with scramble siRNA. After 72 hours incubation, both RNAs and proteins were extracted from the transfected cells using methods described previously. Suppression of the target proteins were assessed both at the transcript and protein levels by Real Time PCR and ELISA as described in their respective sections.

Cell Cycle analysis

In brief, both MOCK and RAGE transfected WM115 cells were harvested using a sterile scrapper after they reached 70-80% confluence. The cells were fixed with 70% ice cold ethanol for 30 mins. After washing with PBS, the cells were permeabilized with 0.25% triton X-100 for 5 mins. After another washing step, the cells were blocked with 3% goat serum for 1 hour. After blocking, the cells were incubated with 5 µg/ml of mouse anti-cyclin E antibody in 1% goat serum in PBS for 45 mins. After another washing step, the cells were incubated with 1/200 of FITC conjugated goat anti-mouse IgG for 30 mins and subsequently washed three times. Prior to PI staining, the cells were treated with 10µl of 10 mg/ml of ribonuclease for 5 mins to avoid double-stranded RNAs staining. After ribonuclease treatment the cells were immediately treated with 50µg/ml of PI. The DNA content and cyclin E expression levels were assessed simultaneously using the FL-1 and FL-2 filters on an Accuri C6 flow cytometer. The data was analyzed using the Flowjo software (TreeStar Inc.)

Statistical Analysis

Data are shown either as Mean ± SEM or Mean ± SD. Comparative analysis between two groups was made by one tail two sample (unpaired) Student's t- test and $p < 0.05$ was considered as significant.

Results

Over-expression of RAGE leads to upregulation of S100B protein

The major goal of this study was to investigate the influence of RAGE over-expression on S100 protein expression in WM115 cells. We found a 3 fold upregulation of S100B in WM115_RAGE (301.2 ± 30.0 nM) cells compared to the MOCK (109.7 ± 11.4 nM) counterparts. S100B protein was also detected in higher levels in the cell supernatants of RAGE cells (27.52 ± 6.0 nM) than in MOCK cells (5.9 ± 3.6 nM) (Table 10). The expression of S100B in WM115_RAGE cells was equivalent to that of WM266_MOCK cells (Figure 18B). The expression of the S100A6 and S100A10 proteins did not change upon RAGE over-expression (Figure 19). Moreover, the S100A2 and S100A4 proteins were not detectable in our experimental conditions in either WM115_MOCK or in WM15_RAGE cells (data not shown).

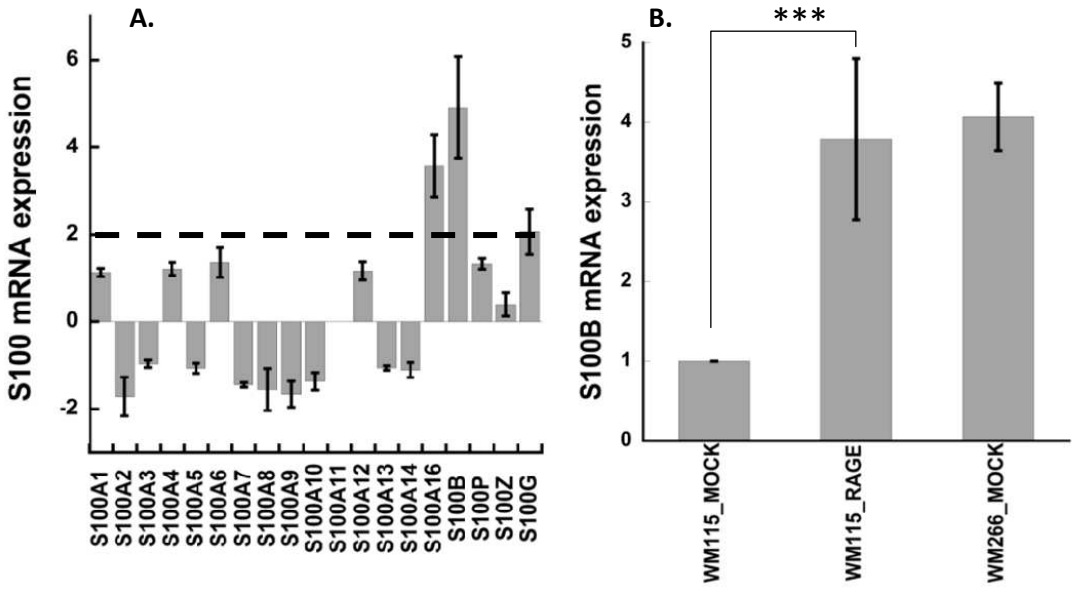

Figure 18: S100 mRNA expression in the transfected WM115 cells by RT_PCR. (A.) Average fold change above the dotted line (cut off value 2) were discussed. (n =3; *p < 0.05).

S100B mRNA expression in WM115_MOCK, WM115_RAGE and WM266_MOCK cells by RT_ PCR (B.). Experiment was performed with at least three independent sets of cDNAs. (n > 3; *p < 0.05).

Table 10: S100B protein concentration in WM115_MOCK, WM115_RAGE cell lysate and cell supernatant by ELISA. ELISA experiments were performed in triplicates with three independent sets of protein lysates. Data represented as Mean ± SD. (n=3; p < 0.05).

Samples	S100B concentration (nM)
WM115_MOCK cell supernatant	6.0 ± 3.7
WM115_RAGE cell supernatant	27.5 ± 6.1
WM115_MOCK cell lysate	109.8 ± 11.4
WM115_RAGE cell lysate	301.2 ± 93.8

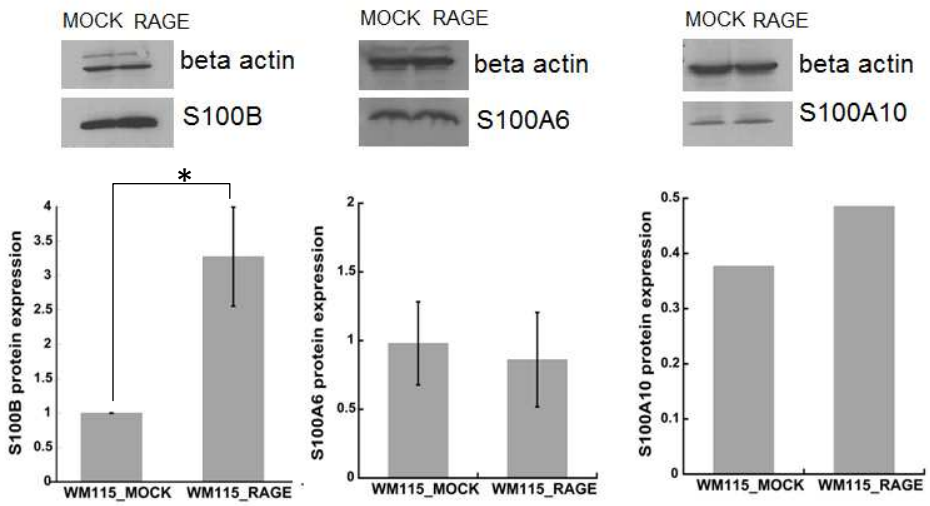

Figure 19: S100B, S100A6 and S100A10 proteins expression in WM115_MOCK and WM115_RAGE cell lysates by Western blot. The graphs represent densitometric analysis of the blots by Image J software. Experiment was performed three independent times (n= 3; *p < 0.05).

p53 and cyclin E are downregulated whereas PDGF-β is upregulated in WM115_RAGE cells

From the Cancer pathway PCR array we found a 2.1 and a 2.4 fold downregulation in p53 and cyclin E respectively at the transcript levels in WM115_RAGE cells as compared to MOCK cells. We also observed an 8.4 fold upregulation in the transcript levels of PDGF-β in the WM115 cells after RAGE over-expression. Following the initial analysis of the cancer pathway PCR array, we chose 15 genes that are involved in the angiogenesis for further investigation. Since genes associated with angiogenesis were highly affected with RAGE over-expression in WM115 cells, we repeated the analysis of the expression of these genes by RT_PCR using sets of primers specific for these genes. Upon repetition, we demonstrated a 4 fold upregulation of PDGF-β in WM115_RAGE cells compared to MOCK cells. To further confirm the expression of p53 and cyclin E at protein levels, Western blots were performed in the cells lysates of WM115_MOCK and the WM115_RAGE cells. The expression of p53 and cyclin E proteins

were found to be significantly reduced in the WM115_RAGE cells compared to MOCK cells (Figure 20). The changes in the expression of cyclin E were further confirmed by flow cytometry. The flow cytometry data showed a significant downregulation in cyclin E protein in all the phases of the cell cycle in WM115_RAGE cells compared to WM115_MOCK cells (Figure 21 & 22).

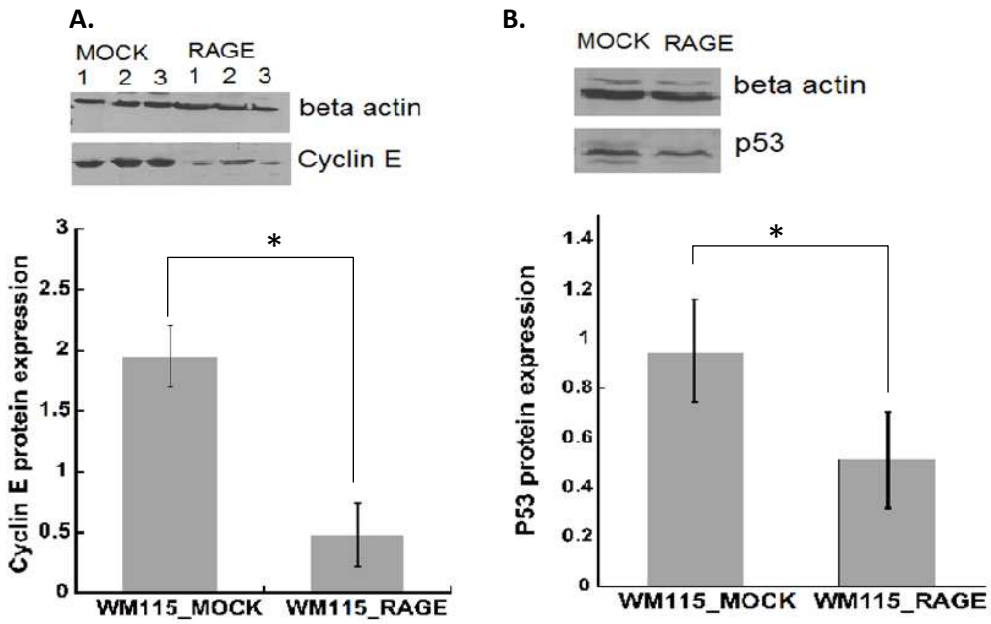

Figure 20: Cyclin E and p53 protein expression in WM115_MOCK and WM115_RAGE cell lysates as determined by Western blot. (A). Cyclin E protein expression in three sets of cell lysates from WM115_MOCK and WM115_RAGE (B).p53 protein expression in WM115_MOCK and WM115_RAGE cell lysates. Each Western blot experiment was performed in triplicate with three independent sets of cell lysates. The graphs represent the densitometric analysis of the corresponding blots. Mean ± SD (n= 3; *$p < 0.05$).

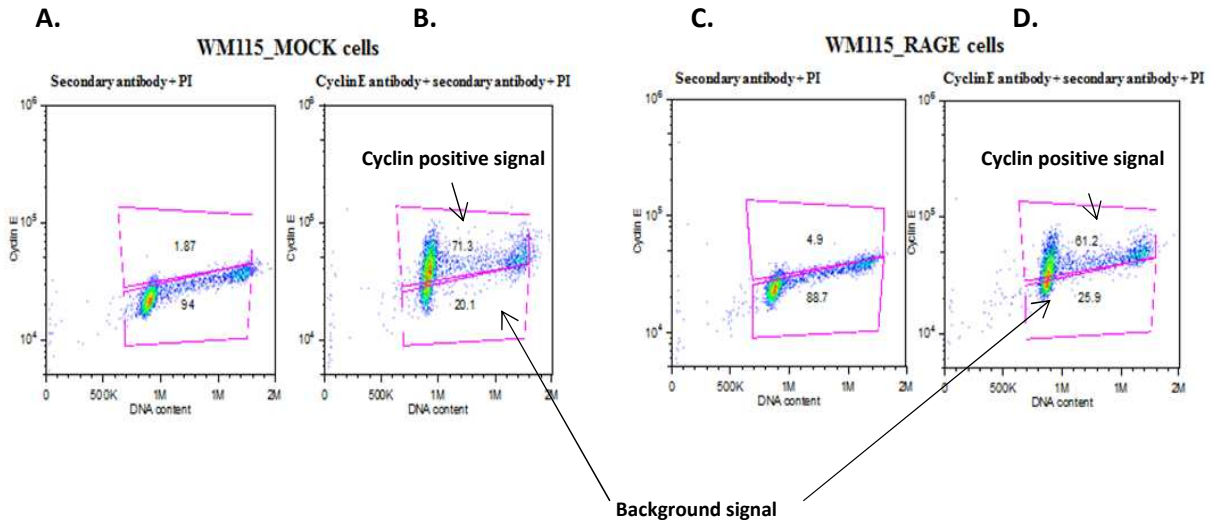

Figure 21: Expression of Cyclin E protein in different cell cycle phases of the WM115_MOCK (A,B) and WM115_RAGE cells (C,D). WM115_MOCK (A.) and WM115_RAGE (C.) cells stained with PI and FITC conjugated secondary antibody. WM115_MOCK (B.) and WM115_RAGE (D.) cells stained with antibody against Cyclin E, FITC conjugated secondary antibody and PI. Background fluorescence was gated in the lower chamber of the graph. The upper chamber of the graph shows Cyclin E expression in the cells in different phases of cell cycle. Experiment was performed three times in triplicate. (n= 3).

Table 11: Percentage of WM115_MOCK and WM115_RAGE cells in different phases of the cell cycle.

siRNA transfection	G1 Phase	S Phase	G2/M phase
WM115_MOCK	78.0 %	13.7 %	9.6 %
WM115_RAGE	72.5 %	16.0 %	9.0 %

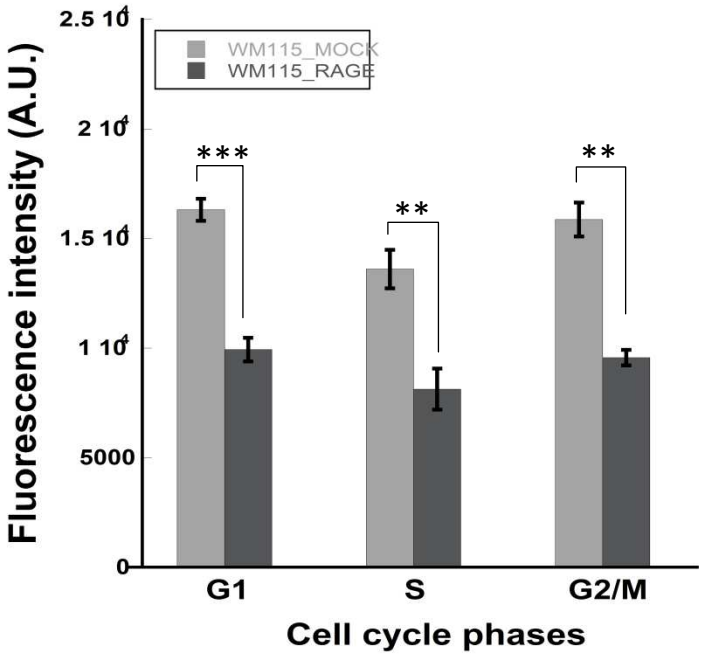

Figure 22: Cyclin E protein expression in different phases of the cell cycle. Experiments were performed three times in triplicate. (n = 3; ***p < 0.001, **p < 0.01).

NF-□B and ERK activities were suppressed whereas AKT activity was unchanged after RAGE over-expression in WM115 cells

RAGE mediated signaling cascades were analyzed by Western blot and NF-□B luciferase assay. The NF-□B luciferase assay results showed a reduced luciferase activity in the WM115_RAGE cell lysates compared to the MOCK cells. Since the gene encoding luciferase in the transfected cells was under the control of NF-□B transcription elements, therefore, the activities of the luciferase enzyme directly reflected the extent of NF-□B activation in these cells. Our results showed a reduced NF-□B activities in the WM115 cells over-expressing RAGE (Figure 23). AKT and ERK activities were assessed by determining the extent of AKT and ERK phosphorylation in the WM115_MOCK and WM115_RAGE cells by Western blot.

We found reduced levels of phosphorylation of ERK in the WM115_RAGE cells as compared to MOCK control cells whereas AKT phosphorylation was found to be unaltered (Figure 24).

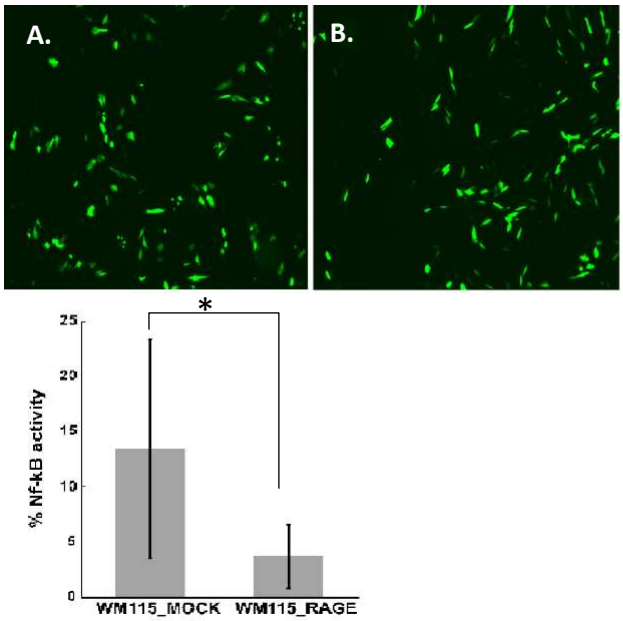

Figure 23: NF-□B activity in WM115_MOCK and WM115_RAGE cells by NF-□B luciferase assay. Figure shows WM115_MOCK (A.) and WM115_RAGE (B.) cells transfected with GFP as transfection control. Graph shows percentage of NF-□B activities in both cells with respect to MEKK positive control. Experiment was performed twice in triplicate (n= 2; *$p < 0.05$).

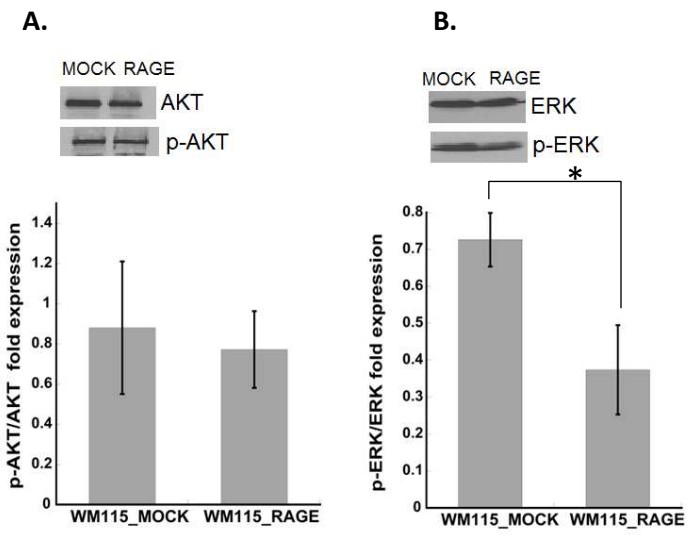

Figure 24: Phosphorylated levels of AKT (A.) and ERK (B.) in the WM115_MOCK and WM115_RAGE cells as determined by Western blot. The graphs represent the densitometric analysis of the corresponding blots. The experiment was performed with three independent sets of protein lysates three independent times ($n = 3$; $*p < 0.05$).

Reduced migration of WM115_RAGE cells upon suppression of RAGE using RAGE specific siRNA

WM115_RAGE cells were transiently transfected with RAGE specific siRNA to suppress the expression of RAGE in these cells. As controls, the set of WM115_RAGE cells were transfected with scramble siRNA. RAGE siRNA transfection in WM115_RAGE cells led to 2.5 fold suppression of RAGE at the protein level compared to the cells transfected with the scramble siRNA (Table 12). Suppression of RAGE resulted in significant increase in proliferation of the WM115_RAGE cells. Moreover, RAGE suppression in the WM115_RAGE cells resulted in a significant reduction in cell migration (Figure 25).

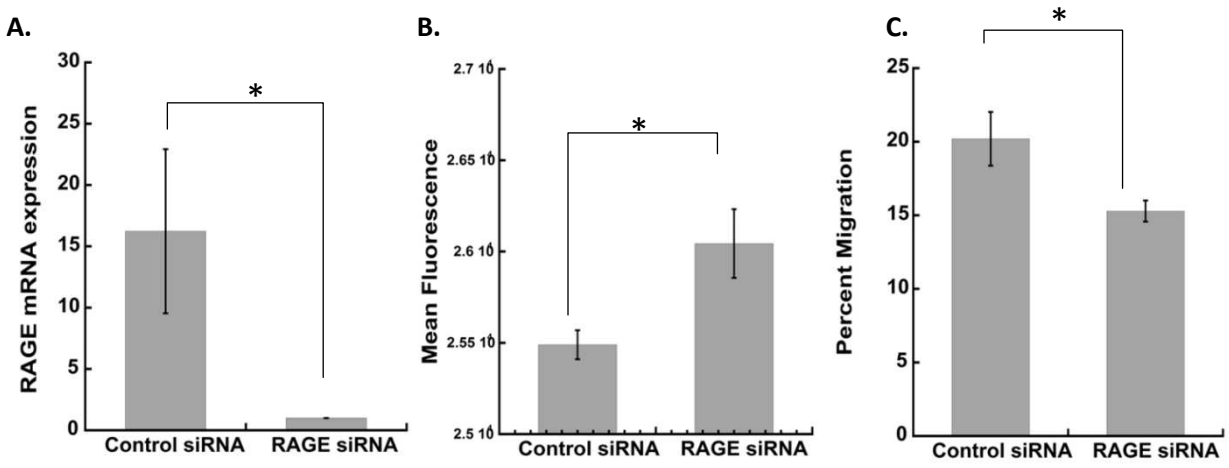

Figure 25: Suppression of RAGE in WM115_RAGE cells by transient transfection with RAGE specific siRNA. (A) RAGE mRNA expression in WM115_RAGE cells after transient transfection with control and RAGE siRNA. (B) Proliferation of WM115_RAGE cells after RAGE siRNA transfection. (C) Percentage of migrated WM115_RAGE cells after RAGE siRNA transfection. Each experiment was performed thrice. (n= 3 ; *p < 0.05). Data shown as Mean ± SD.

Table 12: RAGE concentration in RAGE siRNA transfected WM115_RAGE cells by ELISA. ELISA experiment was performed in triplicate with three indpendent sets of cell lysates. (n= 3 ; P < 0.05). Data shown as Mean ±SD.

siRNA transfection	**RAGE concentration (ng/mg total protein) ± SD**
Control siRNA	54.4 ± 8.7
RAGE siRNA	22.5 ± 8.7

No change in cell migration after S100B siRNA transfection in WM115_RAGE cells

We have shown a 4 fold upregulation of S100B protein in WM115_RAGE cells compared to their MOCK counterparts (Figure 18). To assess the contribution of S100B in RAGE induced cell migration, we have transiently transfected WM115_RAGE cells with a S100B specific siRNA. Transfection with S100B siRNA resulted in a 4 fold suppression of

S100B at protein levels in WM115_RAGE cells. However, suppression of S100B didn't produce any effect on the WM115_RAGE cells migration (Figure 26).

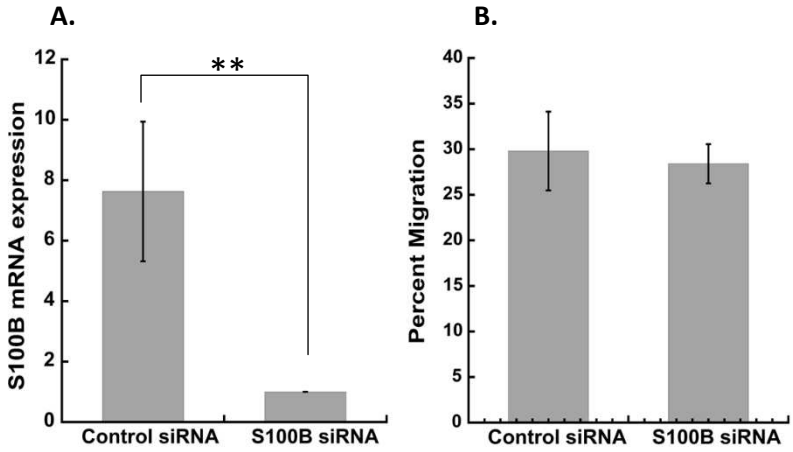

Figure 26: Transient transfection of WM115_RAGE cells with S100B specific siRNA. (A.) S100B mRNA expression in WM115_RAGE cells after transient transfection with control and S100B siRNA. (B.) The percentage of migrated WM115_RAGE cells after S100B siRNA transfection. Experiment was performed three independent times. (n= 3; **p < 0.05). Data shown as Mean ± SD.

Table 13: S100B concentration in S100B siRNA transfected WM115_RAGE cells as determined by ELISA. The experiment was performed in triplicate with three independent sets of cell lysates. (n= 3 ; P < 0.05). Data shown as Mean ± SD.

siRNA transfection	**S100B concentration (nM) ± SD**
Control siRNA	4.03 ± 1.04
S100B siRNA	0.91 ± 0.14

Discussion

Our results have demonstrated the upregulation of S100B in the WM115_RAGE cells compared to the WM115_MOCK cells (Figure 18 & 19). We have also shown an enhanced release of S100B protein in the supernatant of WM115_RAGE cells compared to the MOCK cells (Table 10). Our data suggest that RAGE over-expression leads to enhance S100B expression, which could initiate and amplify RAGE/S100B mediated signaling. In Chapter 1 & 2 our data suggested that RAGE over-expression triggered a proliferative to migratory switching in WM115 cells. RAGE is the only well characterized binding partner for extracellular S100B protein [109]. The contribution of RAGE/S100B mediated signaling in melanoma progression has not been studied yet. To investigate this mechanism we have treated WM115_RAGE cells with an anti-RAGE antibody to block any ligand interaction, including RAGE/S100B interaction. Blocking with anti-RAGE antibody showed no effect on WM115_RAGE cell migration suggesting that either S100B protein acts through a receptor other than RAGE or it does not play any role in RAGE induced melanoma progression. To further investigate S100B's role in RAGE mediated enhanced melanoma cell migration, we transiently suppressed S100B expression in WM115_RAGE cells. Suppression of S100B had no effect on WM115_RAGE cell migration (Figure 26). Our data suggest that in our experimental conditions, S100B might not contribute to enhanced WM115_RAGE cells migration. Our data from Chapter 2 also demonstrated an absence of effect on WM115 cells proliferation and migration upon S100B treatment. These data seem to be in agreement with the results from Chapter 3.

To confirm the role of RAGE in modulating WM115 cells' properties, we transiently transfected WM115_RAGE cells with RAGE specific siRNA. Suppression of RAGE in WM115_RAGE cells led to a reduction in their cell migration and to an increase in cell

proliferation (Figure 24). These data suggest that the changes observed in WM115 cells following RAGE over-expression (Chapter 2), are mediated through RAGE. The precise mechanism by which RAGE can become activated without any ligand is not well understood. We propose that the activation of RAGE in WM115 cells occurs through multimerization of the receptor on the cell surface. We hypothesized that a large number of RAGE molecules expressed on the surface of the WM115 cells tend to oligomerize, which in turn leads to constitutive activation of these cells (Figure 27).

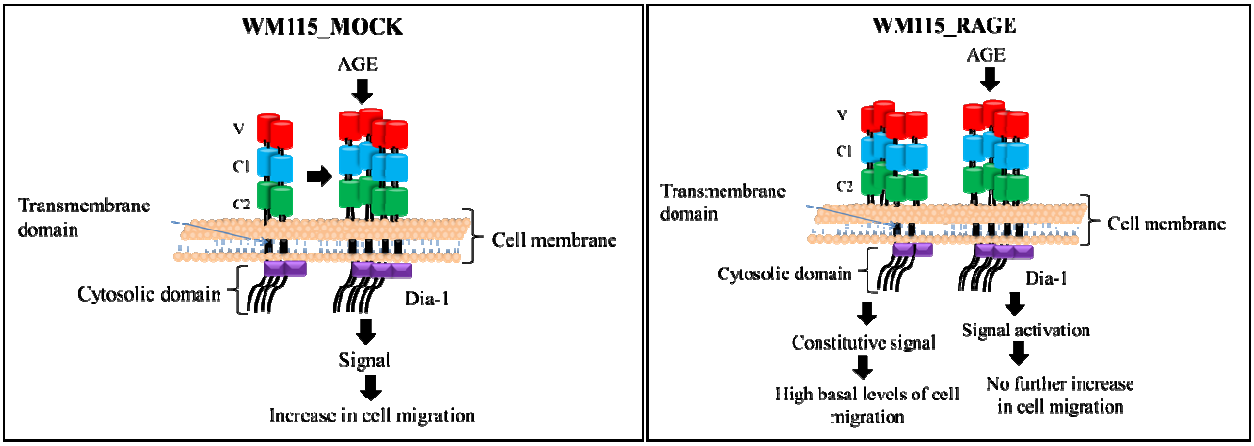

Figure 27: Proposed mechanism of RAGE activation in WM115_MOCK and WM115_RAGE cells. The WM115_MOCK cells with low expression of RAGE upon AGE activation, induce multimerization of RAGE proteins on the cell surface which leads to increase in cell migration. However, WM115_RAGE cells possess large number of RAGE molecules on the cell surface that leads to its multimerization and hence constitutive activation which could not be further activated with AGE activation.

Oligomerization is a key mechanism for RAGE activation [125]. RAGE can oligomerize on the cell surface either upon ligand stimulation or independent of any ligand, depending upon the cell type [126]. The mechanism by which cell surface oligomerization of RAGE leads to its activation is not clear. It has been suggested that cell surface oligomerization of RAGE might affect the interaction of RAGE cytosolic domain with its intracellular binding partner Dia-1, which is a crucial step in RAGE activation. The anti-RAGE antibody used in our study might not

inhibit the oligomerization process because it couldn't inhibit RAGE induced WM115 cell migration. However, the suppression of RAGE by siRNA transfection decreased the total number of RAGE molecules expressed on the cell surface which might reduce the probability of two RAGE molecules to contact each other for the oligomerization process to take place. Our results from Chapter 2 showed an increase in cell migration of WM115_MOCK cells upon AGE treatment. However, WM115_RAGE cells were shown to be insensitive towards AGE activation. We propose that low levels of cell surface RAGE molecules in WM115_MOCK cells, might oligomerize in the presence of AGEs and thereby enhance cell migration. However, RAGE molecules are already in an oligomerization state in the WM115_RAGE cells, and are therefore constitutively activated and thus cannot be further activated with AGEs treatment.

S100B interacts with multiple targets and regulates many cellular properties such as cell cycle, cell morphology, proliferation, motility and metabolism [109]. The tumor suppressor p53 protein is one of the target proteins for S100B in melanoma cells. S100B has been shown to downregulate p53 and to inhibit its tumor suppressive activities in melanoma cells [219]. We have also shown a downregulation in p53 protein in WM115_RAGE cells as compared to WM115_MOCK cells (Figure 20). Suppression of p53 protein found in the WM115_RAGE cells was in agreement with previously published reports and could be mediated via enhanced S100B protein in these cells. As a transcription factor, p53 regulates the expression of different genes associated with tumor progression [364]. Mutation or inactivation of p53 protein is one of the hallmarks of cancer [365]. Although the downregulation of p53 protein in WM115_RAGE cells suggested an increased proliferation in these cells, we observed a decrease in WM115_RAGE cell proliferation compared to control cells (Chapter 2). Apart from regulating cell proliferation, p53 also modulates other cellular functions. Loss of p53 protein has been associated with

enhanced cell migration via Rho GTPase mediated signaling [366-368]. Enhanced motility of WM115_RAGE cells might be associated with loss of p53 protein in these cells.

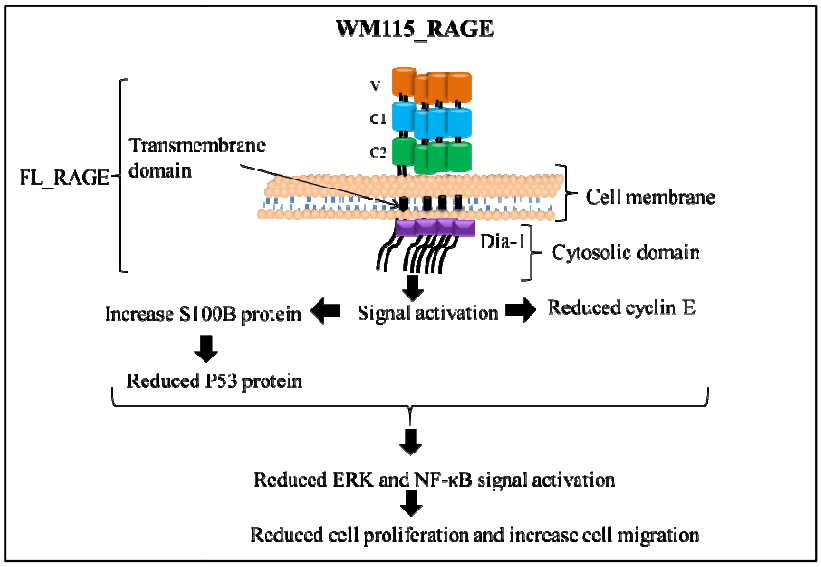

Figure 28: Summary of the results from chapter 2 and 3.RAGE over-expression in WM115 cells results in increased expression of S100B which leads to suppression of p53 protein. RAGE over-expression also leads to suppression in cyclin E expression in WM115 cells. Furthermore, reduced activities of NF-κB and ERK signaling molecules in RAGE over-expressing WM115 cells might result in the proliferation to migration switch observed in these cells.

We have also showed a downregulation in cyclin E in WM115_RAGE cells by Western blot (Figure 20) and flow cytomery (Figure 21 & 22). Cyclin E, a regulatory subunit of cyclin dependent kinase-2, is essential for G1/S transition during the mammalian cell cycle [369, 370]. Previous studies have reported enhanced accumulation of cyclin E in primary melanoma tumors compared to metastatic melanoma tumors [371]. We found a reduced expression of cyclin E in motile WM115_RAGE cells as compared to its less motile counterpart (WM115_MOCK). Therefore, our data appear to be in agreement with these published reports.

Using a commercial cancer pathway gene array, we have investigated the expression levels of 84 genes, representative of six biological pathways involved in transformation and

tumorigenesis (Cell adhesion, angiogenesis, metastasis, apoptosis, cell cycle control and signal transduction) (Table 8). Several genes associated with angiogenesis processes were found to be highly affected by RAGE over-expression in the WM115 cells. We therefore decided to further investigate the changes in transcript levels of 15 selected angiogenesis related genes by RT_PCR. Our data from cancer pathway gene array were found to be reproducible. However, several variations were observed between the two sets of data and these variations might be due to slight variations in the primer sequences. Two different sets of primer pairs specific for a single gene can have different abilities to anneal with the template and therefore can produce different levels of gene amplification. Our results showed a significant upregulation in PDGF-β gene in WM115_RAGE cells compared to MOCK cells. PDGF-β is a platelet derived growth factor known to activate cancer cell survival and motility. Therefore it plays an active role in cancer progression and metastasis [372, 373]. RAGE has been demonstrated to induce the production of a variety of growth factors and cytokines including PDGF-β. AGE-RAGE interaction has been shown to promote pancreatic cancer cells growth through PDGF-β mediated signaling [374]. Upregulation of PDGF-β in WM115_RAGE cells suggest their possible contribution in RAGE mediated WM115 cell motility. However, we have only assessed the transcript levels of PDGF-β but not the protein levels therefore more studies are required to establish its role in RAGE mediated melanoma progression.

CHAPTER 4. EFFECT OF RAGE OVER-EXPRESSION ON MELANOMA TUMOR GROWTH *IN VIVO*

Abstract

As shown in Chapter 2, RAGE stimulates the anchorage independent growth and migration of the WM115 melanoma cell line. To assess the involvement of RAGE in melanoma tumor growth, we have developed a xenograft mouse model of melanoma by grafting WM115_MOCK and WM115_RAGE cells subcutaneously into SCID mice. WM115_RAGE cells showed a larger tumorigenic potential than the WM115_MOCK cells. Tumors generated from WM115_RAGE cells express 194 fold higher RAGE protein than the tumors generated from MOCK cells. We also observed higher levels of sRAGE in WM115_RAGE tumor bearing mice plasma than in MOCK control mice plasma. Several RAGE binding partners were found to be upregulated (S100B: 2.9 ± 0.7 fold, S100A4: 1.4 ± 0.1 fold, S100A6: 1.3 ± 0.1 fold, S100A10: 3.3 ± 1.2 fold) at the protein levels in RAGE over-expressing melanoma tumors compared to their MOCK counterparts. To further investigate the tumorigenic pathway induced by RAGE in WM115 tumors, we have assessed the expression levels of 84 cancer related genes. Our results showed an upregulation in angiogenesis and metastasis inducing factors (interleukin-8, fibroblast growth factor, vascular endothelial growth factor) in RAGE over-expressing melanoma tumors compared to MOCK tumors. Enhanced AKT and ERK activities were found in WM115_RAGE tumors as compared to control tumors. Our data demonstrate a series of signaling events activated by RAGE in melanoma tumors. Furthermore, we could reduce melanoma tumor growth by treating WM115_RAGE tumor bearing mice with anti-RAGE antibodies. In addition, the combination therapy of an anti-RAGE antibody with a well-

established melanoma drug, dacarbazine showed a synergistic tumor suppressive effect in WM115_RAGE tumors bearing mice.

Introduction

Malignant melanoma is the most aggressive form of skin cancer [375]. Unlike primary melanoma tumors, metastatic melanoma tumors are much more challenging to treat. Due to the increasing number of melanoma associated deaths and the lack of treatment options, the FDA has accelerated the approval process of two new anti-melanoma drugs in 2011 [66]. Before that, dacarbazine was the only FDA approved drug for melanoma treatment [376]. Dacarbazine is a chemotherapeutic drug used in various cancer treatments such as malignant melanoma [376], lymphoma [377] and various sarcoma [378]. It acts by alkylating DNA and inhibiting DNA synthesis which leads to cell death [379]. Nonspecific cytotoxicity of dacarbazine leads to several adverse effects [54]. In 2011, the FDA approved Ipilimumab, an antibody based drug against cytotoxic T-lymphocyte antigen 4 and Vemurafenib, a BRAF enzyme inhibitor, for the treatment of metastatic melanoma patients [380, 381]. Despite of major progresses in melanoma therapy, there are still some limitations that need to be addressed. For example, Vemurafenib can only be used in melanoma patients with BRAF V600E mutation but not in patients with wild type BRAF [381, 382]. Acquired resistance is another major disadvantage of Vemurafenib treatment [383]. The T-cell inhibitor Ipilimumab, can also produce life threatening adverse effects [384, 385]. Thus, there is still a critical need to develop safer modes of therapies against melanoma. New target molecules need to be identified to develop therapies against them and to widen treatment options for different populations of melanoma patients. To establish a new molecule as a therapeutic target, the role of this target molecule in the disease progression needs to be identified first and its mechanisms of action need to be understood. RAGE is a multi-ligand

and multi-functional cell surface receptor of the immunoglobin superfamily and is involved in many cancer types. RAGE fuels inflammatory reactions within the tumor microenvironment and initiates several cancer promoting signaling cascades [386]. These inflammatory reactions have been suggested to play important roles in carcinogenesis [387]. Depending upon the activating ligand and the cancer type, RAGE can initiate a diverse array of downstream signaling pathways involved in cancer progression that include AKT [388], ERK [388], JNK [87], p21ras [144], MAP kinases [121], NF-□B [121, 388] and cdc42/rac [80]. RAGE and its ligands such as AGEs, S100 proteins or HMGB-1 are associated with the pathogenesis of different cancer types. Previously, we have shown higher expression levels of RAGE and S100B in certain population of late stage melanoma patients [89]. These data suggested an active contribution of RAGE and its ligands in melanoma progression which needed to be deciphered. Blocking RAGE ligand interaction has been shown to suppress downstream signaling and cancer progression [78]. Anti-RAGE antibodies [78], small molecule inhibitors [135], RAGE blocking peptides [134] are some of the different strategies used to inhibit RAGE ligand interaction. Monoclonal antibodies are currently the most popular strategies for cancer treatment due to their high specificity towards their targets and their moderate side effects [389]. There are two major mechanisms by which antibodies produce anti-cancer effects. Antibodies can either block or stimulate physiological functions of a target protein and thereby suppress tumor growth. Complement dependent cytotoxicity (CDC) and antibody dependent cell mediated cytotoxicity (ADCC) are the other mechanisms by which antibodies produce anti-tumor actions [389]. Antibodies against RAGE have previously been shown to suppress cancer progression by inhibiting the interaction of RAGE with their corresponding ligands. Anti-RAGE antibodies could suppress tumor growth in

murine models of different cancer types including melanoma [133]. That suggest their therapeutic potential in the treatment of melanoma.

However, monotherapy designed against a specific target protein is usually not efficient enough for complete remission of cancer. Combination therapy directing against multiple targets is more efficient in treating cancers that can be considered as multifaceted diseases [390]. Antibodies conjugated with or in combination with chemotherapeutic drugs are being used to improve their overall efficiency and to reduce their possible adverse effects [54]. Several clinical trials are currently ongoing to test the combination of dacarbazine with other drugs for the treatment of metastatic melanoma. The goal of the present study was to decipher the role of RAGE in melanoma tumor growth in mechanistic details and to develop RAGE targeting therapies against melanoma.

Materials and Methods

Cells

The generation and characterization of the WM115_MOCK and WM115_RAGE cells have been described in Chapter 1. The cells were maintained in OPTIMEM containing 4% FBS, 1% penicillin/streptomycin, 0.5 mg/ml (WM115_MOCK cells) or 1mg/ml (WM115_RAGE) of G418 sulfate. The antibiotic G418 sulfate was used to specifically select the transfected WM115 cells. Before injecting the cells into the animals, cells were tested for any mycoplasma contamination.

Xenograft mouse model

Female Severe Combined Immunodeficiency (SCID) mice were purchased from Charles River Laboratories (Wilmington, MA). The animals were maintained in pathogen free conditions

and nourished with sterile food and water. All the animal experiments were conducted according to the guidelines of the Institutional Animal Care and Use Committees (IACUC) at North Dakota State University under an approved protocol. Before starting the experiments, the animals were maintained for 3-4 weeks for allowing them to get adapted to the laboratory environment. All the surgical procedures were in compliance with the NIH's Principles of Laboratory Animal Care. For the experiments, five to six week old mice (20-25 g) were anaesthetized and subcutaneously injected with either WM115_RAGE or WM115_MOCK cells (1 x 106 /50 µl) (8 animals per group). Tumor growth was quantified every three days over a period of 30 days. Tumor volumes were measured using a digital caliper. The following equation was used to calculate tumor volumes: 0.52x L x W2, where W2 is the square width and L is the length of the tumor. After one month of treatment the animals were euthanized and the tumors were excised from both groups of animals and were snap frozen in liquid nitrogen for further studies.

Real Time PCR

RNAs from WM115_MOCK and WM115_RAGE tumors were extracted using the commercially available PARIS kit (Ambion Life Sciences, USA). After quantification and quality assessment, the RNAs were reverse transcribed using the Reverse Transcription System (Promega, WI) according to the manufacturer's instructions (Chapter 1 and 3). The cDNAs were run on a Mx3000 Stratagene RT_PCR system using Brilliant II Ultra fast SYBER Green QPCR Master mix and appropriate primers pairs specific for each gene (Table 7). In order to decipher the downstream mechanisms of RAGE induced melanoma tumor growth a Human Cancer pathwayFinder™ RT² Profiler™ PCR Array (Qiagen, USA) was performed on the cDNAs obtained from WM115_MOCK and WM115_RAGE tumors as described in Chapter 3.

Western blot

Tumor protein lysates were prepared using the PARIS kit (Ambion Life Sciences, USA) as per manufacturer's instructions. 40µg to 100µg of total protein was resolved on 12% to 15% SDS gels and blotted on nitrocellulose membrane. After overnight blocking with 4% BSA/TBS at 4°C, the blotted membrane was incubated with specific antibodies in 1% BSA/TBS/0.1% tween for 1 hour at room temperature. After washing three times with TBS/0.1% tween, the blots were incubated with appropriate secondary antibodies. After a final wash, the blots were developed with ECL substrate (ThermoScientific, IL, USA). The data obtained were analyzed by densiometric analysis using Image-J software.

ELISA

Protein lysates were prepared form the tumors using the PARIS kit (Ambion Life Sciences, USA). The RAGE protein was quantified in the tumor lysates and in the animal plasma using the Quantikine Human RAGE Immunoassay ELISA system according to the manufacturer's instructions. The concentration of S100B protein in the plasma of WM115_MOCK and WM115_RAGE tumor bearing mice was determined with the help of a calibration curve obtained by ELISA. Briefly, rabbit polyclonal anti-S100B antibody was coated in the wells of an ELISA plate over-night at 4 °C. After 3 hours of blocking with 3% BSA/TBS, 50µl of S100B standard and plasma samples were added to the wells and further incubated for 1 hour at room temperature. After washing with TBS-T, 50µl of mouse monoclonal anti-S100B was added to the wells and incubated for 1 hour at room temperature. The wells were washed 3 times with TBS-T and then incubated with alkaline phosphatase conjugated secondary antibody

for 45 mins. After three final washes, 50µl of 1mg/ml of p-NPP substrate (Gold Biotechnology, USA) was added to the wells and the absorption was measured at 405nm.

Immunohistochemistry

Tumors embedded in OCT were sectioned into 7 µm thick slices. The sections were treated with H2O2 in water (3% v/v) to neutralize the endogenous peroxidase activity, blocked by 10% (v/v) normal goat serum to avoid non-specific binding and stained with IgG 2A11. Horseradish peroxidase-conjugated goat anti-mouse antibody was then used as a secondary antibody and the peroxidase activity was detected using 3,3'-diaminobenzidine (DAB) substrate (Vector Laboratories, Burlingame, CA). As a control, parallel tumor sections of WM115_MOCK and WM115_RAGE tumors were stained with hematoxylin/eosin. The hematoxylin solution (Harris Modified), and eosin Y were obtained from Sigma-Aldrich Corporation (St. Louis, MO). The sections were imaged using an Olympus IX-81 microscope (Melville, NY). The images were recorded on a camera that interfaced with a computer and were processed by the HCImage software (Hirakuchi, Hamamatsu, Japan).

IgG 2A11 antibody treatment

WM115_RAGE tumor bearing mice were treated with anti-RAGE antibody. The animals were divided in two groups (n = 8). WM115_RAGE cells were implanted subcutaneously in the animals and tumors developed in both groups as described previously. Group I was treated with PBS (control) and Group II was treated with anti-RAGE antibody (0.5 mg/mice) by intra peritoneal injection every 5 days for two cycles of 21 days each. The animal body weights were measured over the treatment period. Tumor volumes were calculated as per the formula described in the materials and methods of chapter 4.

Cy5.5 labeling of IgG 2A11

Cy5.5 monofunctional hydroxysuccinamide ester (Cy5.5-NHS) was purchased from GE Healthcare Biosciences (Piscataway, NJ). The conjugation of IgG 2A11 with Cy5.5-NHS was carried out as described. Briefly, 1 mg IgG 2A11 was dissolved in 1 ml 10mM Phosphate buffer pH 7.4 containing 150mM of NaCl and was reacted with one molar excess of Cy5.5 NHS at room temperature for 15 mins. The labeled IgG was then purified from non-reacted Cy5.5 by size exclusion chromatography on Sephadex G-50 column (GE Helathcare). The protein concentration of the labeled IgG was determined by the BCA kit (Thermo Scientific, Walthman, Ma) according to manufacturer's instructions. The number of Cy5.5 fluorophores per antibody was determined by absorbance on a Spectraman Spectrofluorimeter (Molecular Devices, Sunnyvale, Ca), using the extinction coefficient of Cy5.5 of (= 250,000M-1 cm-1 at 675nm). The labeling resulted in about 1.3-1.5 fluorophore per molecule of antibody. As negative control, Cy5.5-labeled polygonal mouse IgG was prepared under similar condition. Mouse serum IgG was purchased from Sigma-Aldrich Corporation (St. Louis, MO).

Imaging with Cy5.5 labeled IgG 2A11

The in vivo imaging studies were carried out in real time NIRF reflectance imaging (Kodak Fx Pro, Carestream Health Incorporation, Rochester, NY). In brief, WM115_RAGE tumor bearing mice were divided in three groups (4 animals each group) once the tumor volume reached ≈ 80 mm3. Animals were intravenously injected with Cy5.5-labeled RAGE antibody, or Cy5.5-labeled mouse IgG or PBS only (100μg, 125μL). A group of WM115_MOCK tumor bearing mice (n=4) was used a control and treated with Cy5.5-labeled RAGE antibody in the similar way. Mice were imaged after 0, 4, 24, 48 hours with 1 min image acquisition time. The

images were analyzed using the Kodak Digital Science 1D software (Carestream Health Incorporation, Rochester, NY). The average fluorescence intensities at the region of interest (ROI) were corrected for the background at the adjacent skin.

Combination therapy

WM115_RAGE tumor bearing mice were divided in 6 groups. Group I was treated with PBS as control (8 animals), Group II, III and IV were treated with 50 mg/kg, 25 mg/kg and 12.5 mg/kg of dacarbazine respectively (8 animals each). Group V was treated with a combination of 25 mg/kg dacarbazine + anti-RAGE antibody (4 animals) and Group VI was treated with a combination of 12.5 mg/kg dacarbazine + anti-RAGE antibody (4 animals). Dose regimen of dacarbazine (every 5 days of treatment for two cycles of 21 days each) was followed. At the end of the treatment or if the tumor size exceeded 1200 mm3, the mice were euthanized and the tumors were excised. These tumors were immediately snap frozen for further studies.

Statistical Analysis

Data are shown either as Mean ± SEM or Mean ± SD. Comparative analysis between two groups was made by one tail two sample (unpaired) Student's t- test and $p < 0.05$ was considered as significant.

Results

RAGE over-expressing WM115 cells are more tumorigenic that WM115_MOCK cells

As described in Chapter 1, we have generated and characterized RAGE over-expressing WM115 cells and used WM115_MOCK cells for control cells. The transfected cells were injected in SCID mice and tumor volumes were followed over the period of 30 days. We

observed that both MOCK and RAGE transfected WM115 cells formed tumors with different growth rates (Figure 29). Ten days after the implantation, the WM115_RAGE cells started to form a tumor whereas WM115_MOCK cells took more than 15 days to initiate tumor formation. At the end of the study, WM115_RAGE were two times larger than the WM115_MOCK cells. Upon characterization of the tumors we found a higher expression of RAGE in the tumors established from the WM115_RAGE cells as shown by ELISA, Real Time PCR and Immunohistochemistry (Figure 30 and Table 14). We found 194 fold higher RAGE (13693 ± 137 pg/mg in WM115_RAGE tumors and 70.0 ± 2.8 pg/mg WM115_MOCK tumors) in WM115_RAGE tumors as compared to MOCK tumors. We could also detect the soluble form of RAGE (213.1 ± 66.0 pg/ml) in the plasma of WM115_RAGE tumor bearing mice (Table 14). The levels of soluble RAGE in the plasma from WM115_MOCK tumor bearing mice were undetectable in our experimental conditions.

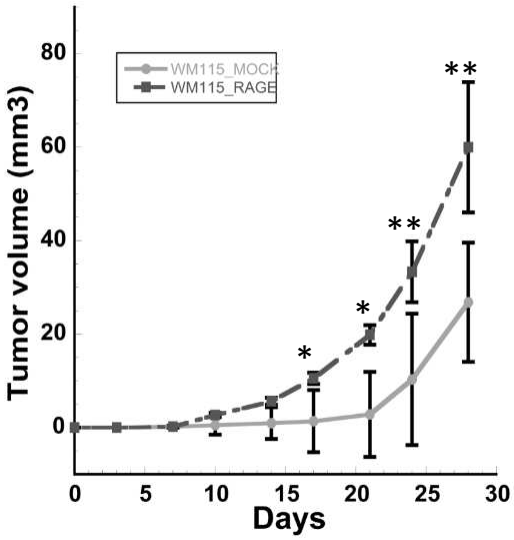

Figure 29: RAGE over-expression enhances melanoma tumor growth in vivo in a xenograft mouse model.$1*10^6$ cells were injected subcutaneously in the mammary tissue of SCID mice. Tumor growth was followed over the period of 30 days. Tumors RAGE expressions at transcript and protein levels are shown in the table 14. Data are represented as Mean ± SEM. (n = 8; **p < 0.01, *p < 0.05).

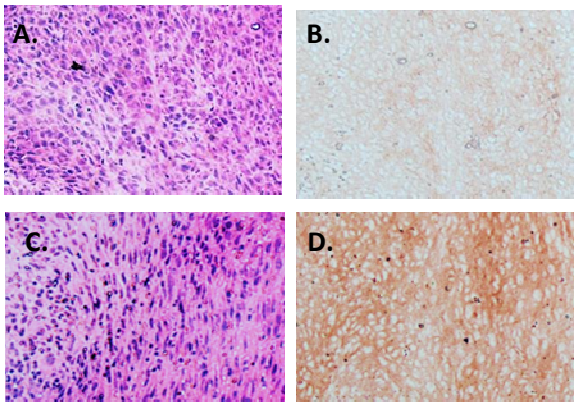

Figure 30: RAGE expression in WM115_MOCK and WM115_RAGE tumors as determined by immunohistochemistry. Tumors sections were stained with anti-RAGE antibody and HRP conjugated secondary antibody (Figure B. and D.). Figure A. and C. are H & E stained images of WM115_MOCK and WM115_RAGE tumors respectively.

Table 14: RAGE protein in tumor lysates and blood plasma samples by ELISA. The assay was performed with three different sets of tumors and blood plasma samples obtained from three different animals. Data shown as Mean ± SD. (n = 3).

Tumors samples	**RAGE expression pg/mg of total protein**	**Fold change**
WM115_MOCK tumor	70.0 ± 2.8	-
WM115_RAGE tumor	13693 ± 137	194 fold
Plasma samples	**RAGE pg /ml of plasma**	**Fold change**
WM115_MOCK plasma	≤ 10	
WM115_RAGE plasma	213.1 ± 66	≥ 21 fold

RAGE ligands are upregulated in RAGE over-expressing melanoma tumors

We found significant upregulation in six S100 genes (S100B, S100A4, S100A6, S100A10, S100A11 and S100A16) in WM115_RAGE tumors as compared to MOCK tumors at transcript levels (Figure 31). However, we decided to further study S100A4, S100A6, S100A10 and S100B at protein levels because these S100 proteins have been previously described to

contribute to melanoma pathogenesis. S100B, S100A4, S100A6 and S100A10 proteins were significantly upregulated 2.9 ± 0.7 fold, 1.4 ± 0.1 fold, 1.3 ± 0.1 fold and 3.3 ± 1.2 fold respectively (Figure 33 and 34). We also detected ≈ 10 nM of S100B in the plasma from WM115_RAGE tumor bearing mice whereas in WM115_MOCK tumor bearing mice, the S100B levels were too low in the blood plasma to be detected in our experimental conditions.

We also compared the expression levels of S100 proteins in RAGE over-expressing cells with the corresponding RAGE over-expressing tumors (Figure 32 and Table 15). We found an 18 and 3 fold increase in S100B mRNA expression in WM115_RAGE tumors and WM115_RAGE cells respectively compared to their MOCK counterparts. At transcript level, we found suppression in S100A2 gene in WM115_RAGE cells compared to the MOCK cells. However, in the corresponding WM115_RAGE tumors we found an upregulation in S100A2 mRNA expression compared to the MOCK tumors (Figure 32 and Table 15). S100A2 protein was not detected in the cells as well as in the corresponding tumors by western blot in our experimental conditions. The transcript levels of S100A4 genes were low in both types of WM115 cells and were not affected with RAGE over-expression. The tumors formed from these cells expressed significant higher levels of S100A4. RAGE over-expressing WM115 tumors expressed 5 fold higher S100A4 mRNAs than the MOCK tumors. The Western blot data shows 2 fold upregulation in S100A4 protein in WM115_RAGE tumors compared to the MOCK tumors.

Similar to S100A4, S100A6 transcripts were also low in the cells and were unaffected by RAGE over-expression. However, the tumors generated from the WM115_RAGE cells showed a 2 fold up regulation in S100A6 transcripts by RT_PCR and about a 1.4 fold upregulation in S100A6 proteins by Western blot as compared to control tumors (Figure 32 and Table 15).

At transcript levels, S100A10 was found to be downregulated in WM115_RAGE cells compared to MOCK cells. By Western blot we could not observe any change in the S100A10 protein between WM115_MOCK and WM115_RAGE cells. However, we found a 8 fold upregulation in S100A10 at transcript levels and 4 fold upregulation at protein levels in WM115_RAGE tumors as compared to MOCK tumors (Figures 32 and 34).

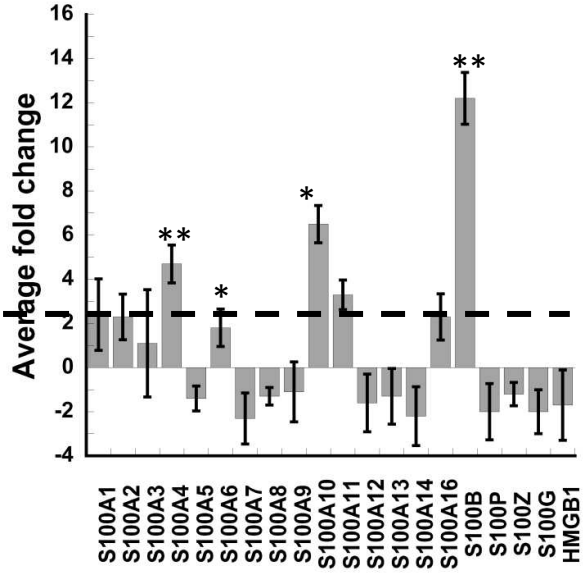

Figure 31: S100 mRNA expressions in WM115_MOCK and WM115_RAGE tumors. cDNAs (10ng/well) obtained from WM115_MOCK and WM115_RAGE tumors were used as templates in RT_PCR. Data obtained are shown as the average fold change in S100 mRNA expression in WM115_RAGE tumors compared to MOCK tumors. Experiment was performed at least three times on three different sets of tumor cDNAs obtained from different animals. Data are represented as Mean ± SD. (n=3; *$p < 0.05$, **$p < 0.01$).

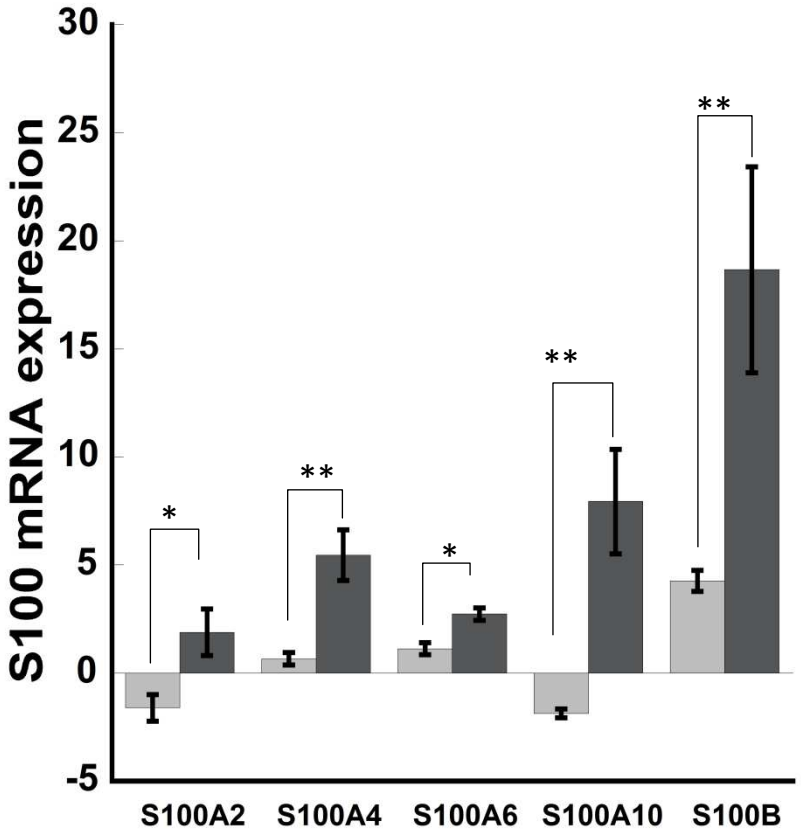

Figure 32: Comparison of S100 mRNA expressions in WM115_MOCK and WM115_RAGE cells and in their corresponding tumors. (n = 3; **p <0.01, *p < 0.05).

Table 15: Comparative analysis of S100 mRNA expression in WM115_MOCK and WM115_RAGE cells and the corresponding tumors.

S100 genes	Cells Δ Ct		Fold Change	Tumors ΔCt		Fold Change
	MOCK	RAGE		MOCK	RAGE	
S100A2	9.7 ± 0.9	10.5 ± 0.8	-1.6 ± 1.6	9.4 ± 0.7	8.3 ± 0.8	1.9 ± 2.6
S100A4	7.5 ± 0.7	7.3 ± 0.7	0.7 ± 0.9	1.9 ± 0.8	-0.3 ± 0.7	5.5 ± 3.4
S100A6	6.9 ± 1.2	6.5 ± 1.2	1.1 ± 0.9	5.6 ± 0.8	4.2 ± 0.9	2.7 ± 0.8
S100A10	4.1 ± 0.3	5.0 ± 0.6	-1.8 ± 0.5	4.2 ± 0.9	1.6 ± 1.0	7.9 ± 5.8
S100B	3.9 ± 1.0	1.9 ± 0.7	4.3 ± 1.5	3.9 ± 0.8	0.1 ± 1.1	18.67 ± 14.3

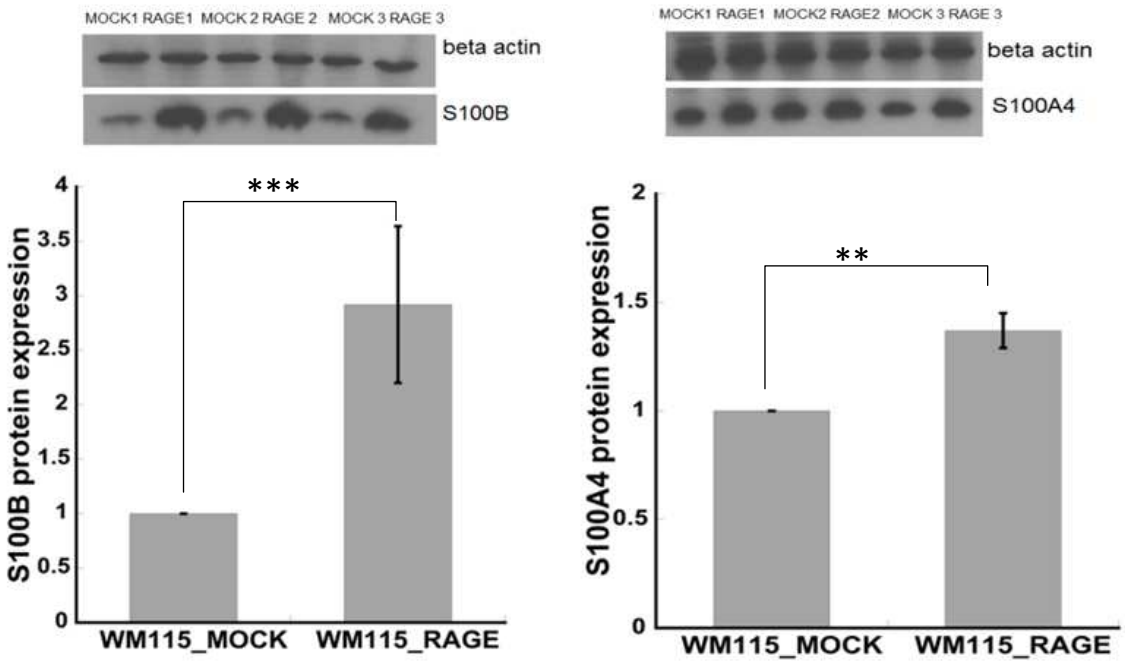

Figure 33: S100B and S100A4 protein expression in WM115_MOCK and WM115_RAGE tumor lysates by Western blot. Western blot was performed two times on three sets of tumor lysates from different animals. The graph represents the densitometric analysis of the blots. (n= 3; ***$p < 0.001$; **$p < 0.01$).

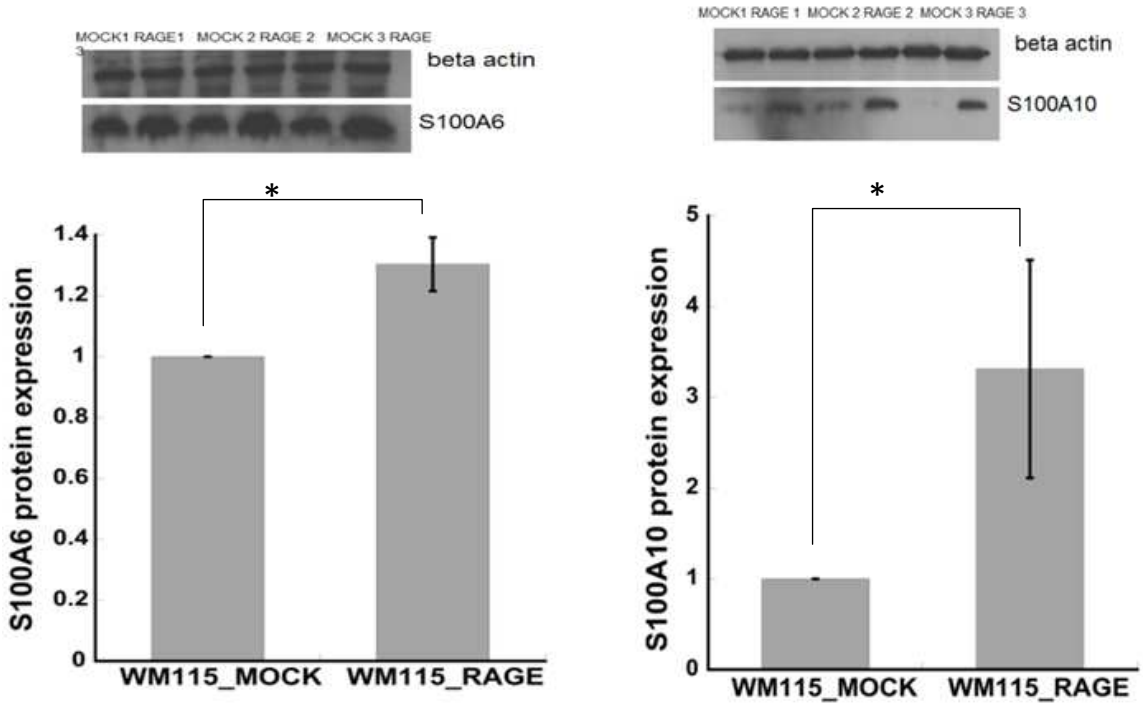

Figure 34: S100A6 and S100A10 protein expression in WM115_MOCK and WM115_RAGE tumor lysates by Western blot. The experiment was performed two times on three sets of tumor lysates from different animals. The graph represents the densitometric analysis of the blots. (n= 3; *$p < 0.05$).

RAGE over-expression alters gene expression of IL-8, p53, Collagen XVIII, VEGF, PDGF-apha and integrin proteins in melanoma tumors

In order to decipher RAGE induced mechanisms in melanoma tumors we performed a RT_PCR gene array of 84 genes involved in cancer progression. We arbitrarily used a 2.5 fold cut off value for the analysis of the array. The results from the cancer pathway gene array demonstrated significant changes in the expression of genes involved in tumorigenesis (Table 16). We found a significant upregulation in IL-8 (5.2 ± 1.6 fold), Collagen XVIII (4.1 ± 2.1 fold), VEGF (3.9 ± 3.3 fold), Thrombospondin 1 (3.9 ± 0.8) and PDGF-alpha (2.5 ± 1.7 fold) and the downregulation in p53 (2.4 ± 1.7 fold), integrin alpha-4 (2.5 ± 1.2 fold) and integrin

alpha-1 (2.4 ± 1.5 fold) at the gene level. We next chose to further study 15 selective genes associated with angiogenesis pathway using primers pairs specific for the genes obtained from the primer bank. Our results from the second set of experiment showed upregulation of IL-8 (9.8 ± 5.2 fold), Collagen XVIII (3.5 ± 2.0 fold), VEGF (2.1 ± 0.88 fold) and PDGF-alpha (3.4 ± 1.9 fold) genes in WM115_RAGE tumors compared to MOCK tumors (Table 17). Our data from both the experiments were reproducible.

Table 16: Cancer pathway gene array in WM115_MOCK and WM115_RAGE tumors. Data are shown as fold changes in WM115_RAGE compared to WM115_MOCK tumors. The array was performed three times with three different tumor cDNAs (n=3, $p < 0.05$).

No.	Genes	Average fold change	SD	Functional role
1.	Integrin, alpha 1	-2.4	0.5	Cell Adhesion
2.	Integrin, alpha 2 (CD49B, alpha 2 subunit of VLA-2 receptor)	1.6	0.6	
3.	Integrin, alpha 3 (antigen CD49C, alpha 3 subunit of VLA-3 receptor)	3.1	0.5	
4.	Integrin, alpha 4 (antigen CD49D, alpha 4 subunit of VLA-4 receptor)	-2.5	0.3	
5.	Integrin, alpha V (vitronectin receptor, alpha polypeptide, antigen CD51)	2.9	0.9	
6.	Integrin, beta 1 (fibronectin receptor, beta polypeptide, antigen CD29 includes MDF2, MSK12	1.4	0.4	
7.	Integrin, beta 3 (platelet glycoprotein IIIa, antigen CD61)	1.2	0.3	
8.	Integrin, beta 5	-2	0.3	
9.				

Table 16: Cancer pathway gene array in WM115_MOCK and WM115_RAGE tumors (continued).

10.	Metastasis suppressor 1	-2.1	1.1	
11.	Pinin, desmosome associated protein	1.2	0.4	
12.	Synuclein, gamma (breast cancer-specific protein 1)			
13.	Angiopoietin 1	-1.6	1.9	Angiogenesis
14.	Angiopoietin 2	2.7	1.5	
15.	Collagen, type XVIII, alpha 1	4.1	1.1	
16.	Fibroblast growth factor receptor 2	1.8	1.1	
17.	Interferon, alpha 1	1.2	0.4	
18.	Interferon, beta 1, fibroblast	1.1	1.0	
19.	Insulin-like growth factor 1 (somatomedin C)	2.2	0.8	
20.	Interleukin 8	5.3	0.7	
21.	Platelet-derived growth factor alpha polypeptide	2.5	0.7	
22.	Platelet-derived growth factor beta polypeptide	1.6	1.5	
23.	TEK tyrosine kinase, endothelial	-1.4	0.3	
24.	Transforming growth factor, beta 1	-1.8	1.1	
25.	Transforming growth factor, beta receptor 1	-1.0	0.7	

Table 16: Cancer pathway gene array in WM115_MOCK and WM115_RAGE tumors (continued).

26.	Thrombospondin 1	3.9	0.8	
27.	Tumor necrosis factor	1.3	0.9	
28.	Vascular endothelial growth factor A	3.9	1.7	
29.	Met proto-oncogene (hepatocyte growth factor receptor)	-1.1	1.1	Invasion and Metastasis
30.	Matrix metallopeptidase 1 (interstitial collagenase)	-1.4	1.2	
31.	Matrix metallopeptidase 2 (gelatinase A, 72kDa gelatinase, 72kDa type IV collagenase)	-1.0	0.8	
32.	Matrix metallopeptidase 9 (gelatinase B, 92kDa gelatinase, 92kDa type IV collagenase)	1.1	0.7	
33.	Metastasis associated 1	-2.8	1.8	
34.	Metastasis associated 1 family, member 2	1.1	1.2	
35.	Non-metastatic cells 1, protein (NM23A) expressed in	-1.3	0.3	
36.	Non-metastatic cells 4, protein expressed in	-1.6	0.6	
37.	Plasminogen activator, urokinase	1.0	0.2	
38.	Plasminogen activator, urokinase receptor	1.5	0.4	
39.	S100 calcium binding protein A4	2.8	0.9	
40.	Serpin peptidase inhibitor, clade B (ovalbumin), member 5	1.5	0.6	
41.	Serpin peptidase inhibitor, clade E (nexin, plasminogen activator inhibitor type 1), member 1	2.6	0.9	

Table 16: Cancer pathway gene array in WM115_MOCK and WM115_RAGE tumors (continued).

42.	TIMP metallopeptidase inhibitor 1	2.5	1.0	
43.	TIMP metallopeptidase inhibitor 3	1.4	0.8	
44.	Twist homolog 1 (Drosophila)	-1.1	1.9	
45.	Apoptotic peptidase activating factor 1	1.1	0.6	Apoptosis and Cell Senescence
46.	BCL2-associated agonist of cell death	1.0	1.2	
47.	BCL2-associated X protein	-1.6	1.0	
48.	B-cell CLL/lymphoma 2	-1.1	1.0	
49.	BCL2-like 1	1.4	0.4	
50.	Caspase 8, apoptosis-related cysteine peptidase	1.5	0.5	
51.	CASP8 and FADD-like apoptosis regulator	1.2	0.7	
52.	Fas (TNF receptor superfamily, member 6)	1.1	0.5	
53.	Granzyme A (granzyme 1, cytotoxic T-lymphocyte-associated serine esterase 3	1.9	0.7	
54.	HIV-1 Tat interactive protein 2, 30kDa	1.2	0.3	
55.	Telomerase reverse transcriptase	1.2	0.4	
56.	Tumor necrosis factor receptor superfamily, member 1A	2.0	0.9	
57.	Tumor necrosis factor receptor superfamily, member 25	1.5	0.6	
58.	Tumor necrosis factor receptor superfamily, member 10b	1.5	0.8	
59.	Ataxia telangiectasia mutated	-1.3	0.9	Cell Cycle Control & DNA Damage
60.	Breast cancer 1, early onset	-1.2	0.3	
61.	Cyclin E1	-1.8	0.2	

Table 16: Cancer pathway gene array in WM115_MOCK and WM115_RAGE tumors (continued).

62.	Cell division cycle 25 homolog A (S. pombe)	-1.3	0.2	
63.	Cyclin-dependent kinase 2	1.0	0.4	
64.	Cyclin-dependent kinase 4	-1.8	0.7	
65.	Cyclin-dependent kinase inhibitor 1A (p21, Cip1)	2.3	0.9	
66.	Cyclin-dependent kinase inhibitor 2A (melanoma, p16, inhibits CDK4)	2.3	0.9	
67.	CHK2 checkpoint homolog (S. pombe)	-1.2	0.6	
68.	E2F transcription factor 1	-1.3	0.1	
69.	Mdm2 p53 binding protein homolog (mouse)	-1.5	1.6	
70.	Retinoblastoma 1	-3.1	1.2	
71.	S100 calcium binding protein A4	2.2	0.9	
72.	Tumor protein p53	-2.4	0.7	
73.	V-AKT murine thymoma viral oncogene homolog 1	-1.8	0.5	Signal Transduction Molecules and Transcription Factors
74.	V-erb-b2 erythroblastic leukemia viral oncogene homolog 2, neuro/glioblastoma derived oncogene homolog (avian)	1.6	0.7	
75.	V-Ets erythroblastosis virus E26 oncogene homolog 2 (avian)	-2.8	1.1	
76.	FBJ murine osteosarcoma viral oncogene homolog	1.3	1.9	
77.	Jun proto-oncogene	-1.3	2.4	
78.	Mitogen-activated protein kinase kinase 1	-1.8	0.1	
79.	V-myc myelocytomatosis viral oncogene homolog (avian)	-1.5	2.4	

Table 16: Cancer pathway gene array in WM115_MOCK and WM115_RAGE tumors (continued).

80.	Nuclear factor of kappa light polypeptide gene enhancer in B-cells 1	1.0	0.5	
81.	Nuclear factor of kappa light polypeptide gene enhancer in B-cells inhibitor, alpha	2.3	1.0	
82.	Phosphoinositide-3-kinase, regulatory subunit 1 (alpha)	-1.4	0.7	
83.	V-raf-1 murine leukemia viral oncogene homolog 1	1.3	0.4	
84.	Synuclein, gamma (breast cancer-specific protein 1)	1.7	0.6	

Table 17: PCR gene array with angiogenesis associated genes in the WM115 tumors. Expression of selective genes associated with angiogenesis processes were assessed using appropriate primer pairs and tumors cDNAs as templates. Experiment was performed more than three times with three independent sets of cDNAs. Data are shown as Mean ± SD (n = 3; **p < 0.01; *p < 0.05)

Number	**Genes**	**Average fold change ± SD**
1.	Angiopoietin 1	2.8 ± 2.9
2.	Angiopoietin 2	1.9 ± 2.6
3.	Collagen, type XVIII, alpha 1	3.6 ± 2.0*
4.	Fibroblast growth factor receptor 2	No Ct
5.	Interferon, alpha 1	3.9 ± 2.4*
6.	Interferon, beta 1, fibroblast	3.1 ± 4.2
7.	Insulin-like growth factor 1 (somatomedin C)	5.9 ± 7.6
8.	Interleukin 8	9.8 ± 5.2**
9.	Platelet-derived growth factor alpha polypeptide	3.4 ± 1.9*
10.	Platelet-derived growth factor beta polypeptide	0.1 ± 1.4
11.	TEK tyrosine kinase, endothelial	-1.8 ± 0.6
12.	Transforming growth factor, beta 1	1.4 ± 0.4
13.	Vascular endothelial growth factor A	2.1 ± 0.9*
14.	Tumor necrosis factor	4.3 ± 6.8
15.	Thrombospondin-1	1.2 ± 0.1

Enhanced AKT, ERK signaling activities in WM115_RAGE tumors

AKT, JNK and ERK signaling cascades are important signaling events activated by RAGE in cancer [87]. We assessed the activities of AKT, JNK and ERK in the tumor lysates by Western blot and we found significant increases in the phosphorylated forms of AKT (1.4 ± 0.3 fold) and ERK (2.0 ± 0.4 fold) in WM115_RAGE tumors as compared to MOCK counterparts (Figure 35 & 36) whereas JNK activity was found to be unchanged (data not shown).

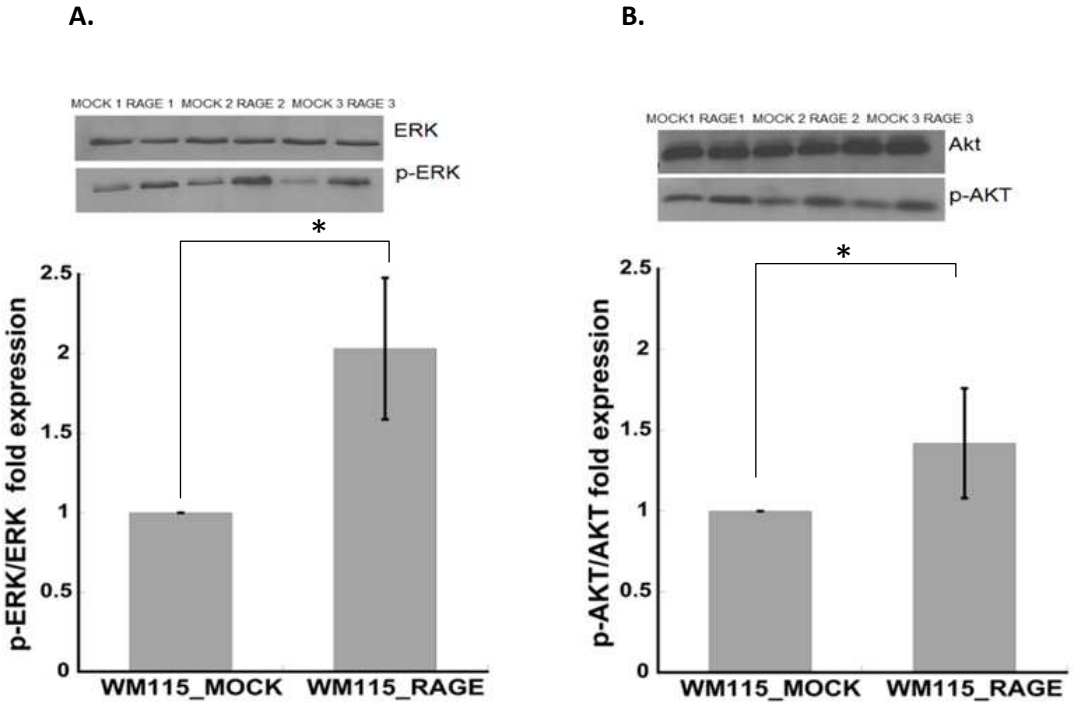

Figure 35: Phosphorylated levels of ERK (A.) and AKT (B.) in WM115_MOCK and WM115_RAGE tumors by Western blot. The graphs represent the densitometric analysis of the corresponding blots. The experiment was performed twice on three different tumors. Data represented as Mean ± SD (n = 3, *p <0.05).

Treatment with IgG 2A11 suppresses melanoma tumor growth

We demonstrate that RAGE over-expression enhances melanoma tumor growth and enhanced RAGE ligand expression. From the results we hypothesized that RAGE-ligand interaction activates signaling cascades and leads to faster tumor growth. To substantiate our statement, we have treated WM115_RAGE tumor bearing mice with an anti-RAGE antibody (IgG 2A11) and PBS as control. IgG 2A11 is a monoclonal antibody generated in mouse immunized with human RAGE protein. IgG 2A11 interacts with human RAGE with nano molar affinity. Blocking RAGE with IgG 2A11 led to significant suppression of tumor growth. On the last day of treatment, we found ≈1.6 fold reduction in tumor volume with IgG 2A11 treatment as compared to control (Figure 36). Also, the animal body weights were unaffected during the antibody treatment suggesting no severe side effects of the antibody (Table 18).

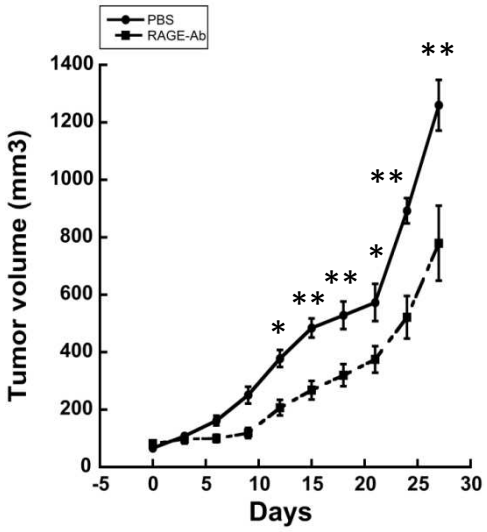

Figure 36: Tumor growth rate upon IgG 2A11 treatment in WM115_RAGE tumor bearing mice. WM115_RAGE tumor bearing mice were treated with 0.5 mg/mice of IgG 2A11 every 5 days for two cycles of 21 days each. A group of mice was treated with PBS as control. Tumor volumes were calculated as mentioned previously (n= 8: *$p < 0.05$).

Table 18: Body weights of WM115_RAGE tumors bearing mice during the treatment with IgG 2A11 and DITC. The mice were treated with PBS, 2A11, 50 mg/kg of DITC, 25 mg/kg of DITC, 12.5 mg/kg of DITC and two combinations of 2A11 with DITC. The body weights were monitored over the period of the treatment. Data are shown as Mean ± SEM.

Day	**PBS**	**2A11**	**2A11 + 25 mg/kg DITC**	**2A11 + 12.5 mg/kg DITC**	**50 mg/kg DITC**	**25 mg/kg DITC**	**12.5 mg/kg DITC**
0	25.6 ± 0.3	25.1 ± 0.3	24.4 ± 0.9	24.3 ± 0.9	22.9 ± 0.3	22.3 ± 0.5	23.8 ± 0 .7
3	24.6 ± 0.1	25.5 ± 0.3	23.3 ± 0.8	23.4 ± 0.7	22.8 ± 0.2	21.4 ± 0.5	23.9 ± 0.7
6	24.7 ± 0.5	24.4 ± 0.5	23.2 ± 0.7	23.4 ± 0.6	22.8 ± 0.4	21.8 ± 0.6	23.7 ± 0.8
9	26.3 ± 0.3	25.8 ± 0.3	24.1 ± 0.8	23.4 ± 0.6	23.1 ± 0.5	21.7 ± 0.5	24.1 ± 0.8
12	21.9 ± 0.3	25.7 ± 0.1	23.8 ± 0.7	23.6 ± 0.3	23.2 ± 0.2	22.1 ± 0.3	23.6 ± 0.6
15	21.9 ± 0.4	25.8 ± 0.2	23.9 ± 0.7	24.2 ± 0.3	23.1 ± 0.3	22.4 ± 0.6	23.9 ± 0.6
18	22.0 ± 0.4	25.5 ± 0.2	23.8 ± 0.8	24.4 ± 0.5	23.4 ± 0.3	22.6 ± 0.6	23.8 ± 0.6
21	21.8 ± 0.4	26.0 ± 0.5	24.2 ± 0.9	23.9 ± 0.4	23.7 ± 0.2	22.3 ± 0.6	23.6 ± 0.5
24	22.0 ± 0.3	25.4 ± 0.3	24.0 ± 0.7	24.3 ± 0.2	23.5 ± 0.2	22.0 ± 0.7	23.7 ± 0.5
27	21.9 ± 0.2	25.9 ± 0.2	24.4 ± 0.8	24.4 ± 0.6	23.4 ± 0.2	22.4 ± 0.6	23.9 ± 0.5
30			24.3 ± 0.6	24.7 ± 0.6	23.9 ± 0.3	22.6 ± 0.6	23.9 ± 0.6
33			24.4 ± 0.6	24.7 ± 0.8	23.9 ± 0.3	22.4 ± 0.7	23.8 ± 0.6
36			24.8 ± 0.6	24.4 ± 0.5	23.9 ± 0.2	22.5 ± 0.4	24.3 ± 0.6
39			24.6 ± 0.8	24.9 ± 0.5	23.8 ± 0.2	22.8 ± 0.5	24.4 ± 0.6
42			24.5 ± 0.9	25.4 ± 0.6	23.6 ± 0.2	22.6 ± 0.6	24.1 ± 0.5

Table 19: Tumor volumes (mm3) from WM115_RAGE tumors bearing mice during the treatment of IgG 2A11 and DITC. Mice were treated with PBS, 2A11, 50 mg/kg of DITC, 25 mg/kg of DITC, 12.5 mg/kg of DITC and combination of 2A11 with DITC. Tumor volumes were measured over the period of treatment. Data are shown as Mean ± SEM.

Day	**PBS**	**2A11**	**2A11 + 25 mg/kg DITC**	**2A11 + 12.5 mg/kg DITC**	**50 mg/kg DITC**	**25 mg/kg DITC**	**12.5 mg/kg DITC**
0	66.4 ± 6.0	81.7 ± 9.0	76.4 ± 5.0	74.8 ± 6.0	72.5 ± 7.0	72.7 ± 6.0	72.3 ± 13
3	108.0 ± 7.0	97.9 ± 15	82.4 ± 7.0	87.4 ± 3.0	90.6 ± 11	102.4 ± 9.0	85.3 ± 14
6	162.0 ± 16	99.9 ± 12	80.8 ± 8.0	99.5 ± 7.0	100.0 ± 13	113.2 ± 17	121.3 ± 21
9	250.6 ± 29	118.7 ± 17	57.3 ± 4.0	96.1 ± 13	89.1 ± 12	141.7 ± 20	150.4 ± 24
12	378.1 ± 30	206.9 ± 26	59.4 ± 7.0	85.6 ± 13	77.7 ± 13	125.3 ± 15	152.6 ± 26
15	484.0 ± 33	268.1 ± 32	53.5 ± 7.0	78.0 ± 10	71.7 ± 13	103.4 ± 13	176.6 ± 29
18	528.2 ± 47	319.8 ± 38	45.3 ± 6.0	75.8 ± 9.0	59.7 ± 10	93.5 ± 11	134.4 ± 23
21	573.0 ± 64	374.9 ± 46	40.3 ± 8.0	80.5 ± 11	46.0 ± 7.0	88.5 ± 10	100.3 ± 22
24	892.2 ± 43	521.6 ± 74	40.3 ± 8.0	79.9 ± 7.0	71.1 ± 14	89.1 ± 16	120.4 ± 23
27	1259.6 ± 88	779.1 ± 130	40.3 ± 8.0	73.6 ± 9.0	73.1 ± 15	89.6 ± 18	128.0 ± 22
30	0	0	34.8 ± 4	71.5 ± 6.0	71.3 ± 23	64.6 ± 12	115.6 ± 20
33	0	0	34.8 ± 4	64.5 ± 0.4	78.2 ± 32	64.6 ± 12	109.9 ± 19
36	0	0	34.8 ± 4	58.3 ± 3.0	78.2 ± 32	63.8 ± 11	100.2 ± 17
39	0	0	34.8 ± 4	61.4 ± 2.0	88.2 ± 42	63.8 ± 11	100.2 ± 17
42	0	0	20.4 ± 5	67.1 ± 2.0	151.8 ± 107	85.6 ± 18	160.1 ± 35

Cy5.5 conjugated IgG 2A11 is localized within the tumor with minimal distribution in other organs

To assess the biodistribution of IgG 2A11 we have conjugated the IgG 2A11 antibody with Cy5.5 as described in materials and methods. As control, we have conjugated a non specific mouse IgG with Cy5.5 using a similar method. WM115_MOCK and WM115_RAGE tumors bearing mice were intravenously injected with Cy5.5 conjugated antibodies. PBS was injected in the control group. Whole animal body imaging clearly demonstrated a higher accumulation of IgG 2A11 in WM115_RAGE tumors as compared to WM115_MOCK tumors (Figure 37). Fluorescence images of tumor sections after Cy5.5 conjugated antibodies injection also demonstrated a significant higher fluorescence in WM115_RAGE tumors as compared to MOCK tumors.

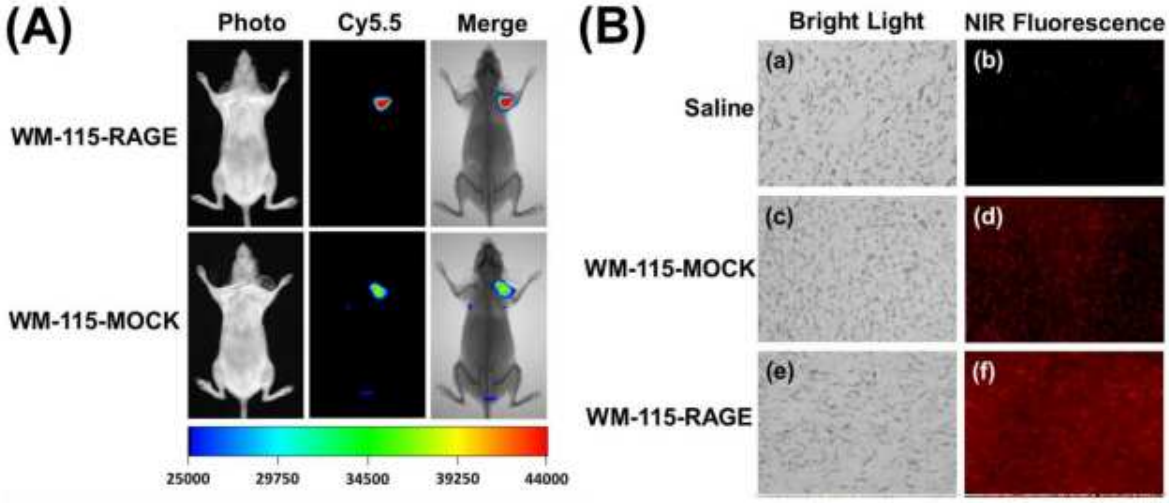

Figure 37: Distribution of Cy5.5 conjugated IgG 2A11 in WM115_MOCK and WM115_RAGE tumor bearing mice. Figure (A.) shows whole animal images of WM115_MOCK and WM115_RAGE tumors bearing mice after Cy5.5 conjugated IgG2A11 injection. Figure (B.) shows fluorescence images of WM115_MOCK and WM115_RAGE tumor sections after injection with Cy5.5 conjugated IgG2A11 and saline.

Combination of IgG 2A11 with Dacarbazine produce synergistic tumor suppressive activities

We could achieve 1.6 fold suppression in tumor growth with IgG 2A11 treatment alone. In an attempt to improve the therapeutic potential of IgG 2A11, we have treated WM115_RAGE tumor bearing mice with three different doses of dacarbazine (50mg/mg, 25 mg/kg and 12.5 mg/kg) and two combinations of dacarbazine (25 mg/kg and 12.5 mg/kg) with IgG 2A11. Our results demonstrate that the combination therapy of IgG 2A11 with dacarbazine synergistically enhance the therapeutic potential of IgG 2A11. The combination of IgG 2A11 with 12.5 mg/kg and 25 mg/kg of dacarbazine led to significant reduction in tumor growth compared to the treatment with dacarbazine alone. A combination therapy of IgG 2A11 with 25 mg/kg of dacarbazine produced significantly improved tumor suppressive activities than the treatment with 50 mg/kg of dacarbazine alone. Similarly, the tumor suppressive effect of the combination of IgG 2A11 with 12.5 mg/kg of dacarbazine was equivalent to that of 25 mg/kg of dacarbazine alone. On the 42^{th} day of treatment regimen, the average tumor volumes of the mice receiving a combination of IgG 2A11 with 25 mg/kg of dacarbazine (20.47 mm^3) was ≈7 fold smaller than those of the group receiving 50 mg/kg of dacarbazine (151.8 mm3) alone. Similarly, the average tumor volumes of mice receiving a combination of IgG 2A11 with 12.5 mg/kg of dacarbazine (67.1 mm^3) was ≈1.3 fold smaller than those in the group receiving 25 mg/kg of dacarbazine alone (Figure 38).

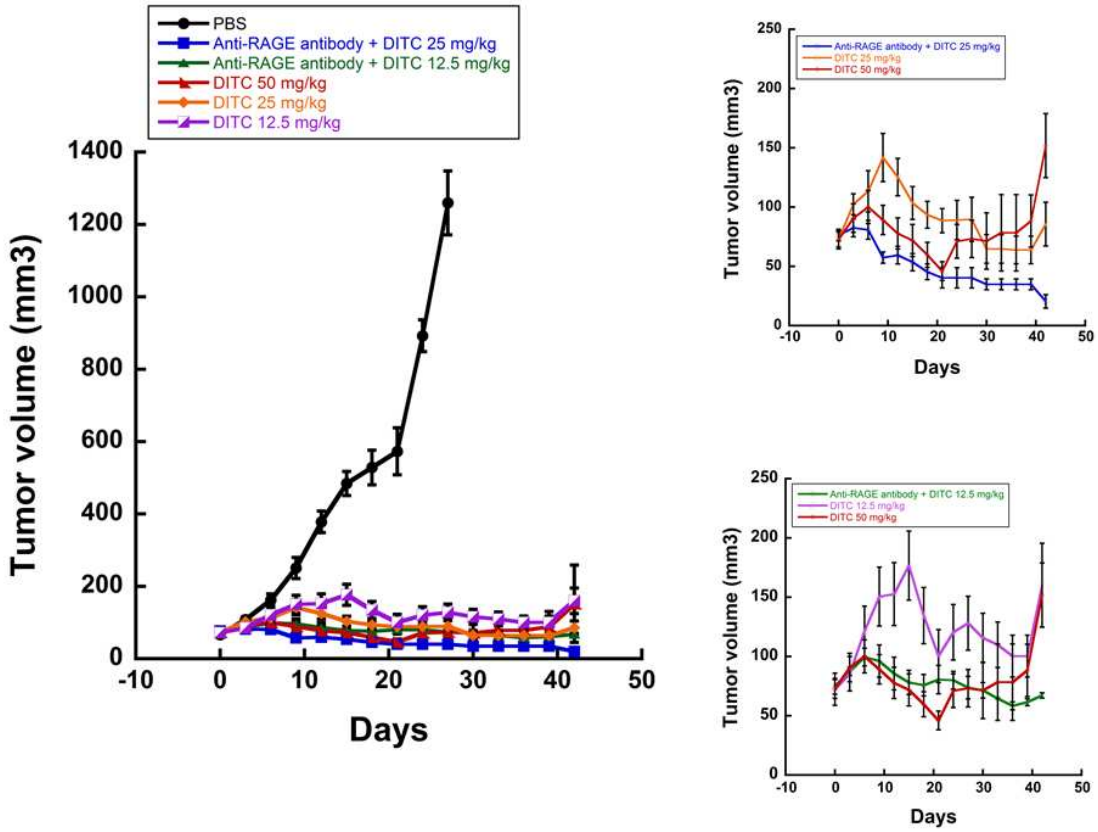

Figure 38: Combined therapy of IgG 2A11 with dacarbazine (DITC) in WM115_RAGE tumor bearing mice. Graph demonstrates tumor volumes of the groups treated with 50 mg/kg DITC alone (red), 25 mg/kg DITC alone (orange), 12.5 mg/kg DITC alone (pink), combination of 12.5 mg/kg DITC with IgG 2A11 (green) and combination of 25 mg/kg DITC with IgG 2A11 (blue). Data are shown as Mean ± SEM. (n = 4 or 8, *p < 0.05).

Discussion

In this study we have investigated RAGE as a new target in melanoma and also introduced anti-RAGE antibody as a therapeutic strategy for the set of melanoma patients with high expression levels of RAGE. We have shown that RAGE over-expression in melanoma led to enhanced tumor growth. The formation of tumors under the skin of immune- deficient mice is a multistep process that involves cell proliferation, cell spreading, cell migration and cell invasion [391, 392]. In Chapter 2 we demonstrated that RAGE over-expression increases the

anchorage independent growth, migration and invasion of WM115 cells, which are critical features for tumor formation and growth. However, we have also shown less proliferative traits of WM115_RAGE cells than their MOCK counterparts. Contrary to this, we have found increased growth of RAGE over-expressing WM115 tumors compared to MOCK tumors. These data suggests that the tumor microenvironment might switch the WM115_RAGE cells to a more proliferative state once injected under the mouse skin. Apart from cancer cells, the tumor also consists of non-cancer stromal cells which are acquired from the host body [393]. These cells which are embedded in extracellular matrix create a tumor microenvironment which is a major influencing factor on cancer growth [394, 395]. We propose that the enhanced tumorigenic growth of WM115_RAGE cells might be the result of a crosstalk between cancer cells and the surrounding activated stromal cells. RAGE and its various ligands have been previously reported to trigger an inflammatory tumor microenvironment and contribute in cancer pathogenesis [396]. Furthermore, we have also assessed the expression of five S100 proteins (S100B, S100A2, S100A4, S100A6, S100A10) which are known to be associated with melanoma. We found the upregulation in these S100 proteins in RAGE over-expressing melanoma tumors at both the transcript and protein levels. These data suggest a feedback regulation of these S100 proteins through RAGE to enhance, sustain and prolong signal activation to promote melanoma tumor growth. Previous reports have demonstrated that RAGE expression can be induced in its ligand rich tissue microenvironment [397]. We have presented a novel functional role of RAGE in regulating S100 proteins in melanoma tumor. S100 proteins are Ca^{+2} binding protein of the EF hand superfamily involved in melanoma pathogenesis [224]. Expression of S100B protein correlates with melanoma progression and serum concentration of S100B is used as a biomarker for melanoma [6]. S100B promotes melanoma progression by downregulating tumor suppressive

protein p53 [219]. Upregulation of S100B in WM115_RAGE tumors is significantly higher than that in WM115_RAGE cells as compared to their respective counterparts (Figure 35). Our data suggest that over-expression of RAGE in WM115 cells trigger S100B expression not only from cancer cells but also from surrounding stromal cells.

S100A2 has been previously shown to be down regulated in many cancer types as compared to their corresponding normal tissues and therefore it can be considered as a tumor suppressor protein [300, 398]. In squamous cell carcinoma, S100A2 has been shown to inhibit cell migration which supports its role as a tumor suppressor protein [259]. However, its precise role as a tumor suppressor has not been established yet. Our lab has also shown a significant down regulation of S100A2 transcripts levels in stage III and stage IV melanoma patients as compared to the normal skin [89]. Our results from chapter 3 showed a down regulation of S100A2 mRNA levels in WM115_RAGE cells as compared to MOCK control cells. However, in the corresponding WM115_RAGE tumors a significant upregulation of S100A2 mRNA levels was found compared to MOCK control tumors. However, the expression of S100A2 protein in the WM115 cells and their corresponding tumors was too low and could not be detected by Western blot in our experimental conditions.

S100A4 is another member of S100 protein superfamily also known as “Metastasin” due to its association with cancer metastasis [399]. RAGE/S100A4 interaction is rather complex and not very clear. We could not detect S100A4 protein in neither of the WM115 cell types (WM115_MOCK and WM115_RAGE cells) but we found enhanced S100A4 in WM115_RAGE tumors compared to MOCK tumors (Figure 33). This suggests that either the host stromal cells are the source of S100A4 protein or it has been induced in tumor cells by surrounding stromal cells. The induction of S100A4 protein by the tumor microenvironment in xenograft tumors of

human cancer cell lines has been reported previously [393]. S100A4 was not detected in either cell types, but in tumors, S100A4 was not only expressed but also significantly increased in response to RAGE over-expression.

S100A6 protein also referred as “Calcyclin” has been reported to interact with RAGE and to induce apoptosis via JNK signaling in neuroblastoma [108]. A positive correlation between S100A6 expression and melanoma metastasis has been reported [89]. Here, we showed a significant upregulation in S100A6 protein in WM115_RAGE tumors compared to MOCK tumors (Figure 34). RAGE mediated upregulation of S100A6 in WM115_RAGE tumors suggests an important role of S100A6 in melanoma progression.

S100A10, also referred as “Plasminogen Receptor” is another member of the S100 superfamily. It interacts with plasminogen and facilities its conversion to plasmin. Plasmin leads to the proteolytic cleavage of the extracellular matrix and in turn enhanced cell migration and invasion [321]. However S100A10 is unable to interact with RAGE but it has been implicated to play a role in cancer progression and metastasis. S100A10 has also been detected in melanoma cells but its role in melanoma progression is not clear. We showed an upregulation of S100A10 in WM115_RAGE tumors compared to MOCK tumors (Figure 34). S100A6 and S100A10 were unchanged in WM115 cells due to RAGE over-expression but found to be significantly upregulated in RAGE over-expressing WM115 tumors. These data suggest that the tumor microenvironment might contribute to the induction of these S100 proteins. The upregulation of S100A4, S100A6, S100A10 and S100B proteins in RAGE over-expressing melanoma tumors suggests their direct or indirect contribution in RAGE mediated enhanced melanoma tumor growth.

The cancer pathway array results demonstrate an upregulation of IL-8, Collagen XVIII, VEGF, PDGF-alpha and downregulation of p53 in WM115_RAGE tumors as compared to MOCK control (Table 16 & 17). Apart from the cancer cells RAGE is also expressed in other tumor associated cells such as macrophages, mast cells and endothelial cells [400]. Upon interaction with different ligands, RAGE triggers inflammatory responses within the tumor microenvironment. Activated inflammatory cells release various cytokines/chemokines, growth factors, adhesion molecules and certain RAGE ligands at the tumor site [103]. IL-8 is a growth factor important for melanoma cell proliferation and migration via CXC receptor [401, 402]. IL-8 also promotes cancer angiogenesis by enhancing endothelial cells proliferation and survival [403]. VEGF as its name implies, is a vascular endothelial growth factor which promotes angiogenesis via VEGF receptor [404]. PDGF-alpha is a potent mitogen and chemo attractant for fibroblasts and plays important roles in cancer progression and angiogenesis [405, 406]. Collagen XVIII is also known as Endostatin and is a component of basement membrane and known to be anti-angiogenic [407, 408]. Upregulation of IL-8, VEGF, PDGF-alpha in RAGE over-expressing melanoma tumors suggest that RAGE creates a growth factor rich tumor microenvironment that collectively contributes to enhanced melanoma tumor growth. The downregulation of p53 protein in WM115_RAGE tumors is in agreement with previous reports demonstrating negative correlation between S100B and p53 proteins in melanoma cells [219]. The increase expression of S100B protein in WM115_RAGE tumors might suppress p53 protein expression. However, the results from the cancer pathway gene array in WM115_MOCK and WM115_RAGE cells do not correlate with the results from their corresponding tumors (Table 8 & 9). We did not find any upregulation in IL-8, VEGF, PDGF-alpha genes in WM115_RAGE cells that were upregulated in the corresponding tumors as compared to their MOCK

counterparts. Contrary to this our results demonstrate the upregulation in PDGF-β gene in RAGE over-expressing WM115 cells compared to the MOCK cells. These data further emphasize the contribution of tumor microenvironment in modulating RAGE induced signaling involved in melanoma progression.

Upon analysis of further downstream signaling mediated by RAGE we found enhanced activities of AKT and ERK in WM115_RAGE tumors. ERK signaling was shown to be suppressed in WM115 cells due to RAGE over-expression. Moreover, AKT activities were not altered in WM115 cells after RAGE over-expression (Figure 23). The tumorigenic microenvironment might be responsible for inducing this functional and signaling switching in the WM115 cells inside the tumors.

Furthermore blocking of RAGE by anti-RAGE antibody (IgG 2A11) could significantly suppress melanoma tumor growth. IgG 2A11 used in this study was previously characterized for RAGE binding and its potential to compete with S100B for binding to RAGE was also determined (data not shown). Blocking RAGE binding sites could inhibit ligand interaction and thus inhibit RAGE induced downstream signaling. Our data suggest that the interaction of S100 proteins with RAGE might be involved in RAGE mediated enhanced melanoma tumor growth. Another possible mechanism of IgG 2A11 in suppressing melanoma tumor growth could be via antibody mediated receptor internalization. Antibody mediated internalization of RAGE might reduce the availability of RAGE on cell surface for RAGE ligands.

Animal's weights were monitored throughout the treatment period in order to assess any possible adverse effect of IgG 2A11. Most of the cytotoxic anticancer drugs non specifically kill healthy cells which directly affects animal's body weights. We found no change in animal's

weight in IgG 2A11 treated animals compared to control group. Also, the imaging studies of Cy5.5 conjugated IgG 2A11 showed a significantly higher accumulation in WM115_RAGE tumors compared to the other tissues. A higher Cy5.5 fluorescence observed in WM115_RAGE tumors compared to MOCK control suggests an enhanced localization of IgG 2A11 in WM115_RAGE tumors.

In the next set of study we have treated WM115_RAGE tumor bearing mice with a combination of IgG 2A11 and varied concentration of dacarbazine. Combination therapy produce synergistic tumor suppressive activities. Dacarbazine is a chemotherapeutic drug, extensively used for the treatment of melanoma. However, repetitive treatment with dacarbazine triggers an escape mechanism by increasing expression of IL-8 and VEGF in melanoma cells and therefore leads to enhanced melanoma tumor growth and metastasis [53, 409]. IgG 2A11 is believed to inhibit melanoma tumor growth by blocking RAGE mediated signaling in the tumor. Our results from cancer pathway gene array showed an upregulation of IL-8 and VEGF mRNAs in the RAGE over-expressing WM115 tumors compared to the MOCK control (Tables 16 and 17). We believe that the ability of IgG 2A11 in inhibiting RAGE mediated signaling, might overcome possible escape mechanism induced in the WM115 tumors upon dacarbazine treatment. Therefore combination therapy of dacarbazine with IgG 2A11 produced synergistic tumor suppressive effects as compared to dacarbazine alone. Melanoma has complex pathophysiology with multiple genetic and molecular aberrations [410]. Multi-targeted therapy for melanoma therefore presents the advantage of enhancing the overall efficiency of the therapy.

In summary we have demonstrated the role of RAGE in melanoma tumor growth and deciphered the downstream signal mechanisms. We have shown that RAGE over-expression modulates WM115 tumor microenvironment by increasing the expression of S100 proteins,

cytokines and growth factors inside the tumor. Furthermore, we have demonstrated that blocking RAGE with an anti-RAGE antibody could suppress RAGE induced melanoma tumor growth which could be further improved by a combination therapy of anti-RAGE antibody with dacarbazine.

SUPPLEMENTARY FIGURE

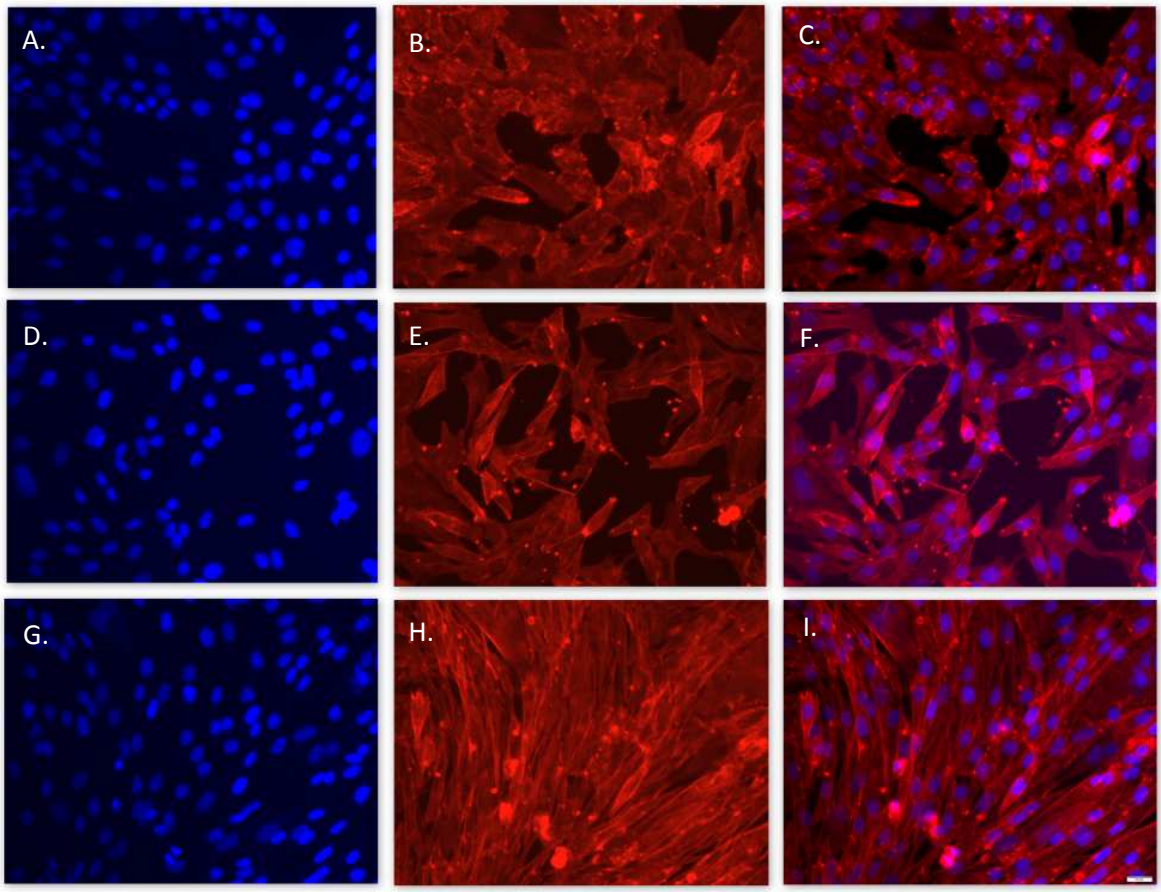

Figure 39: Filamentous actin staining with rhodamine conjugated phalloidin in WM115_MOCK (top), WM115_RAGE-I (middle) and WM115_RAGE (bottom) cells. Images A, D and G show nuclei staining with Hoechst dye. Images B, E and H show actin staining with phalloidin. C, F and I are the merged images.

CONCLUSIONS AND FUTURE DIRECTIONS

The present study suggests that RAGE plays a significant role in melanoma progression by triggering a metastatic like phenotype in the WM115 melanoma cells and by promoting tumor growth in the xenograft mouse model generated from the same cells.

RAGE over-expression led to phenotypic changes in WM115 cells from a epithelial like polyglonal morphology to a mesenchymal like elongated morphology. Phenotypic changes induced by RAGE in WM115 cells might translate into proliferative to migratory switch in these cells. Our results demonstrated an enhanced migration but reduced proliferation of the WM115 cells upon RAGE over-expression. Moreover, we showed that RAGE induced its own ligand (S100B protein) expression in WM115 cells. However, S100B protein did not appear to contribute to RAGE mediated enhanced WM115 cells motility. RAGE mediated enhanced motilities in the WM115_RAGE cells seems to be independent of any ligand stimulation and might be through cell surface oligomerization of RAGE molecules in the WM115_RAGE cells

Furthermore, we showed a downregulation in tumor suppressor p53 that is one of the binding targets of S100B, in WM115_RAGE cells compared to MOCK cells. Interestingly, we didn’t observe any change in cell cycle due to reduced p53 protein levels in WM115_RAGE cells. Apart from cell cycle regulation, p53 protein is also associated with cell migration, therefore, we suggest that enhanced cell migration of the WM115_RAGE cells is mediated through p53 protein. Furthermore, we also showed a downregulation in cyclin E protein in RAGE over-expressing WM115 cells. RAGE over-expression resulted in decreased ERK and NF-kB signaling activities in WM115 cells. Decreased cyclin E, ERK and NF-kB signaling activities might be involved in reduced cell proliferation obtained in WM115_RAGE cells.

Upon subcutaneous implantation of the transfected WM115 cells in mice, WM115_RAGE cells showed a stronger tumorigenic potential compared to the MOCK control cells. Furthermore, the tumors generated from WM115_RAGE cells showed upregulation of S100B, S100A4, S100A6 and S100A10 proteins compared to MOCK tumors suggesting an active participation of the host derived tumor microenvironment in modulating the RAGE mediated signaling pathways. Moreover, enhanced expression of several cytokines, growth factors and angiogenic factors (IL-8, VEGF-A, Angiopoitin-2) in WM115_RAGE tumors further emphasize the influence of the tumorigenic microenvironment in RAGE induced signaling in melanoma tumors. We showed a reduced ERK signaling in RAGE over-expressing WM115 cells, however, an enhanced ERK signaling activation was observed in the corresponding WM115 tumors. Likewise, AKT signaling was not found to be activated in RAGE over-expressing WM115 cells but in the corresponding tumors we found a significant higher activation of AKT signaling compared to MOCK tumors. We have shown that RAGE over-expressing WM115 cells were less proliferative compared to MOCK cells, but the tumors generated from these cells were shown to grow faster than their MOCK counterparts. The mechanism that alters the cellular behavior of the cancer cells inside the tumors is not understood yet. We propose an interplay between RAGE over-expressing WM115 cells and the surrounding host cells of the tumors that modulates the cellular properties of cancer cells at molecular levels inside the tumors.

Furthermore, treatment with anti-RAGE antibody could significantly suppress the melanoma tumor growth compared to PBS controls. Moreover, combination therapy of anti-RAGE antibody together with dacarbazine resulted in synergistic tumor suppressive effects.

These data suggest that RAGE blocking antibody could be an efficient strategy to inhibit RAGE mediated melanoma progression.

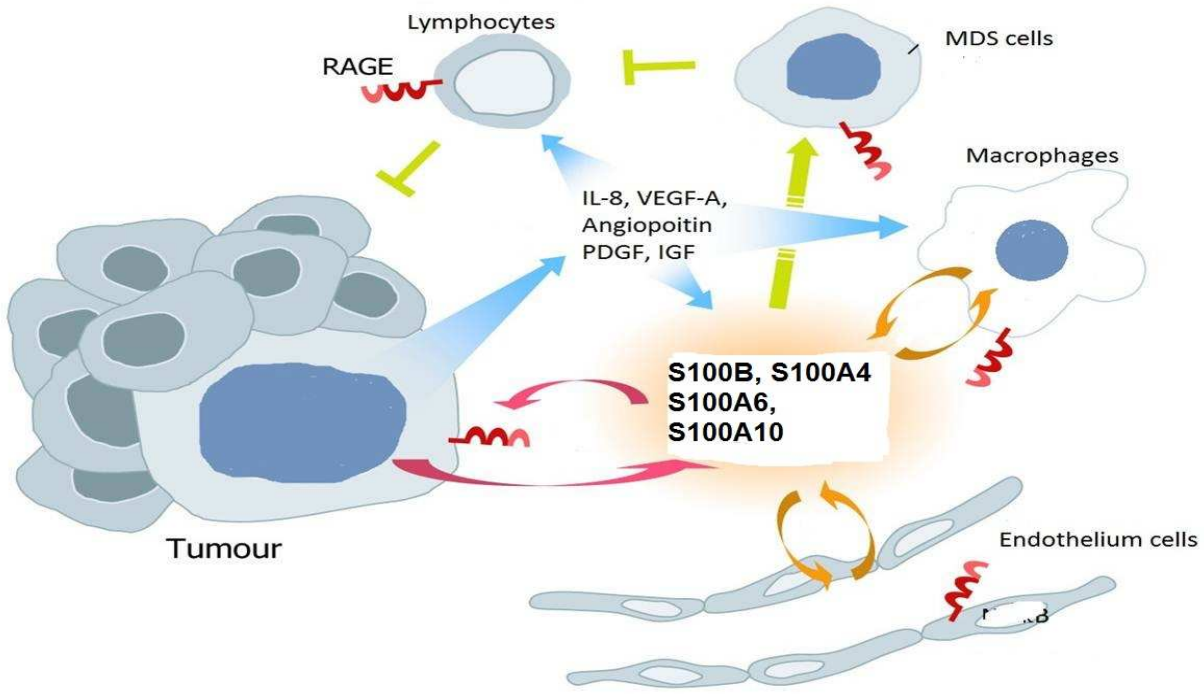

Figure 40: Schematic representation of RAGE mediated melanoma progression. Over-expression of RAGE in the melanoma cells resulted in upregulation of RAGE ligands (S100B, S100A4, S100A6 and S100A10) and cytokines inside the tumor. Modified from [386].

In the present study we have demonstrated the role of RAGE in melanoma progression and also introduced anti-RAGE antibody as a therapeutic strategy for melanoma treatment. However, there are few questions that still need to be answered.

What is the mechanism behind RAGE mediated switching of melanoma cells between proliferative to migratory states? What is the role of actin remodeling in enhanced WM115_RAGE cells migration and invasion potential?

What is the mechanism underlying RAGE mediated modulation of S100B protein in melanoma cells? What is the molecular mechanism involved in behavioral switch induced in the

transfected WM115 cells after their implantation under the mouse skin? How host derived tumor microenvironment affects the cellular properties of cancer cells?

The above mentioned questions would be answered in the future in order to better understand the role of RAGE in melanoma progression.

REFERENCES

[1] Purdue MP, Freeman L, Anderson WF, Tucker MA. Recent trends in incidence of cutaneous melanoma among US Caucasian young adults. The Journal of investigative dermatology. 2008;128:2905-8.

[2] Berking C, Takemoto R, Satyamoorthy K, Elenitsas R, Herlyn M. Basic fibroblast growth factor and ultraviolet B transform melanocytes in human skin. The American journal of pathology. 2001;158:943-53.

[3] Palmieri G, Capone M, Ascierto M, Gentilcore G, Stroncek D, Casula M, et al. Main roads to melanoma. J Transl Med. 2009;7:86.

[4] Ando H, Ichihashi M, Hearing VJ. Role of the ubiquitin proteasome system in regulating skin pigmentation. International journal of molecular sciences. 2009;10:4428-34.

[5] Balch CM, Gershenwald JE, Soong S-j, Thompson JF, Atkins MB, Byrd DR, et al. Final version of 2009 AJCC melanoma staging and classification. Journal of Clinical Oncology. 2009;27:6199-206.

[6] Gogas H, Eggermont A, Hauschild A, Hersey P, Mohr P, Schadendorf D, et al. Biomarkers in melanoma. Annals of oncology. 2009;20:8-13.

[7] Narayanan DL, Saladi RN, Fox JL. Review: Ultraviolet radiation and skin cancer. International journal of dermatology. 2010;49:978-86.

[8] Howlader N, Noone A, Krapcho M, Neyman N, Aminou R, Altekruse S, et al. SEER cancer statistics review, 1975–2009 (vintage 2009 populations). Bethesda, MD: National Cancer Institute. 2012.

[9] Bhatia S, Tykodi SS, Thompson JA. Treatment of metastatic melanoma: an overview. Oncology (Williston Park, NY). 2009;23:488.

[10] Herlyn M, Balaban G, Bennicelli J, Guerry D, Halaban R, Herlyn D, et al. Primary melanoma cells of the vertical growth phase: similarities to metastatic cells. Journal of the National Cancer Institute. 1985;74:283-9.

[11] Haass NK, Smalley KS, Herlyn M. The role of altered cell–cell communication in melanoma progression. Journal of molecular histology. 2004;35:309-18.

[12] Li G, Satyamoorthy K, Herlyn M. N-cadherin-mediated intercellular interactions promote survival and migration of melanoma cells. Cancer research. 2001;61:3819-25.

[13] Haass NK, Smalley KS, Li L, Herlyn M. Adhesion, migration and communication in melanocytes and melanoma. Pigment cell research. 2005;18:150-9.

[14] Hsu M, Wheelock M, Johnson K, Herlyn M. Shifts in cadherin profiles between human normal melanocytes and melanomas. The journal of investigative dermatology Symposium proceedings/the Society for Investigative Dermatology, Inc European Society for Dermatological Research1996. p. 188-94.

[15] Kuphal S, Bosserhoff A. Influence of the cytoplasmic domain of E-cadherin on endogenous N-cadherin expression in malignant melanoma. Oncogene. 2005;25:248-59.

[16] Robert G, Gaggioli C, Bailet O, Chavey C, Abbe P, Aberdam E, et al. SPARC represses E-cadherin and induces mesenchymal transition during melanoma development. Cancer research. 2006;66:7516-23.

[17] Geiger TR, Peeper DS. Metastasis mechanisms. Biochimica et Biophysica Acta (BBA)-Reviews on Cancer. 2009;1796:293-308.

[18] McConkey DJ, Choi W, Marquis L, Martin F, Williams MB, Shah J, et al. Role of epithelial-to-mesenchymal transition (EMT) in drug sensitivity and metastasis in bladder cancer. Cancer and Metastasis Reviews. 2009;28:335-44.
[19] Niu R, Zhang L, Xi G, Wei X, Yang Y, Shi Y, et al. Up-regulation of Twist induces angiogenesis and correlates with metastasis in hepatocellular carcinoma. J Exp Clin Cancer Res. 2007;26:385-94.
[20] Hoek KS, Eichhoff OM, Schlegel NC, Döbbeling U, Kobert N, Schaerer L, et al. In vivo switching of human melanoma cells between proliferative and invasive states. Cancer research. 2008;68:650-6.
[21] Perego M, Tortoreto M, Tragni G, Mariani L, Deho P, Carbone A, et al. Heterogeneous phenotype of human melanoma cells with in vitro and in vivo features of tumor-initiating cells. Journal of Investigative Dermatology. 2010;130:1877-86.
[22] Hendrix MJ, Seftor EA, Hess AR, Seftor RE. Molecular plasticity of human melanoma cells. Oncogene. 2003;22:3070-5.
[23] Hoek KS, Goding CR. Cancer stem cells versus phenotype-switching in melanoma. Pigment cell & melanoma research. 2010;23:746-59.
[24] Hendrix MJ, Seftor EA, Hess AR, Seftor RE. Vasculogenic mimicry and tumour-cell plasticity: lessons from melanoma. Nature Reviews Cancer. 2003;3:411-21.
[25] Dalton WS, Friend SH. Cancer biomarkers—an invitation to the table. Science. 2006;312:1165-8.
[26] Strimbu K, Tavel JA. What are biomarkers? Current opinion in HIV and AIDS. 2010;5:463-6.
[27] Ludwig JA, Weinstein JN. Biomarkers in cancer staging, prognosis and treatment selection. Nature Reviews Cancer. 2005;5:845-56.
[28] Karley D, Gupta D, Tiwari A. Biomarker for cancer: A great promise for future. World Journal of Oncology. 2011;2:151-7.
[29] Leclerc E, Fritz G, Vetter SW, Heizmann CW. Binding of S100 proteins to RAGE: an update. Biochimica et Biophysica Acta (BBA)-Molecular Cell Research. 2009;1793:993-1007.
[30] Gaynor R, Irie R, Morton D, Herschman HR. S100 protein is present in cultured human malignant melanomas. 1980:400-1.
[31] Cao MG, Auge J, Molina R, Marti R, Carrera C, Castel T, et al. Melanoma inhibiting activity protein (MIA), beta-2 microglobulin and lactate dehydrogenase (LDH) in metastatic melanoma. Anticancer research. 2007;27:595-9.
[32] De Gast B, Smit L, Haanen J, Bonfrer H. The biomarker serum S100B identifies responders and prolonged survival in stage IV melanoma. J Clin Oncol (Meeting Abstracts)2004. p. 7519.
[33] Garbe C, Schadendorf D, Stolz W, Volkenandt M, Reinhold U, Kortmann RD, et al. Short German guidelines: malignant melanoma. JDDG: Journal der Deutschen Dermatologischen Gesellschaft. 2008;6:S9-S14.
[34] Garnier J-P, Letellier S, Cassinat B, Lebbé C, Kerob D, Baccard M, et al. Clinical value of combined determination of plasma L-DOPA/tyrosine ratio, S100B, MIA and LDH in melanoma. European Journal of Cancer. 2007;43:816-21.
[35] Palmer SR, Erickson LA, Ichetovkin I, Knauer DJ, Markovic SN. Circulating serologic and molecular biomarkers in malignant melanoma. Mayo Clinic Proceedings: Elsevier; 2011. p. 981-90.
[36] Ho J, de Moura MB, Lin Y, Vincent G, Thorne S, Duncan LM, et al. Importance of glycolysis and oxidative phosphorylation in advanced melanoma. Mol Cancer. 2012;11:76.

[37] Koukourakis M, Giatromanolaki A, Sivridis E, Bougioukas G, Didilis V, Gatter K, et al. Lactate dehydrogenase-5 (LDH-5) overexpression in non-small-cell lung cancer tissues is linked to tumour hypoxia, angiogenic factor production and poor prognosis. British journal of cancer. 2003;89:877-85.
[38] Hill BR, Levi C. Elevation of a serum component in neoplastic disease. Cancer research. 1954;14:513-5.
[39] Bogdahn U, Apfel R, Hahn M, Gerlach M, Behl C, Hoppe J, et al. Autocrine tumor cell growth-inhibiting activities from human malignant melanoma. Cancer research. 1989;49:5358-63.
[40] Blesch A, Boßerhoff A-K, Apfel R, Behl C, Hessdoerfer B, Schmitt A, et al. Cloning of a novel malignant melanoma-derived growth-regulatory protein, MIA. Cancer research. 1994;54:5695-701.
[41] Stahlecker J, Gauger A, Bosserhoff A, Büttner R, Ring J, Hein R. MIA as a reliable tumor marker in the serum of patients with malignant melanoma. Anticancer research. 2000;20:5041-4.
[42] Krähn G, Kaskel P, Sander S, Waizenhöfer P, Wortmann S, Leiter U, et al. S100 beta is a more reliable tumor marker in peripheral blood for patients with newly occurred melanoma metastases compared with MIA, albumin and lactate-dehydrogenase. Anticancer research. 2001;21:1311-6.
[43] Deichmann M, Benner A, Bock M, Jäckel A, Uhl K, Waldmann V, et al. S100-Beta, melanoma-inhibiting activity, and lactate dehydrogenase discriminate progressive from nonprogressive American Joint Committee on Cancer stage IV melanoma. Journal of Clinical Oncology. 1999;17:1891-6.
[44] Vakiani E, Solit DB. KRAS and BRAF: drug targets and predictive biomarkers. The Journal of pathology. 2011;223:220-30.
[45] Flaherty KT, Puzanov I, Kim KB, Ribas A, McArthur GA, Sosman JA, et al. Inhibition of mutated, activated BRAF in metastatic melanoma. New England Journal of Medicine. 2010;363:809-19.
[46] Garrido MC, Bastian BC. KIT as a therapeutic target in melanoma. Journal of Investigative Dermatology. 2009;130:20-7.
[47] Howell Jr PM, Liu S, Ren S, Behlen C, Fodstad O, Riker AI. Epigenetics in human melanoma. Cancer control: journal of the Moffitt Cancer Center. 2009;16:200-18.
[48] Garbe C, Eigentler TK, Keilholz U, Hauschild A, Kirkwood JM. Systematic review of medical treatment in melanoma: current status and future prospects. The oncologist. 2011;16:5-24.
[49] Thomas JM, Newton-Bishop J, A'Hern R, Coombes G, Timmons M, Evans J, et al. Excision margins in high-risk malignant melanoma. New England Journal of Medicine. 2004;350:757-66.
[50] Garbe C, Peris K, Hauschild A, Saiag P, Middleton M, Spatz A, et al. Diagnosis and treatment of melanoma: European consensus-based interdisciplinary guideline. European Journal of Cancer. 2010;46:270-83.
[51] Khan N, Khan MK, Almasan A, Singh AD, Macklis R. The evolving role of radiation therapy in the management of malignant melanoma. International Journal of Radiation Oncology* Biology* Physics. 2011;80:645-54.
[52] Lee C, Collichio F, Ollila D, Moschos S. Historical review of melanoma treatment and outcomes. Clinics in dermatology. 2013;31:141-7.
[53] Lev DC, Ruiz M, Mills L, McGary EC, Price JE, Bar-Eli M. Dacarbazine Causes Transcriptional Up-Regulation of Interleukin 8 and Vascular Endothelial Growth Factor in

Melanoma Cells: A Possible Escape Mechanism from Chemotherapy1. Molecular Cancer Therapeutics. 2003;2:753-63.
[54] Robert C, Thomas L, Bondarenko I, O'Day S, Weber J, Garbe C, et al. Ipilimumab plus dacarbazine for previously untreated metastatic melanoma. New England Journal of Medicine. 2011;364:2517-26.
[55] Phan GQ, Yang JC, Sherry RM, Hwu P, Topalian SL, Schwartzentruber DJ, et al. Cancer regression and autoimmunity induced by cytotoxic T lymphocyte-associated antigen 4 blockade in patients with metastatic melanoma. Proceedings of the National Academy of Sciences. 2003;100:8372-7.
[56] Downey SG, Klapper JA, Smith FO, Yang JC, Sherry RM, Royal RE, et al. Prognostic factors related to clinical response in patients with metastatic melanoma treated by CTL-associated antigen-4 blockade. Clinical Cancer Research. 2007;13:6681-8.
[57] Pardoll DM. The blockade of immune checkpoints in cancer immunotherapy. Nature Reviews Cancer. 2012;12:252-64.
[58] Hodi FS, O'Day SJ, McDermott DF, Weber RW, Sosman JA, Haanen JB, et al. Improved survival with ipilimumab in patients with metastatic melanoma. New England Journal of Medicine. 2010;363:711-23.
[59] Camacho LH, Antonia S, Sosman J, Kirkwood JM, Gajewski TF, Redman B, et al. Phase I/II trial of tremelimumab in patients with metastatic melanoma. Journal of Clinical Oncology. 2009;27:1075-81.
[60] Mansh M. Ipilimumab and cancer immunotherapy: a new hope for advanced stage melanoma. The Yale journal of biology and medicine. 2011;84:381-9.
[61] Tseng H-W, Li W-T, Hsieh J-F. Targeted Agents for the Treatment of Melanoma: An Overview. 2013:231-51.
[62] Ledford H. Melanoma drug wins US approval. nature. 2011;471:561.
[63] Lipson EJ, Drake CG. Ipilimumab: an anti-CTLA-4 antibody for metastatic melanoma. Clinical Cancer Research. 2011;17:6958-62.
[64] Ascierto PA, Kirkwood JM, Grob J-J, Simeone E, Grimaldi AM, Maio M, et al. The role of BRAF V600 mutation in melanoma. J Transl Med. 2012;10:85-93.
[65] Amaria R, Lewis K, Jimeno A. Vemurafenib: the road to personalized medicine in melanoma. Drugs of today (Barcelona, Spain: 1998). 2012;48:109-18.
[66] Mullard A. 2011 FDA drug approvals. Nature Reviews Drug Discovery. 2012;11:91-4.
[67] Luke JJ, Hodi FS. Vemurafenib and BRAF inhibition: a new class of treatment for metastatic melanoma. Clinical Cancer Research. 2012;18:9-14.
[68] Sumimoto H, Imabayashi F, Iwata T, Kawakami Y. The BRAF–MAPK signaling pathway is essential for cancer-immune evasion in human melanoma cells. The Journal of experimental medicine. 2006;203:1651-6.
[69] Tse KF, Jeffers M, Pollack VA, McCabe DA, Shadish ML, Khramtsov NV, et al. CR011, a fully human monoclonal antibody-auristatin E conjugate, for the treatment of melanoma. Clinical Cancer Research. 2006;12:1373-82.
[70] Yang HM, Reisfeld RA. Doxorubicin conjugated with a monoclonal antibody directed to a human melanoma-associated proteoglycan suppresses the growth of established tumor xenografts in nude mice. Proceedings of the National Academy of Sciences. 1988;85:1189-93.
[71] Pollack VA, Alvarez E, Tse KF, Torgov MY, Xie S, Shenoy SG, et al. Treatment parameters modulating regression of human melanoma xenografts by an antibody–drug

conjugate (CR011-vcMMAE) targeting GPNMB. Cancer chemotherapy and pharmacology. 2007;60:423-35.
[72] Alley SC, Okeley NM, Senter PD. Antibody–drug conjugates: targeted drug delivery for cancer. Current opinion in chemical biology. 2010;14:529-37.
[73] Ornes S. Antibody–drug conjugates. Proceedings of the National Academy of Sciences of the United States of America. 2013;110:13695.
[74] Ciccocioppo R, Vanoli A, Klersy C, Imbesi V, Boccaccio V, Manca R, et al. Role of the advanced glycation end products receptor in Crohn's disease inflammation. World journal of gastroenterology: WJG. 2013;19:8269-81.
[75] Oliveira MIA, Souza EMd, Pedrosa FdO, Réa RR, Alves AdSC, Picheth G, et al. RAGE receptor and its soluble isoforms in diabetes mellitus complications. Jornal Brasileiro de Patologia e Medicina Laboratorial. 2013;49:97-108.
[76] Neeper M, Schmidt A, Brett J, Yan S, Wang F, Pan Y, et al. Cloning and expression of a cell surface receptor for advanced glycosylation end products of proteins. Journal of Biological Chemistry. 1992;267:14998-5004.
[77] Srikrishna G, Huttunen HJ, Johansson L, Weigle B, Yamaguchi Y, Rauvala H, et al. N - Glycans on the receptor for advanced glycation end products influence amphoterin binding and neurite outgrowth. Journal of neurochemistry. 2002;80:998-1008.
[78] Taguchi A, Blood DC, del Toro G, Canet A, Lee DC, Qu W, et al. Blockade of RAGE–amphoterin signalling suppresses tumour growth and metastases. nature. 2000;405:354-60.
[79] Park H, Boyington JC. The 1.5 Å crystal structure of human receptor for advanced glycation endproducts (RAGE) ectodomains reveals unique features determining ligand binding. Journal of Biological Chemistry. 2010;285:40762-70.
[80] Hudson BI, Kalea AZ, del Mar Arriero M, Harja E, Boulanger E, D'Agati V, et al. Interaction of the RAGE cytoplasmic domain with diaphanous-1 is required for ligand-stimulated cellular migration through activation of Rac1 and Cdc42. Journal of Biological Chemistry. 2008;283:34457-68.
[81] Raucci A, Cugusi S, Antonelli A, Barabino SM, Monti L, Bierhaus A, et al. A soluble form of the receptor for advanced glycation endproducts (RAGE) is produced by proteolytic cleavage of the membrane-bound form by the sheddase a disintegrin and metalloprotease 10 (ADAM10). The FASEB Journal. 2008;22:3716-27.
[82] Park IH, Yeon SI, Youn JH, Choi JE, Sasaki N, Choi I-H, et al. Expression of a novel secreted splice variant of the receptor for advanced glycation end products (RAGE) in human brain astrocytes and peripheral blood mononuclear cells. Molecular immunology. 2004;40:1203-11.
[83] Hudson BI, Carter AM, Harja E, Kalea AZ, Arriero M, Yang H, et al. Identification, classification, and expression of RAGE gene splice variants. The FASEB Journal. 2008;22:1572-80.
[84] Vazzana N, Santilli F, Cuccurullo C, Davì G. Soluble forms of RAGE in internal medicine. Internal and emergency medicine. 2009;4:389-401.
[85] Zhang L, Bukulin M, Kojro E, Roth A, Metz VV, Fahrenholz F, et al. Receptor for advanced glycation end products is subjected to protein ectodomain shedding by metalloproteinases. Journal of Biological Chemistry. 2008;283:35507-16.
[86] Galichet A, Weibel M, Heizmann CW. Calcium-regulated intramembrane proteolysis of the RAGE receptor. Biochemical and biophysical research communications. 2008;370:1-5.

[87] Kalea AZ, See F, Harja E, Arriero M, Schmidt AM, Hudson BI. Alternatively spliced RAGEv1 inhibits tumorigenesis through suppression of JNK signaling. Cancer research. 2010;70:5628-38.
[88] Tesarova P, Kalousová M, Jáchymová M, Mestek O, Petruzelka L, Zima T. Receptor for advanced glycation end products (RAGE)-soluble form (sRAGE) and gene polymorphisms in patients with breast cancer. Cancer investigation. 2007;25:720-5.
[89] Leclerc E, Heizmann CW, Vetter SW. RAGE and S100 protein transcription levels are highly variable in human melanoma tumors and cells. Gen Physiol Biophys. 2009;28:65-75.
[90] Yamagishi S, Matsui T. Soluble form of a receptor for advanced glycation end products (sRAGE) as a biomarker. Frontiers in bioscience (Elite edition). 2010;2:1184-95.
[91] Wendt T, Tanji N, Guo J, Hudson BI, Bierhaus A, Ramasamy R, et al. Glucose, glycation, and RAGE: implications for amplification of cellular dysfunction in diabetic nephropathy. Journal of the American Society of Nephrology. 2003;14:1383-95.
[92] Huttunen HJ, Kuja-Panula J, Sorci G, Agneletti AL, Donato R, Rauvala H. Coregulation of neurite outgrowth and cell survival by amphoterin and S100 proteins through receptor for advanced glycation end products (RAGE) activation. Journal of Biological Chemistry. 2000;275:40096-105.
[93] Hori O, Brett J, Slattery T, Cao R, Zhang J, Chen JX, et al. The receptor for advanced glycation end products (RAGE) is a cellular binding site for amphoterin Mediation of neurite outgrowth and co-expression of rage and amphoterin in the developing nervous system. Journal of Biological Chemistry. 1995;270:25752-61.
[94] Nishiyama H, Knöpfel T, Endo S, Itohara S. Glial protein S100B modulates long-term neuronal synaptic plasticity. Proceedings of the National Academy of Sciences. 2002;99:4037-42.
[95] Sakaguchi T, Yan SF, Du Yan S, Belov D, Rong LL, Sousa M, et al. Central role of RAGE-dependent neointimal expansion in arterial restenosis. Journal of Clinical Investigation. 2003;111:959-72.
[96] Buckley ST, Ehrhardt C. The receptor for advanced glycation end products (RAGE) and the lung. Journal of Biomedicine and Biotechnology. 2010;2010:1-12.
[97] Englert JM, Hanford LE, Kaminski N, Tobolewski JM, Tan RJ, Fattman CL, et al. A role for the receptor for advanced glycation end products in idiopathic pulmonary fibrosis. The American journal of pathology. 2008;172:583-91.
[98] Bartling B, Hofmann H-S, Weigle B, Silber R-E, Simm A. Down-regulation of the receptor for advanced glycation end-products (RAGE) supports non-small cell lung carcinoma. Carcinogenesis. 2005;26:293-301.
[99] Schmidt AM, Vianna M, Gerlach M, Brett J, Ryan J, Kao J, et al. Isolation and characterization of two binding proteins for advanced glycosylation end products from bovine lung which are present on the endothelial cell surface. Journal of Biological Chemistry. 1992;267:14987-97.
[100] Hofmann MA, Drury S, Fu C, Qu W, Taguchi A, Lu Y, et al. RAGE mediates a novel proinflammatory axis: a central cell surface receptor for S100/calgranulin polypeptides. Cell. 1999;97:889-901.
[101] Sousa MM, Du Yan S, Stern D, Saraiva MJ. Interaction of the receptor for advanced glycation end products (RAGE) with transthyretin triggers nuclear transcription factor kB (NF-kB) activation. Laboratory investigation. 2000;80:1101-10.

[102] Deane R, Du Yan S, Submamaryan RK, LaRue B, Jovanovic S, Hogg E, et al. RAGE mediates amyloid-β peptide transport across the blood-brain barrier and accumulation in brain. Nature medicine. 2003;9:907-13.
[103] Chavakis T, Bierhaus A, Al-Fakhri N, Schneider D, Witte S, Linn T, et al. The Pattern Recognition Receptor (RAGE) Is a Counterreceptor for Leukocyte Integrins A Novel Pathway for Inflammatory Cell Recruitment. The Journal of experimental medicine. 2003;198:1507-15.
[104] He M, Kubo H, Morimoto K, Fujino N, Suzuki T, Takahasi T, et al. Receptor for advanced glycation end products binds to phosphatidylserine and assists in the clearance of apoptotic cells. EMBO reports. 2011;12:358-64.
[105] Ruan BH, Li X, Winkler AR, Cunningham KM, Kuai J, Greco RM, et al. Complement C3a, CpG oligos, and DNA/C3a complex stimulate IFN-α production in a receptor for advanced glycation end product-dependent manner. The Journal of Immunology. 2010;185:4213-22.
[106] Fritz G. RAGE: a single receptor fits multiple ligands. Trends in biochemical sciences. 2011;36:625-32.
[107] Koch M, Chitayat S, Dattilo BM, Schiefner A, Diez J, Chazin WJ, et al. Structural basis for ligand recognition and activation of RAGE. Structure. 2010;18:1342-52.
[108] Leclerc E, Fritz G, Weibel M, Heizmann CW, Galichet A. S100B and S100A6 differentially modulate cell survival by interacting with distinct RAGE (receptor for advanced glycation end products) immunoglobulin domains. Journal of Biological Chemistry. 2007;282:31317-31.
[109] Donato R, Sorci G, Riuzzi F, Arcuri C, Bianchi R, Brozzi F, et al. S100B's double life: intracellular regulator and extracellular signal. Biochimica et Biophysica Acta (BBA)-Molecular Cell Research. 2009;1793:1008-22.
[110] Sparvero LJ, Asafu-Adjei D, Kang R, Tang D, Amin N, Im J, et al. RAGE (Receptor for Advanced Glycation Endproducts), RAGE ligands, and their role in cancer and inflammation. J Transl Med. 2009;7:17.
[111] Yan SF, Ramasamy R, Schmidt AM. The receptor for advanced glycation endproducts (RAGE) and cardiovascular disease. Expert Rev Mol Med. 2009;11:1-12.
[112] Stern DM, Yan SD, Yan SF, Schmidt AM. Receptor for advanced glycation endproducts (RAGE) and the complications of diabetes. Ageing research reviews. 2002;1:1-15.
[113] Morbini P, Villa C, Campo I, Zorzetto M, Inghilleri S, Luisetti M. The receptor for advanced glycation end products and its ligands: a new inflammatory pathway in lung disease? Modern Pathology. 2006;19:1437-45.
[114] Münch G, Westcott B, Menini T, Gugliucci A. Advanced glycation endproducts and their pathogenic roles in neurological disorders. Amino Acids. 2012;42:1221-36.
[115] Hirose A, Tanikawa T, Mori H, Okada Y, Tanaka Y. Advanced glycation end products increase endothelial permeability through the RAGE/Rho signaling pathway. FEBS letters. 2010;584:61-6.
[116] O'Neill LA, Kaltschmidt C. NF-kB: a crucial transcription factor for glial and neuronal cell function. Trends in neurosciences. 1997;20:252-8.
[117] Pahl HL. Activators and target genes of Rel/NF-κB transcription factors. Oncogene. 1999;18:6853-66.
[118] Bucciarelli L, Wendt T, Rong L, Lalla E, Hofmann M, Goova M, et al. RAGE is a multiligand receptor of the immunoglobulin superfamily: implications for homeostasis and chronic disease. Cellular and Molecular Life Sciences CMLS. 2002;59:1117-28.

[119] Ramasamy R, Vannucci SJ, Du Yan SS, Herold K, Yan SF, Schmidt AM. Advanced glycation end products and RAGE: a common thread in aging, diabetes, neurodegeneration, and inflammation. Glycobiology. 2005;15:16-28.
[120] Johnson GL, Lapadat R. Mitogen-activated protein kinase pathways mediated by ERK, JNK, and p38 protein kinases. Science. 2002;298:1911-2.
[121] Hermani A, De Servi B, Medunjanin S, Tessier PA, Mayer D. S100A8 and S100A9 activate MAP kinase and NF-κB signaling pathways and trigger translocation of RAGE in human prostate cancer cells. Experimental cell research. 2006;312:184-97.
[122] Zill H, Günther R, Erbersdobler HF, Fölsch UR, Faist V. RAGE expression and AGE-induced MAP kinase activation in Caco-2 cells. Biochemical and biophysical research communications. 2001;288:1108-11.
[123] Chou MM, Blenis J. The 70 kDa S6 kinase complexes with and is activated by the Rho family G proteins Cdc42 and Rac1. Cell. 1996;85:573-83.
[124] Viberti GC. Increased capillary permeability in diabetes mellitus and its relationship to microvascular angiopathy. The American journal of medicine. 1983;75:81-4.
[125] Zong H, Madden A, Ward M, Mooney MH, Elliott CT, Stitt AW. Homodimerization is essential for the receptor for advanced glycation end products (RAGE)-mediated signal transduction. Journal of Biological Chemistry. 2010;285:23137-46.
[126] Wei W, Lampe L, Park S, Vangara BS, Waldo GS, Cabantous S, et al. Disulfide bonds within the C2 domain of RAGE play key roles in its dimerization and biogenesis. PloS one. 2012;7:e50736.
[127] Yatime L, Andersen GR. Structural insights into the oligomerization mode of the human receptor for advanced glycation end-products. FEBS journal. 2013;280:6556-68.
[128] Sevillano N, Girón MD, Salido M, Vargas AM, Vilches J, Salto R. Internalization of the receptor for advanced glycation end products (RAGE) is required to mediate intracellular responses. Journal of Biochemistry. 2009;145:21-30.
[129] Perrone L, Peluso G, Melone MA. RAGE recycles at the plasma membrane in S100B secretory vesicles and promotes Schwann cells morphological changes. Journal of cellular physiology. 2008;217:60-71.
[130] Bro S, Flyvbjerg A, Binder CJ, Bang CA, Denner L, Olgaard K, et al. A neutralizing antibody against receptor for advanced glycation end products (RAGE) reduces atherosclerosis in uremic mice. Atherosclerosis. 2008;201:274-80.
[131] Lutterloh EC, Opal SM, Pittman DD, Keith JC, Tan X-Y, Clancy BM, et al. Inhibition of the RAGE products increases survival in experimental models of severe sepsis and systemic infection. Critical Care. 2007;11:122-30.
[132] Christaki E, Opal SM, Keith Jr JC, Kessimian N, Palardy JE, Parejo NA, et al. A monoclonal antibody against RAGE alters gene expression and is protective in experimental models of sepsis and pneumococcal pneumonia. Shock. 2011;35:492-8.
[133] Abe R, Shimizu T, Sugawara H, Watanabe H, Nakamura H, Choei H, et al. Regulation of human melanoma growth and metastasis by AGE–AGE receptor interactions. Journal of Investigative Dermatology. 2004;122:461-7.
[134] Arumugam T, Ramachandran V, Gomez SB, Schmidt AM, Logsdon CD. S100P-derived RAGE antagonistic peptide reduces tumor growth and metastasis. Clinical Cancer Research. 2012;18:4356-64.

[135] Arumugam T, Ramachandran V, Logsdon CD. Effect of cromolyn on S100P interactions with RAGE and pancreatic cancer growth and invasion in mouse models. Journal of the National Cancer Institute. 2006;98:1806-18.
[136] Singh R, Barden A, Mori T, Beilin L. Advanced glycation end-products: a review. Diabetologia. 2001;44:129-46.
[137] Goldberg T, Cai W, Peppa M, Dardaine V, Baliga BS, Uribarri J, et al. Advanced glycoxidation end products in commonly consumed foods. Journal of the American Dietetic Association. 2004;104:1287-91.
[138] Uribarri J, Woodruff S, Goodman S, Cai W, Chen X, Pyzik R, et al. Advanced glycation end products in foods and a practical guide to their reduction in the diet. Journal of the American Dietetic Association. 2010;110:911-6. .
[139] Ulrich P, Cerami A. Protein glycation, diabetes, and aging. Recent progress in hormone research. 2001;56:1-22.
[140] Miyazaki A, Nakayama H, Horiuchi S. Scavenger receptors that recognize advanced glycation end products. Trends in cardiovascular medicine. 2002;12:258-62.
[141] Basta G, Lazzerini G, Massaro M, Simoncini T, Tanganelli P, Fu C, et al. Advanced glycation end products activate endothelium through signal-transduction receptor RAGE a mechanism for amplification of inflammatory responses. Circulation. 2002;105:816-22.
[142] Chen Q, Dong L, Wang L, Kang L, Xu B. Advanced glycation end products impair function of late endothelial progenitor cells through effects on protein kinase Akt and cyclooxygenase-2. Biochemical and biophysical research communications. 2009;381:192-7.
[143] Bierhaus A, Chevion S, Chevion M, Hofmann M, Quehenberger P, Illmer T, et al. Advanced glycation end product-induced activation of NF-κB is suppressed by α-lipoic acid in cultured endothelial cells. Diabetes. 1997;46:1481-90.
[144] Lander HM, Tauras JM, Ogiste JS, Hori O, Moss RA, Schmidt AM. Activation of the receptor for advanced glycation end products triggers a p21 ras-dependent mitogen-activated protein kinase pathway regulated by oxidant stress. Journal of Biological Chemistry. 1997;272:17810-4.
[145] Abe R, Yamagishi S-i. AGE-RAGE system and carcinogenesis. Current pharmaceutical design. 2008;14:940-5.
[146] Vlassara H. The AGE-receptor in the pathogenesis of diabetic complications. Diabetes/metabolism research and reviews. 2001;17:436-43.
[147] Schmidt AM, Du Yan S, Wautier J-L, Stern D. Activation of receptor for advanced glycation end products a mechanism for chronic vascular dysfunction in diabetic vasculopathy and atherosclerosis. Circulation Research. 1999;84:489-97.
[148] Yan SF, Ramasamy R, Schmidt AM. The RAGE axis a fundamental mechanism signaling danger to the vulnerable vasculature. Circulation Research. 2010;106:842-53.
[149] HEIJST JW, Niessen HW, Hoekman K, Schalkwijk CG. Advanced Glycation End Products in Human Cancer Tissues: Detection of Nε-(Carboxymethyl) lysine and Argpyrimidine. Annals of the New York Academy of Sciences. 2005;1043:725-33.
[150] Gnanasekar M, Thirugnanam S, Ramaswamy K. Short hairpin RNA (shRNA) constructs targeting high mobility group box-1 (HMGB1) expression leads to inhibition of prostate cancer cell survival and apoptosis. International journal of oncology. 2009;34:425-31.
[151] Markowitz J, Chen I, Gitti R, Baldisseri DM, Pan Y, Udan R, et al. Identification and characterization of small molecule inhibitors of the calcium-dependent S100B-p53 tumor suppressor interaction. Journal of medicinal chemistry. 2004;47:5085-93.

[152] Saleem M, Kweon M-H, Johnson JJ, Adhami VM, Elcheva I, Khan N, et al. S100A4 accelerates tumorigenesis and invasion of human prostate cancer through the transcriptional regulation of matrix metalloproteinase 9. Proceedings of the National Academy of Sciences. 2006;103:14825-30.
[153] Stein U, Arlt F, Walther W, Smith J, Waldman T, Harris ED, et al. The Metastasis-Associated Gene S100A4 Is a Novel Target of β-catenin/T-cell Factor Signaling in Colon Cancer. Gastroenterology. 2006;131:1486-500.
[154] Andersen K, Nesland JM, Holm R, Flørenes VA, Fodstad Ø, Mælandsmo GM. Expression of S100A4 combined with reduced E-cadherin expression predicts patient outcome in malignant melanoma. Modern Pathology. 2004;17:990-7.
[155] Ohuchida K, Mizumoto K, Ishikawa N, Fujii K, Konomi H, Nagai E, et al. The role of S100A6 in pancreatic cancer development and its clinical implication as a diagnostic marker and therapeutic target. Clinical Cancer Research. 2005;11:7785-93.
[156] Lange SS, Mitchell DL, Vasquez KM. High mobility group protein B1 enhances DNA repair and chromatin modification after DNA damage. Proceedings of the National Academy of Sciences. 2008;105:10320-5.
[157] Müller S, Scaffidi P, Degryse B, Bonaldi T, Ronfani L, Agresti A, et al. The double life of HMGB1 chromatin protein: architectural factor and extracellular signal. The EMBO journal. 2001;20:4337-40.
[158] Chen Y, Sun W, Gao R, Su Y, Umehara H, Dong L, et al. The role of high mobility group box chromosomal protein 1 in rheumatoid arthritis. Rheumatology. 2013;52:1739-47.
[159] Huang L, Yao Y, Sheng Z. Novel insights for high mobility group box 1 protein-mediated cellular immune response in sepsis: A systemic review. World J Emerg Med. 2012;3:165-71.
[160] Dumitriu IE, Baruah P, Manfredi AA, Bianchi ME, Rovere-Querini P. HMGB1: guiding immunity from within. Trends in immunology. 2005;26:381-7.
[161] Li J, Kokkola R, Tabibzadeh S, Yang R, Ochani M, Qiang X, et al. Structural basis for the proinflammatory cytokine activity of high mobility group box 1. Molecular Medicine. 2003;9:37-45.
[162] Banerjee S, Kundu TK. The acidic C-terminal domain and A-box of HMGB-1 regulates p53-mediated transcription. Nucleic acids research. 2003;31:3236-47.
[163] Bianchi ME, Beltrame M. Upwardly mobile proteins. EMBO reports. 2000;1:109-14.
[164] Czapla L, Peters JP, Rueter EM, Olson WK, Maher III LJ. Understanding apparent DNA flexibility enhancement by HU and HMGB architectural proteins. Journal of molecular biology. 2011;409:278-89.
[165] Scaffidi P, Misteli T, Bianchi ME. Release of chromatin protein HMGB1 by necrotic cells triggers inflammation. nature. 2002;418:191-5.
[166] Wang H, Yang H, Tracey K. Extracellular role of HMGB1 in inflammation and sepsis. Journal of internal medicine. 2004;255:320-31.
[167] Sims GP, Rowe DC, Rietdijk ST, Herbst R, Coyle AJ. HMGB1 and RAGE in inflammation and cancer. Annual review of immunology. 2009;28:367-88.
[168] Ito I, Fukazawa J, Yoshida M. Post-translational methylation of high mobility group box 1 (HMGB1) causes its cytoplasmic localization in neutrophils. Journal of Biological Chemistry. 2007;282:16336-44.
[169] Bonaldi T, Talamo F, Scaffidi P, Ferrera D, Porto A, Bachi A, et al. Monocytic cells hyperacetylate chromatin protein HMGB1 to redirect it towards secretion. The EMBO journal. 2003;22:5551-60.

[170] Ito N, DeMarco RA, Mailliard RB, Han J, Rabinowich H, Kalinski P, et al. Cytolytic cells induce HMGB1 release from melanoma cell lines. Journal of leukocyte biology. 2007;81:75-83.
[171] Wake H, Mori S, Liu K, Takahashi HK, Nishibori M. Histidine-rich glycoprotein inhibited high mobility group box 1 in complex with heparin-induced angiogenesis in matrigel plug assay. European journal of pharmacology. 2009;623:89-95.
[172] Rauvala H, Rouhiainen A. Physiological and pathophysiological outcomes of the interactions of HMGB1 with cell surface receptors. Biochimica et Biophysica Acta (BBA)-Gene Regulatory Mechanisms. 2010;1799:164-70.
[173] Schlueter C, Weber H, Meyer B, Rogalla P, Röser K, Hauke S, et al. Angiogenetic signaling through hypoxia: HMGB1: an angiogenetic switch molecule. The American journal of pathology. 2005;166:1259-63.
[174] Flohr AM, Rogalla P, Meiboom M, Borrmann L, Krohn M, Thode-Halle B, et al. Variation of HMGB1 expression in breast cancer. Anticancer research. 2001;21:3881-5.
[175] Chung HW, Lee S-G, Kim H, Hong DJ, Chung JB, Stroncek D, et al. Serum high mobility group box-1 (HMGB1) is closely associated with the clinical and pathologic features of gastric cancer. J Transl Med. 2009;7:38-48.
[176] Sasahira T, Kirita T, Oue N, Bhawal UK, Yamamoto K, Fujii K, et al. High mobility group box-1-inducible melanoma inhibitory activity is associated with nodal metastasis and lymphangiogenesis in oral squamous cell carcinoma. Cancer science. 2008;99:1806-12.
[177] Bosserhoff AK. Melanoma inhibitory activity (MIA): an important molecule in melanoma development and progression. Pigment cell research. 2005;18:411-6.
[178] Kostova N, Zlateva S, Ugrinova I, Pasheva E. The expression of HMGB1 protein and its receptor RAGE in human malignant tumors. Molecular and cellular biochemistry. 2010;337:251-8.
[179] Zhang J, Zhu J-S, Zhou Z, Chen W-X, Chen N-W. Inhibitory effects of ethyl pyruvate administration on human gastric cancer growth via regulation of the HMGB1-RAGE and Akt pathways in vitro and in vivo. Oncology reports. 2012;27:1511-9.
[180] Tang D, Kang R, Cheh C-W, Livesey KM, Liang X, Schapiro NE, et al. HMGB1 release and redox regulates autophagy and apoptosis in cancer cells. Oncogene. 2010;29:5299-310.
[181] Wang D, Lippard SJ. Cellular processing of platinum anticancer drugs. Nature Reviews Drug Discovery. 2005;4:307-20.
[182] Heizmann CW, Fritz G, Schafer B. S100 proteins: structure, functions and pathology. Front Biosci. 2002;7:1356-68.
[183] Donato R. Intracellular and extracellular roles of S100 proteins. Microscopy research and technique. 2003;60:540-51.
[184] Marenholz I, Heizmann CW, Fritz G. S100 proteins in mouse and man: from evolution to function and pathology (including an update of the nomenclature). Biochemical and biophysical research communications. 2004;322:1111-22.
[185] Svenningsson P, Greengard P. p11 (S100A10)—an inducible adaptor protein that modulates neuronal functions. Current opinion in pharmacology. 2007;7:27-32.
[186] Allore R, O'Hanlon D, Price R, Neilson K, Willard H, Cox D, et al. Gene encoding the beta subunit of S100 protein is on chromosome 21: implications for Down syndrome. Science. 1988;239:1311-3.
[187] Broome A-M, Ryan D, Eckert RL. S100 protein subcellular localization during epidermal differentiation and psoriasis. Journal of Histochemistry & Cytochemistry. 2003;51:675-85.

[188] Mandinova A, Atar D, Schafer B, Spiess M, Aebi U, Heizmann CW. Distinct subcellular localization of calcium binding S100 proteins in human smooth muscle cells and their relocation in response to rises in intracellular calcium. Journal of cell science. 1998;111:2043-54.
[189] Gerlach R, Demel G, König H-G, Gross U, Prehn J, Raabe A, et al. Active secretion of S100B from astrocytes during metabolic stress. Neuroscience. 2006;141:1697-701.
[190] Stary M, Schneider M, Sheikh SP, Weitzer G. Parietal endoderm secreted S100A4 promotes early cardiomyogenesis in embryoid bodies. Biochemical and biophysical research communications. 2006;343:555-63.
[191] Rammes A, Roth J, Goebeler M, Klempt M, Hartmann M, Sorg C. Myeloid-related protein (MRP) 8 and MRP14, calcium-binding proteins of the S100 family, are secreted by activated monocytes via a novel, tubulin-dependent pathway. Journal of Biological Chemistry. 1997;272:9496-502.
[192] Michetti F, Corvino V, Geloso MC, Lattanzi W, Bernardini C, Serpero L, et al. The S100B protein in biological fluids: more than a lifelong biomarker of brain distress. Journal of neurochemistry. 2012;120:644-59.
[193] Gifford J, Walsh M, Vogel H. Structures and metal-ion-binding properties of the Ca2+-binding helix-loop-helix EF-hand motifs. Biochem J. 2007;405:199-221.
[194] Donato R. Functional roles of S100 proteins, calcium-binding proteins of the EF-hand type. Biochimica et Biophysica Acta (BBA)-Molecular Cell Research. 1999;1450:191-231.
[195] Santamaria-Kisiel L, Rintala-Dempsey A, Shaw G. Calcium-dependent and-independent interactions of the S100 protein family. Biochem J. 2006;396:201-14.
[196] Heizmann CW, Cox JA. New perspectives on S100 proteins: a multi-functional Ca 2+-, Zn 2+-and Cu 2+-binding protein family. Biometals. 1998;11:383-97.
[197] Halawi A, Abbas O, Mahalingam M. S100 proteins and the skin: a review. Journal of the European Academy of Dermatology and Venereology. 2013:405-14.
[198] Passey RJ, Xu K, Hume DA, Geczy CL. S100A8: emerging functions and regulation. Journal of leukocyte biology. 1999;66:549-56.
[199] Moroz O, Antson A, Dodson E, Burrell H, Grist S, Lloyd R, et al. The structure of S100A12 in a hexameric form and its proposed role in receptor signalling. Acta Crystallographica Section D: Biological Crystallography. 2002;58:407-13.
[200] Xie J, Burz DS, He W, Bronstein IB, Lednev I, Shekhtman A. Hexameric calgranulin C (S100A12) binds to the receptor for advanced glycated end products (RAGE) using symmetric hydrophobic target-binding patches. Journal of Biological Chemistry. 2007;282:4218-31.
[201] Ellis EF, Willoughby KA, Sparks SA, Chen T. S100B protein is released from rat neonatal neurons, astrocytes, and microglia by in vitro trauma and anti-S100 increases trauma-induced delayed neuronal injury and negates the protective effect of exogenous S100B on neurons. Journal of neurochemistry. 2007;101:1463-70.
[202] Davey GE, Murmann P, Heizmann CW. Intracellular Ca2+ and Zn2+ levels regulate the alternative cell density-dependent secretion of S100B in human glioblastoma cells. Journal of Biological Chemistry. 2001;276:30819-26.
[203] Donato R. RAGE: a single receptor for several ligands and different cellular responses: the case of certain S100 proteins. Current molecular medicine. 2007;7:711-24.
[204] Salama I, Malone P, Mihaimeed F, Jones J. A review of the S100 proteins in cancer. European Journal of Surgical Oncology (EJSO). 2008;34:357-64.

[205] Mecocci P, Parnetti L, Romano G, Scarelli A, Chionne F, Cecchetti R, et al. Serum anti-GFAP and anti-S100 autoantibodies in brain aging, Alzheimer's disease and vascular dementia. Journal of neuroimmunology. 1995;57:165-70.
[206] Rothermundt M, Peters M, Prehn JH, Arolt V. S100B in brain damage and neurodegeneration. Microscopy research and technique. 2003;60:614-32.
[207] Remppis A, Greten T, Schäfer BW, Hunziker P, Erne P, Katus HA, et al. Altered expression of the Ca 2+ binding protein S100A1 in human cardiomyopathy. Biochimica et Biophysica Acta (BBA)-Molecular Cell Research. 1996;1313:253-7.
[208] Foell D, Frosch M, Sorg C, Roth J. Phagocyte-specific calcium-binding S100 proteins as clinical laboratory markers of inflammation. Clinica Chimica Acta. 2004;344:37-51.
[209] Arumugam T, Simeone DM, Van Golen K, Logsdon CD. S100P promotes pancreatic cancer growth, survival, and invasion. Clinical Cancer Research. 2005;11:5356-64.
[210] Fuentes MK, Nigavekar SS, Arumugam T, Logsdon CD, Schmidt AM, Park JC, et al. RAGE activation by S100P in colon cancer stimulates growth, migration, and cell signaling pathways. Diseases of the colon & rectum. 2007;50:1230-40.
[211] Ghavami S, Rashedi I, Dattilo BM, Eshraghi M, Chazin WJ, Hashemi M, et al. S100A8/A9 at low concentration promotes tumor cell growth via RAGE ligation and MAP kinase-dependent pathway. Journal of leukocyte biology. 2008;83:1484-92.
[212] Thierolf M, Hagmann ML, Pfeffer M, Berntenis N, Wild N, Roeßler M, et al. Towards a comprehensive proteome of normal and malignant human colon tissue by 2-D-LC-ESI-MS and 2-DE proteomics and identification of S100A12 as potential cancer biomarker. PROTEOMICS-Clinical Applications. 2008;2:11-22.
[213] Marenholz I, Heizmann CW. S100A16, a ubiquitously expressed EF-hand protein which is up-regulated in tumors. Biochemical and biophysical research communications. 2004;313:237-44.
[214] Sapkota D, Costea DE, Ibrahim SO, Johannessen AC, Bruland O. S100A14 Interacts with S100A16 and Regulates Its Expression in Human Cancer Cells. PloS one. 2013;8:e76058.
[215] Briggs MW, Sacks DB. IQGAP proteins are integral components of cytoskeletal regulation. EMBO reports. 2003;4:571-4.
[216] Watanabe T, Wang S, Noritake J, Sato K, Fukata M, Takefuji M, et al. Interaction with IQGAP1 links APC to Rac1, Cdc42, and actin filaments during cell polarization and migration. Developmental cell. 2004;7:871-83.
[217] Lin J, Yang Q, Yan Z, Markowitz J, Wilder PT, Carrier F, et al. Inhibiting S100B restores p53 levels in primary malignant melanoma cancer cells. Journal of Biological Chemistry. 2004;279:34071-7.
[218] Lin J, Blake M, Tang C, Zimmer D, Rustandi RR, Weber DJ, et al. Inhibition of p53 transcriptional activity by the S100B calcium-binding protein. Journal of Biological Chemistry. 2001;276:35037-41.
[219] Lin J, Yang Q, Wilder PT, Carrier F, Weber DJ. The calcium-binding protein S100B down-regulates p53 and apoptosis in malignant melanoma. Journal of Biological Chemistry. 2010;285:27487-98.
[220] Wilder PT, Charpentier TH, Liriano MA, Gianni K, Varney KM, Pozharski E, et al. In vitro screening and structural characterization of inhibitors of the S100B-p53 interaction. International journal of high throughput screening. 2010;2010:109-26.
[221] Smith J, Stewart BJ, Glaysher S, Peregrin K, Knight LA, Weber DJ, et al. The effect of pentamidine on melanoma. Anti-cancer drugs. 2010;21:181-5.

[222] Suzuki F, Kato K, Nakajima T. Hormonal Regulation of Adipose S-100 Protein Release. Journal of neurochemistry. 1984;43:1336-41.
[223] Abib RT, Quincozes-Santos A, Nardin P, Wofchuk ST, Perry ML, Gonçalves C-A, et al. Epicatechin gallate increases glutamate uptake and S100B secretion in C6 cell lineage. Molecular and cellular biochemistry. 2008;310:153-8.
[224] Harpio R, Einarsson R. S100 proteins as cancer biomarkers with focus on S100B in malignant melanoma. Clinical biochemistry. 2004;37:512-8.
[225] Brochez L, Naeyaert JM. Serological markers for melanoma. British Journal of Dermatology. 2000;143:256-68.
[226] Korfias S, Stranjalis G, Papadimitriou A, Psachoulia C, Daskalakis G, Antsaklis A, et al. Serum S-100B protein as a biochemical marker of brain injury: a review of current concepts. Current medicinal chemistry. 2006;13:3719-31.
[227] Raabe A, Grolms C, Sorge O, Zimmermann M, Seifert V. Serum S-100B protein in severe head injury. Neurosurgery. 1999;45:477-83.
[228] Mazzini GS, Schaf DV, Vinadé ER, Horowitz E, Bruch RS, Brunm LM, et al. Increased S100B serum levels in dilated cardiomyopathy patients. Journal of cardiac failure. 2007;13:850-4.
[229] Mazzini GS, Schaf DV, Oliveira ÁR, Gonçalves CA, Belló-Klein A, Bordignon S, et al. The ischemic rat heart releases S100B. Life sciences. 2005;77:882-9.
[230] Barger SW, Van Eldik LJ, Mattson MP. S100β protects hippocampal neurons from damage induced by glucose deprivation. Brain research. 1995;677:167-70.
[231] Iwasaki Y, Shiojima T, Kinoshita M. S100 β prevents the death of motor neurons in newborn rats after sciatic nerve section. Journal of the neurological sciences. 1997;151:7-12.
[232] Huttunen H, Kuja-Panula J, Sorci G, Agneletti A, Donato R, Rauvala H. Coregulation of neurite outgrowth and cell survival by amphotericin and S100 proteins through RAGE activation. J Biol Chem. 2000;75:40096-105.
[233] Businaro R, Leone S, Fabrizi C, Sorci G, Donato R, Lauro G, et al. S100B protects LAN-5 neuroblastoma cells against Aβ amyloid-induced neurotoxicity via RAGE engagement at low doses but increases Aβ amyloid neurotoxicity at high doses. Journal of neuroscience research. 2006;83:897-906.
[234] Esposito G, Imitola J, Lu J, De Filippis D, Scuderi C, Ganesh VS, et al. Genomic and functional profiling of human Down syndrome neural progenitors implicates S100B and aquaporin 4 in cell injury. Human molecular genetics. 2008;17:440-57.
[235] Sathe K, Maetzler W, Lang JD, Mounsey RB, Fleckenstein C, Martin HL, et al. S100B is increased in Parkinson's disease and ablation protects against MPTP-induced toxicity through the RAGE and TNF-α pathway. Brain. 2012;135:3336-47.
[236] Sheng JG, Mrak RE, Rovnaghi CR, Kozlowska E, Van Eldik LJ, Griffin WST. Human brain S100β and S100β mRNA expression increases with age: pathogenic implications for Alzheimer's disease. Neurobiology of aging. 1996;17:359-63.
[237] Dyck RH, Bogoch II, Marks A, Melvin NR, Teskey GC. Enhanced epileptogenesis in S100B knockout mice. Molecular brain research. 2002;106:22-9.
[238] Schmitt A, Bertsch T, Henning U, Tost H, Klimke A, Henn FA, et al. Increased serum S100B in elderly, chronic schizophrenic patients: negative correlation with deficit symptoms. Schizophrenia research. 2005;80:305-13.

[239] Andreazza AC, Cassini C, Rosa AR, Leite MC, de Almeida L, Nardin P, et al. Serum S100B and antioxidant enzymes in bipolar patients. Journal of psychiatric research. 2007;41:523-9.
[240] Machado-Vieira R, Lara D, Portela L, Goncalves C, Soares J, Kapczinski F, et al. Elevated serum S100B protein in drug-free bipolar patients during first manic episode: a pilot study. European neuropsychopharmacology. 2002;12:269-72.
[241] Steiner J, Bogerts B, Schroeter ML, Bernstein H-G. S100B protein in neurodegenerative disorders. Clinical Chemistry and Laboratory Medicine. 2011;49:409-24.
[242] Torabian S, Kashani-Sabet M. Biomarkers for melanoma. Current opinion in oncology. 2005;17:167-71.
[243] Mocellin S, Zavagno G, Nitti D. The prognostic value of serum S100B in patients with cutaneous melanoma: A meta-analysis. International journal of cancer. 2008;123:2370-6.
[244] Stuckert J, Tarhini A, Lee S, Sander C, Kirkwood J. Interferon alfa-induced autoimmunity and serum S100 levels as predictive and prognostic biomarkers in high-risk melanoma in the ECOG-intergroup phase II trial E2696. Journal of Clinical Oncology. 2007;25:8506.
[245] Tarhini AA, Stuckert J, Lee S, Sander C, Kirkwood JM. Prognostic significance of serum S100B protein in high-risk surgically resected melanoma patients participating in Intergroup Trial ECOG 1694. Journal of Clinical Oncology. 2009;27:38-44.
[246] Engelkamp D, Schäfer B, Mattei MG, Erne P, Heizmann CW. Six S100 genes are clustered on human chromosome 1q21: identification of two genes coding for the two previously unreported calcium-binding proteins S100D and S100E. Proceedings of the National Academy of Sciences. 1993;90:6547-51.
[247] Luthra MG, Ajani JA, Izzo J, Ensor J, Wu T-T, Rashid A, et al. Decreased expression of gene cluster at chromosome 1q21 defines molecular subgroups of chemoradiotherapy response in esophageal cancers. Clinical Cancer Research. 2007;13:912-9.
[248] Heo S-H, Choi Y-J, Lee J-H, Lee J-M, Cho J-Y. S100A2 level changes are related to human periodontitis. Molecules and cells. 2011;32:445-50.
[249] Botelho HM, Koch M, Fritz G, Gomes CM. Metal ions modulate the folding and stability of the tumor suppressor protein S100A2. FEBS journal. 2009;276:1776-86.
[250] Gimona M, Lando Z, Dolginov Y, Vandekerckhove J, Kobayashi R, Sobieszek A, et al. Ca2+-dependent interaction of S100A2 with muscle and nonmuscle tropomyosins. Journal of cell science. 1997;110:611-21.
[251] Mueller A, Schäfer BW, Ferrari S, Weibel M, Makek M, Höchli M, et al. The calcium-binding protein S100A2 interacts with p53 and modulates its transcriptional activity. Journal of Biological Chemistry. 2005;280:29186-93.
[252] Kirschner RD, Sänger K, Müller GA, Engeland K. Transcriptional activation of the tumor suppressor and differentiation gene S100A2 by a novel p63-binding site. Nucleic acids research. 2008;36:2969-80.
[253] Lapi E, Iovino A, Fontemaggi G, Soliera A, Iacovelli S, Sacchi A, et al. S100A2 gene is a direct transcriptional target of p53 homologues during keratinocyte differentiation. Oncogene. 2006;25:3628-37.
[254] Lee SW, Tomasetto C, Swisshelm K, Keyomarsi K, Sager R. Down-regulation of a member of the S100 gene family in mammary carcinoma cells and reexpression by azadeoxycytidine treatment. Proceedings of the National Academy of Sciences. 1992;89:2504-8.

[255] Feng G, Xu X-c, Youssef EM, Lotan R. Diminished expression of S100A2, a putative tumor suppressor, at early stage of human lung carcinogenesis. Cancer research. 2001;61:7999-8004.
[256] Suzuki F, Oridate N, Homma A, Nakamaru Y, Nagahashi T, Yagi K, et al. S100A2 expression as a predictive marker for late cervical metastasis in stage I and II invasive squamous cell carcinoma of the oral cavity. Oncology reports. 2005;14:1493-8.
[257] Maelandsmo GM, Flørenes VA, Mellingsaeter T, Hovig E, Kerbel RS, Fodstad Ø. Differential expression patterns of S100A2, S100A4 and S100A6 during progression of human malignant melanoma. International journal of cancer. 1997;74:464-9.
[258] Gupta S, Hussain T, MacLennan GT, Fu P, Patel J, Mukhtar H. Differential expression of S100A2 and S100A4 during progression of human prostate adenocarcinoma. Journal of Clinical Oncology. 2003;21:106-12.
[259] Nagy N, Brenner C, Markadieu N, Chaboteaux C, Camby I, Schäfer BW, et al. S100A2, a putative tumor suppressor gene, regulates in vitro squamous cell carcinoma migration. Laboratory investigation. 2001;81:599-612.
[260] Hough CD, Cho KR, Zonderman AB, Schwartz DR, Morin PJ. Coordinately up-regulated genes in ovarian cancer. Cancer research. 2001;61:3869-76.
[261] Moskaluk CA, Abdrabbo MK, Harper J, Yoshida C, Riggins GJ, Frierson HF, et al. Gastric cancers overexpress S100A calcium-binding proteins. Cancer research. 2002;62:6823-6.
[262] Smith S, Gugger M, Hoban P, Ratschiller D, Watson S, Field J, et al. S100A2 is strongly expressed in airway basal cells, preneoplastic bronchial lesions and primary non-small cell lung carcinomas. British journal of cancer. 2004;91:1515-24.
[263] IMAZAWA M, HIBI K, FUJITAKE S-I, KODERA Y, ITO K, AKIYAMA S, et al. S100A2 overexpression is frequently observed in esophageal squamous cell carcinoma. Anticancer research. 2005;25:1247-50.
[264] Wolf S, Haase-Kohn C, Pietzsch J. S100A2 in cancerogenesis: a friend or a foe? Amino Acids. 2011;41:849-61.
[265] Bulk E, Sargin B, Krug U, Hascher A, Jun Y, Knop M, et al. S100A2 Induces Metastasis in Non–Small Cell Lung Cancer. Clinical Cancer Research. 2009;15:22-9.
[266] Klopper JP, Sharma V, Bissonnette R, Haugen BR. Combination PPAR and RXR Agonist Treatment in Melanoma Cells: Functional Importance of S100A2. PPAR research. 2010;10:1-8.
[267] Chen M, Sinha M, Luxon BA, Bresnick AR, O'Connor KL. Integrin α6β4 controls the expression of genes associated with cell motility, invasion, and metastasis, including S100A4/metastasin. Journal of Biological Chemistry. 2009;284:1484-94.
[268] Marenholz I, Lovering RC, Heizmann CW. An update of the S100 nomenclature. Biochimica et Biophysica Acta (BBA)-Molecular Cell Research. 2006;1763:1282-3.
[269] Tarabykina S, Scott DJ, Herzyk P, Hill TJ, Tame JR, Kriajevska M, et al. The dimerization interface of the metastasis-associated protein S100A4 (Mts1) in vivo and in vitro studies. Journal of Biological Chemistry. 2001;276:24212-22.
[270] Boye K, Mælandsmo GM. S100A4 and metastasis: a small actor playing many roles. The American journal of pathology. 2010;176:528-35.
[271] Cabezón T, Celis JE, Skibshøj I, Klingelhöfer J, Grigorian M, Gromov P, et al. Expression of S100A4 by a variety of cell types present in the tumor microenvironment of human breast cancer. International journal of cancer. 2007;121:1433-44.

[272] Tarabykina S, L Griffiths T, Tulchinsky E, Mellon J, Bronstein I, Kriajevska M. Metastasis-associated protein S100A4: spotlight on its role in cell migration. Current cancer drug targets. 2007;7:217-28.
[273] Li Z-H, Bresnick AR. The S100A4 metastasis factor regulates cellular motility via a direct interaction with myosin-IIA. Cancer research. 2006;66:5173-80.
[274] Grigorian M, Andresen S, Tulchinsky E, Kriajevska M, Carlberg C, Kruse C, et al. Tumor Suppressor p53 Protein Is a New Target for the Metastasis-associated Mts1/S100A4 Protein FUNCTIONAL CONSEQUENCES OF THEIR INTERACTION. Journal of Biological Chemistry. 2001;276:22699-708.
[275] Semov A, Moreno MJ, Onichtchenko A, Abulrob A, Ball M, Ekiel I, et al. Metastasis-associated protein S100A4 induces angiogenesis through interaction with Annexin II and accelerated plasmin formation. Journal of Biological Chemistry. 2005;280:20833-41.
[276] Kiryushko D, Novitskaya V, Soroka V, Klingelhofer J, Lukanidin E, Berezin V, et al. Molecular mechanisms of Ca2+ signaling in neurons induced by the S100A4 protein. Molecular and cellular biology. 2006;26:3625-38.
[277] Yammani RR, Carlson CS, Bresnick AR, Loeser RF. Increase in production of matrix metalloproteinase 13 by human articular chondrocytes due to stimulation with S100A4: Role of the receptor for advanced glycation end products. Arthritis & Rheumatism. 2006;54:2901-11.
[278] Lawrie A, Spiekerkoetter E, Martinez EC, Ambartsumian N, Sheward WJ, MacLean MR, et al. Interdependent serotonin transporter and receptor pathways regulate S100A4/Mts1, a gene associated with pulmonary vascular disease. Circulation Research. 2005;97:227-35.
[279] Ebralidze A, Tulchinsky E, Grigorian M, Afanasyeva A, Senin V, Revazova E, et al. Isolation and characterization of a gene specifically expressed in different metastatic cells and whose deduced gene product has a high degree of homology to a Ca2+-binding protein family. Genes & development. 1989;3:1086-93.
[280] Grum-Schwensen B, Klingelhofer J, Berg CH, El-Naaman C, Grigorian M, Lukanidin E, et al. Suppression of tumor development and metastasis formation in mice lacking the S100A4 (mts1) gene. Cancer research. 2005;65:3772-80.
[281] Lo J-F, Yu C-C, Chiou S-H, Huang C-Y, Jan C-I, Lin S-C, et al. The epithelial-mesenchymal transition mediator S100A4 maintains cancer-initiating cells in head and neck cancers. Cancer research. 2011;71:1912-23.
[282] Kalluri R. EMT: when epithelial cells decide to become mesenchymal-like cells. The Journal of clinical investigation. 2009;119:1417-9.
[283] Bjørnland K, Winberg JO, Ødegaard OT, Hovig E, Loennechen T, Aasen AO, et al. S100A4 Involvement in Metastasis Deregulation of Matrix Metalloproteinases and Tissue Inhibitors of Matrix Metalloproteinases in Osteosarcoma Cells Transfected with an Anti-S100A4 Ribozyme. Cancer research. 1999;59:4702-8.
[284] Ambartsumian N, Klingelhöfer J, Grigorian M, Christensen C, Kriajevska M, Tulchinsky E, et al. The metastasis-associated Mts1 (S100A4) protein could act as an angiogenic factor. Oncogene. 2001;20.
[285] Nowotny M, Spiechowicz M, Jastrzebska B, Filipek A, Kitagawa K, Kuznicki J. Calcium-regulated interaction of Sgt1 with S100A6 (calcyclin) and other S100 proteins. Journal of Biological Chemistry. 2003;278:26923-8.
[286] Filipek A. S100A6 and CacyBP/SIP–two proteins discovered in ehrlich ascites tumor cells that are potentially involved in the degradation of β-Catenin. Chemotherapy. 2005;52:32-4.

[287] Leśniak W, Słomnicki ŁP, Filipek A. S100A6–New facts and features. Biochemical and biophysical research communications. 2009;390:1087-92.
[288] Stradal TB, Gimona M. Ca2+-dependent association of S100A6 (Calcyclin) with the plasma membrane and the nuclear envelope. Journal of Biological Chemistry. 1999;274:31593-6.
[289] Leśniak W, Szczepańska A, Kuźnicki J. Calcyclin (S100A6) expression is stimulated by agents evoking oxidative stress via the antioxidant response element. Biochimica et Biophysica Acta (BBA)-Molecular Cell Research. 2005;1744:29-37.
[290] Breen EC, Fu Z, Normand H. Calcyclin gene expression is increased by mechanical strain in fibroblasts and lung. American journal of respiratory cell and molecular biology. 1999;21:746-52.
[291] Lewington A, Padanilam B, Hammerman M. Induction of calcyclin after ischemic injury to rat kidney. American Journal of Physiology-Renal Physiology. 1997;273:F380-F5.
[292] Ghezzo F, Lauret E, Ferrari S, Baserga R. Growth factor regulation of the promoter for calcyclin, a growth-regulated gene. Journal of Biological Chemistry. 1988;263:4758-63.
[293] Tsoporis JN, Izhar S, Parker TG. Expression of S100A6 in cardiac myocytes limits apoptosis induced by tumor necrosis factor-alpha. J Biol Chem. 2008;283:30174-83.
[294] Hong E-J, Park S-H, Choi K-C, Leung P, Jeung E-B. Identification of estrogen-regulated genes by microarray analysis of the uterus of immature rats exposed to endocrine disrupting chemicals. Reprod Biol Endocrinol. 2006;4:40-9.
[295] Busch AK, Cordery D, Denyer GS, Biden TJ. Expression profiling of palmitate-and oleate-regulated genes provides novel insights into the effects of chronic lipid exposure on pancreatic β-cell function. Diabetes. 2002;51:977-87.
[296] Courtois-Coutry N, Le Moellic C, Boulkroun S, Fay M, Cluzeaud F, Escoubet B, et al. Calcyclin Is an Early Vasopressin-induced Gene in the Renal Collecting Duct ROLE IN THE LONG TERM REGULATION OF ION TRANSPORT. Journal of Biological Chemistry. 2002;277:25728-34.
[297] Kucharczak J, Pannequin J, Camby I, Decaestecker C, Kiss R, Martinez J. Gastrin induces over-expression of genes involved in human U373 glioblastoma cell migration. Oncogene. 2001;20:7021-8.
[298] Joo JH, Kim JW, Lee Y, Yoon SY, Kim JH, Paik S-G, et al. Involvement of NF-κB in the regulation of S100A6 gene expression in human hepatoblastoma cell line HepG2. Biochemical and biophysical research communications. 2003;307:274-80.
[299] Króliczak W, Pietrzak M, Puzianowska-Kuznicka M. P53-dependent suppression of the human calcyclin gene (S100A6): the role of Sp1 and of NFkappaB. Acta Biochim Pol. 2008;55:559-70.
[300] Rehman I, Cross SS, Catto JW, Leiblich A, Mukherjee A, Azzouzi AR, et al. Promoter hyper-methylation of calcium binding proteins S100A6 and S100A2 in human prostate cancer. The Prostate. 2005;65:322-30.
[301] Wang X-H, Zhang L-H, Zhong X-Y, Xing X-F, Liu Y-Q, Niu Z-J, et al. S100A6 overexpression is associated with poor prognosis and is epigenetically up-regulated in gastric cancer. The American journal of pathology. 2010;177:586-97.
[302] Słomnicki ŁP, Nawrot B, Leśniak W. S100A6 binds p53 and affects its activity. The international journal of biochemistry & cell biology. 2009;41:784-90.

[303] Filipek A, Jastrzebska B, Nowotny M, Kuznicki J. CacyBP/SIP, a calcyclin and Siah-1-interacting protein, binds EF-hand proteins of the S100 family. Journal of Biological Chemistry. 2002;277:28848-52.
[304] Fernandez-Fernandez MR, Rutherford TJ, Fersht AR. Members of the S100 family bind p53 in two distinct ways. Protein Science. 2008;17:1663-70.
[305] Komatsu K, Murata K, Kameyama M, Ayaki M, Mukai M, Ishiguro S, et al. Expression of S100A6 and S100A4 in matched samples of human colorectal mucosa, primary colorectal adenocarcinomas and liver metastases. Oncology. 2002;63:192-200.
[306] Kim JW, Kim JH, Yoon SY, Joo JH, Lee Y, Lee KS, et al. S100A6 protein as a marker for differential diagnosis of cholangiocarcinoma from hepatocellular carcinoma. Hepatology research. 2002;23:274-86.
[307] Ribé A, McNutt NS. S100A6 protein expression is different in Spitz nevi and melanomas. Modern Pathology. 2003;16:505-11.
[308] De Petris L, Orre LM, Kanter L, Pernemalm M, Koyi H, Lewensohn R, et al. Tumor expression of S100A6 correlates with survival of patients with stage I non-small-cell lung cancer. Lung Cancer. 2009;63:410-7.
[309] Yang YQ, Zhang LJ, Dong H, Jiang CL, Zhu ZG, Wu JX, et al. Upregulated expression of S100A6 in human gastric cancer. Journal of digestive diseases. 2007;8:186-93.
[310] Nedjadi T, Kitteringham N, Campbell F, Jenkins R, Park B, Navarro P, et al. S100A6 binds to annexin 2 in pancreatic cancer cells and promotes pancreatic cancer cell motility. British journal of cancer. 2009;101:1145-54.
[311] Donato R. S100: a multigenic family of calcium-modulated proteins of the EF-hand type with intracellular and extracellular functional roles. The international journal of biochemistry & cell biology. 2001;33:637-68.
[312] Madureira PA, O'Connell PA, Surette AP, Miller VA, Waisman DM. The biochemistry and regulation of S100A10: a multifunctional plasminogen receptor involved in oncogenesis. BioMed Research International. 2012.
[313] Lindsey J, Lusher M, Anderton J, Gilbertson R, Ellison D, Clifford S. Epigenetic deregulation of multiple S100 gene family members by differential hypomethylation and hypermethylation events in medulloblastoma. British journal of cancer. 2007;97:267-74.
[314] Kwon M, MacLeod TJ, Zhang Y, Waisman DM. S100A10, annexin A2, and annexin a2 heterotetramer as candidate plasminogen receptors. Front Biosci. 2005;10:300-25.
[315] He K-L, Deora AB, Xiong H, Ling Q, Weksler BB, Niesvizky R, et al. Endothelial cell annexin A2 regulates polyubiquitination and degradation of its binding partner S100A10/p11. Journal of Biological Chemistry. 2008;283:19192-200.
[316] Hou Y, Yang L, Mou M, Hou Y, Zhang A, Pan N, et al. Annexin A2 regulates the levels of plasmin, S100A10 and fascin in L5178Y cells. Cancer investigation. 2008;26:809-15.
[317] Bharadwaj A, Bydoun M, Holloway R, Waisman D. Annexin A2 heterotetramer: structure and function. International journal of molecular sciences. 2013;14:6259-305.
[318] MacLeod TJ, Kwon M, Filipenko NR, Waisman DM. Phospholipid-associated Annexin A2-S100A10 Heterotetramer and Its Subunits characterization of the interaction with tissue plasminogen activator, plasminogen, and plasmin. Journal of Biological Chemistry. 2003;278:25577-84.
[319] Zhang L, Fogg DK, Waisman DM. RNA interference-mediated silencing of the S100A10 gene attenuates plasmin generation and invasiveness of Colo 222 colorectal cancer cells. Journal of Biological Chemistry. 2004;279:2053-62.

[320] Surette AP, Madureira PA, Phipps KD, Miller VA, Svenningsson P, Waisman DM. Regulation of fibrinolysis by S100A10 in vivo. Blood. 2011;118:3172-81.
[321] Phipps KD, Surette AP, O'Connell PA, Waisman DM. Plasminogen receptor S100A10 is essential for the migration of tumor-promoting macrophages into tumor sites. Cancer research. 2011;71:6676-83.
[322] Dalgleish AG, O'Byrne K. Inflammation and Cancer. The Link Between Inflammation and Cancer: Springer; 2006. p. 1-38.
[323] O'Connell PA, Madureira PA, Berman JN, Liwski RS, Waisman DM. Regulation of S100A10 by the PML-RAR-α oncoprotein. Blood. 2011;117:4095-105.
[324] Howell MD, Fairchild HR, Kim BE, Bin L, Boguniewicz M, Redzic JS, et al. Th2 cytokines act on S100/A11 to downregulate keratinocyte differentiation. Journal of Investigative Dermatology. 2008;128:2248-58.
[325] Rehman I, Azzouzi A-R, Cross SS, Deloulme JC, Catto JW, Wylde N, et al. Dysregulated expression of S100A11 (calgizzarin) in prostate cancer and precursor lesions. Human pathology. 2004;35:1385-91.
[326] Hao J, Wang K, Yue Y, Tian T, Xu A, Hao J, et al. Selective expression of S100A11 in lung cancer and its role in regulating proliferation of adenocarcinomas cells. Molecular and cellular biochemistry. 2012;359:323-32.
[327] Sakaguchi M, Huh N-h. S100A11, a dual growth regulator of epidermal keratinocytes. Amino Acids. 2011;41:797-807.
[328] Gerke V, Creutz CE, Moss SE. Annexins: linking Ca2+ signalling to membrane dynamics. Nature reviews Molecular cell biology. 2005;6:449-61.
[329] Gorsler T, Murzik U, Ulbricht T, Hentschel J, Hemmerich P, Melle C. DNA damage-induced translocation of S100A11 into the nucleus regulates cell proliferation. BMC cell biology. 2010;11:100-10.
[330] Van Ginkel PR, Gee RL, Walker TM, Hu D-N, Heizmann CW, Polans AS. The identification and differential expression of calcium-binding proteins associated with ocular melanoma. Biochimica et Biophysica Acta (BBA)-Molecular Cell Research. 1998;1448:290-8.
[331] Hsieh H-L, Schäfer BW, Sasaki N, Heizmann CW. Expression analysis of S100 proteins and RAGE in human tumors using tissue microarrays. Biochemical and biophysical research communications. 2003;307:375-81.
[332] Iwatsuki M, Mimori K, Yokobori T, Ishi H, Beppu T, Nakamori S, et al. Epithelial–mesenchymal transition in cancer development and its clinical significance. Cancer science. 2010;101:293-9.
[333] Kalluri R, Weinberg RA. The basics of epithelial-mesenchymal transition. The Journal of clinical investigation. 2009;119:1420.
[334] Schmittgen TD, Livak KJ. Analyzing real-time PCR data by the comparative CT method. Nature protocols. 2008;3:1101-8.
[335] Guo Y, Ma J, Wang J, Che X, Narula J, Bigby M, et al. Inhibition of human melanoma growth and metastasis in vivo by anti-CD44 monoclonal antibody. Cancer research. 1994;54:1561-5.
[336] Sbai O, Devi TS, Melone MA, Feron F, Khrestchatisky M, Singh LP, et al. RAGE–TXNIP axis is required for S100B-promoted Schwann cell migration, fibronectin expression and cytokine secretion. Journal of cell science. 2010;123:4332-9.

[337] Geroldi D, Falcone C, Emanuele E. Soluble receptor for advanced glycation end products: from disease marker to potential therapeutic target. Current medicinal chemistry. 2006;13:1971-8.
[338] Heldin P, Karousou E, Bernert B, Porsch H, Nishitsuka K, Skandalis SS. Importance of hyaluronan-CD44 interactions in inflammation and tumorigenesis. Connective tissue research. 2008;49:215-8.
[339] Ahrens T, Assmann V, Fieber C, Termeer CC, Herrlich P, Hofmann M, et al. CD44 is the principal mediator of hyaluronic-acid-induced melanoma cell proliferation. Journal of Investigative Dermatology. 2001;116:93-101.
[340] Goodison S, Urquidi V, Tarin D. CD44 cell adhesion molecules. Molecular Pathology. 1999;52:189-96.
[341] Kajita M, Itoh Y, Chiba T, Mori H, Okada A, Kinoh H, et al. Membrane-type 1 matrix metalloproteinase cleaves CD44 and promotes cell migration. The Journal of cell biology. 2001;153:893-904.
[342] Yamazaki D, Kurisu S, Takenawa T. Involvement of Rac and Rho signaling in cancer cell motility in 3D substrates. Oncogene. 2009;28:1570-83.
[343] Zink D, Fischer AH, Nickerson JA. Nuclear structure in cancer cells. Nature Reviews Cancer. 2004;4:677-87.
[344] Gardel ML, Schneider IC, Aratyn-Schaus Y, Waterman CM. Mechanical integration of actin and adhesion dynamics in cell migration. Annual review of cell and developmental biology. 2010;26:315-33.
[345] Yamazaki D, Kurisu S, Takenawa T. Regulation of cancer cell motility through actin reorganization. Cancer science. 2005;96:379-86.
[346] Xiong F, Leonov S, Howard AC, Xiong S, Zhang B, Mei L, et al. Receptor for advanced glycation end products (RAGE) prevents endothelial cell membrane resealing and regulates F-actin remodeling in a beta-catenin-dependent manner. J Biol Chem. 2011;286:35061-70.
[347] Geller AC, Annas GD. Epidemiology of melanoma and nonmelanoma skin cancer. Seminars in oncology nursing: Elsevier; 2003. p. 2-11.
[348] Quintana E, Shackleton M, Foster HR, Fullen DR, Sabel MS, Johnson TM, et al. Phenotypic heterogeneity among tumorigenic melanoma cells from patients that is reversible and not hierarchically organized. Cancer cell. 2010;18:510-23.
[349] Albino AP, Le Strange R, Oliff AI, Furth ME, Old LJ. Transforming ras genes from human melanoma: a manifestation of tumour heterogeneity? 1984:69-72.
[350] Cree IA, Neale MH, Myatt NE, de Takats PG, Hall P, Grant J, et al. Heterogeneity of chemosensitivity of metastatic cutaneous melanoma. Anti-cancer drugs. 1999;10:437-44.
[351] Facchetti F, Previdi S, Ballarini M, Minucci S, Perego P, La Porta CA. Modulation of pro- and anti-apoptotic factors in human melanoma cells exposed to histone deacetylase inhibitors. Apoptosis. 2004;9:573-82.
[352] Truzzi F, Marconi A, Lotti R, Dallaglio K, French LE, Hempstead BL, et al. Neurotrophins and their receptors stimulate melanoma cell proliferation and migration. Journal of Investigative Dermatology. 2008;128:2031-40.
[353] Mårtenson ED, Hansson L, Nilsson B, Von Schoultz E, Brahme EM, Ringborg U, et al. Serum S-100b protein as a prognostic marker in malignant cutaneous melanoma. Journal of Clinical Oncology. 2001;19:824-31.

[354] Indurthi VS, Leclerc E, Vetter SW. Interaction between glycated serum albumin and AGE-receptors depends on structural changes and the glycation reagent. Archives of biochemistry and biophysics. 2012;528:185-96.
[355] Ke X-S, Qu Y, Goldfinger N, Rostad K, Hovland R, Akslen LA, et al. Epithelial to mesenchymal transition of a primary prostate cell line with switches of cell adhesion modules but without malignant transformation. PloS one. 2008;3:e3368.
[356] Lei Q-Y, Zhang H, Zhao B, Zha Z-Y, Bai F, Pei X-H, et al. TAZ promotes cell proliferation and epithelial-mesenchymal transition and is inhibited by the hippo pathway. Molecular and cellular biology. 2008;28:2426-36.
[357] Moutasim KA, Nystrom ML, Thomas GJ. Cell migration and invasion assays. Cancer Cell Culture: Springer; 2011. p. 333-43.
[358] Friedl P, Gilmour D. Collective cell migration in morphogenesis, regeneration and cancer. Nature reviews Molecular cell biology. 2009;10:445-57.
[359] Wang L-H. Molecular signaling regulating anchorage-independent growth of cancer cells. The Mount Sinai journal of medicine, New York. 2004;71:361-7.
[360] Guadamillas MC, Cerezo A, del Pozo MA. Overcoming anoikis–pathways to anchorage-independent growth in cancer. Journal of cell science. 2011;124:3189-97.
[361] Kim Y-N, Koo KH, Sung JY, Yun U-J, Kim H. Anoikis resistance: an essential prerequisite for tumor metastasis. International journal of cell biology. 2012;2012.
[362] Savagner P. The epithelial–mesenchymal transition (EMT) phenomenon. Annals of oncology. 2010;21:89-92.
[363] Kloster MM, Naderi EH, Carlsen H, Blomhoff HK, Naderi S. Hyperactivation of NF-kappaB via the MEK signaling is indispensable for the inhibitory effect of cAMP on DNA damage-induced cell death. Mol Cancer. 2011;10:45-58.
[364] Joerger A, Fersht A. Structure–function–rescue: the diverse nature of common p53 cancer mutants. Oncogene. 2007;26:2226-42.
[365] Hollstein M, Sidransky D, Vogelstein B, Harris CC. p53 mutations in human cancers. Science. 1991;253:49-53.
[366] Gadea G, de Toledo M, Anguille C, Roux P. Loss of p53 promotes RhoA–ROCK-dependent cell migration and invasion in 3D matrices. The Journal of cell biology. 2007;178:23-30.
[367] Muller PA, Vousden KH, Norman JC. p53 and its mutants in tumor cell migration and invasion. The Journal of cell biology. 2011;192:209-18.
[368] Guo F, Zheng Y. Rho family GTPases cooperate with p53 deletion to promote primary mouse embryonic fibroblast cell invasion. Oncogene. 2004;23:5577-85.
[369] Resnitzky D, Gossen M, Bujard H, Reed S. Acceleration of the G1/S phase transition by expression of cyclins D1 and E with an inducible system. Molecular and cellular biology. 1994;14:1669-79.
[370] Sherr CJ, Roberts JM. Living with or without cyclins and cyclin-dependent kinases. Genes & development. 2004;18:2699-711.
[371] Bales ES, Dietrich C, Bandyopadhyay D, Schwahn DJ, Xu W, Didenko V, et al. High levels of expression of p27KIP1 and cyclin E in invasive primary malignant melanomas. Journal of Investigative Dermatology. 1999;113:1039-46.
[372] Cao R, Björndahl MA, Religa P, Clasper S, Garvin S, Galter D, et al. PDGF-BB induces intratumoral lymphangiogenesis and promotes lymphatic metastasis. Cancer cell. 2004;6:333-45.

[373] Xue Y, Lim S, Yang Y, Wang Z, Jensen LDE, Hedlund E-M, et al. PDGF-BB modulates hematopoiesis and tumor angiogenesis by inducing erythropoietin production in stromal cells. Nature medicine. 2012;18:100-10.
[374] Alexiou P, Chatzopoulou M, Pegklidou K, Demopoulos V. RAGE: a multi-ligand receptor unveiling novel insights in health and disease. Current medicinal chemistry. 2010;17:2232-52.
[375] De Gruijl F. Skin cancer and solar UV radiation. European Journal of Cancer. 1999;35:2003-9.
[376] Atallah E, Flaherty L. Treatment of metastatic malignant melanoma. Current treatment options in oncology. 2005;6:185-93.
[377] Vechten M, Helfand SC, Jeglum K. Treatment of relapsed canine lymphoma with doxorubicin and dacarbazine. Journal of Veterinary Internal Medicine. 1990;4:187-91.
[378] Bramwell V, Quirt I, Warr D, Verma S, Young V, Knowling M, et al. Combination chemotherapy with doxorubicin, dacarbazine, and ifosfamide in advanced adult soft tissue sarcoma. Journal of the National Cancer Institute. 1989;81:1496-9.
[379] Shiraishi A, Sakumi K, Sekiguchi M. Increased susceptibility to chemotherapeutic alkylating agents of mice deficient in DNA repair methyltransferase. Carcinogenesis. 2000;21:1879-83.
[380] Culver ME, Gatesman ML, Mancl EE, Lowe DK. Ipilimumab: a novel treatment for metastatic melanoma. Annals of Pharmacotherapy. 2011;45:510-9.
[381] Sosman JA, Kim KB, Schuchter L, Gonzalez R, Pavlick AC, Weber JS, et al. Survival in BRAF V600–mutant advanced melanoma treated with vemurafenib. New England Journal of Medicine. 2012;366:707-14.
[382] Chapman PB, Hauschild A, Robert C, Haanen JB, Ascierto P, Larkin J, et al. Improved survival with vemurafenib in melanoma with BRAF V600E mutation. New England Journal of Medicine. 2011;364:2507-16.
[383] Liu F, Cao J, Wu J, Sullivan K, Shen J, Ryu B, et al. Stat3-targeted therapies overcome the acquired resistance to vemurafenib in melanomas. Journal of Investigative Dermatology. 2013;133:2041-9.
[384] Weber J. Ipilimumab: controversies in its development, utility and autoimmune adverse events. Cancer immunology, immunotherapy. 2009;58:823-30.
[385] Hansel TT, Kropshofer H, Singer T, Mitchell JA, George AJ. The safety and side effects of monoclonal antibodies. Nature Reviews Drug Discovery. 2010;9:325-38.
[386] Riehl A, Németh J, Angel P, Hess J. The receptor RAGE: Bridging inflammation and cancer. Cell Commun Signal. 2009;7:7-12.
[387] Shacter E, Weitzman SA. Chronic inflammation and cancer. Oncology. 2002;16:217-30.
[388] Tafani M, Schito L, Pellegrini L, Villanova L, Marfe G, Anwar T, et al. Hypoxia-increased RAGE and P2X7R expression regulates tumor cell invasion through phosphorylation of Erk1/2 and Akt and nuclear translocation of NF-κB. Carcinogenesis. 2011;32:1167-75.
[389] Scott AM, Wolchok JD, Old LJ. Antibody therapy of cancer. Nature Reviews Cancer. 2012;12:278-87.
[390] Li F, Zhao C, Wang L. Molecular-targeted agents combination therapy for cancer: Developments and potentials. International journal of cancer. 2014;134:1257-69.
[391] Shih J-Y, Yuan A, Chen JJ-W, Yang P-C. Tumor-associated macrophage: its role in cancer invasion and metastasis. J Cancer Mol. 2006;2:101-6.

[392] Gupta SC, Kim JH, Prasad S, Aggarwal BB. Regulation of survival, proliferation, invasion, angiogenesis, and metastasis of tumor cells through modulation of inflammatory pathways by nutraceuticals. Cancer and Metastasis Reviews. 2010;29:405-34.
[393] Wetting HL, Hadler-Olsen E, Magnussen S, Rikardsen O, Steigen SE, Sundkvist E, et al. S100A4 expression in xenograft tumors of human carcinoma cell lines is induced by the tumor microenvironment. The American journal of pathology. 2011;178:2389-96.
[394] Li H, Fan X, Houghton J. Tumor microenvironment: the role of the tumor stroma in cancer. Journal of cellular biochemistry. 2007;101:805-15.
[395] Mueller MM, Fusenig NE. Friends or foes—bipolar effects of the tumour stroma in cancer. Nature Reviews Cancer. 2004;4:839-49.
[396] Rojas A, Figueroa H, Morales E. Fueling inflammation at tumor microenvironment: the role of multiligand/RAGE axis. Carcinogenesis. 2010;31:334-41.
[397] Schmidt AM, Yan SD, Yan SF, Stern DM. The biology of the receptor for advanced glycation end products and its ligands. Biochimica et Biophysica Acta (BBA)-Molecular Cell Research. 2000;1498:99-111.
[398] Wicki R, Franz C, Scholl FA, Heizmann CW, Schäfer BW. Repression of the candidate tumor suppressor gene S100A2 in breast cancer is mediated by site-specific hypermethylation. Cell calcium. 1997;22:243-54.
[399] Sherbet G, Lakshmi M. S100A4 (MTS1) calcium binding protein in cancer growth, invasion and metastasis. Anticancer research. 1998;18:2415-21.
[400] Gebhardt C, Riehl A, Durchdewald M, Németh J, Fürstenberger G, Müller-Decker K, et al. RAGE signaling sustains inflammation and promotes tumor development. The Journal of experimental medicine. 2008;205:275-85.
[401] Singh RK, Gutman M, Radinsky R, Bucana CD, Fidler IJ. Expression of interleukin 8 correlates with the metastatic potential of human melanoma cells in nude mice. Cancer research. 1994;54:3242-7.
[402] Norgauer J, Metzner B, Schraufstätter I. Expression and growth-promoting function of the IL-8 receptor beta in human melanoma cells. The Journal of Immunology. 1996;156:1132-7.
[403] Li A, Dubey S, Varney ML, Dave BJ, Singh RK. IL-8 directly enhanced endothelial cell survival, proliferation, and matrix metalloproteinases production and regulated angiogenesis. The Journal of Immunology. 2003;170:3369-76.
[404] Ferrara N. VEGF and the quest for tumour angiogenesis factors. Nature Reviews Cancer. 2002;2:795-803.
[405] Seppä H, Grotendorst G, Seppä S, Schiffmann E, Martin GR. Platelet-derived growth factor in chemotactic for fibroblasts. The Journal of cell biology. 1982;92:584-8.
[406] Nissen LJ, Cao R, Hedlund E-M, Wang Z, Zhao X, Wetterskog D, et al. Angiogenic factors FGF2 and PDGF-BB synergistically promote murine tumor neovascularization and metastasis. Journal of Clinical Investigation. 2007;117:2766-77.
[407] Zatterstrom UK, Felbor U, Fukai N, Olsen BR. Collagen XVIII/endostatin structure and functional role in angiogenesis. Cell structure and function. 2000;25:97.
[408] Halfter W, Dong S, Schurer B, Cole GJ. Collagen XVIII is a basement membrane heparan sulfate proteoglycan. Journal of Biological Chemistry. 1998;273:25404-12.
[409] Lev DC, Onn A, Melinkova VO, Miller C, Stone V, Ruiz M, et al. Exposure of melanoma cells to dacarbazine results in enhanced tumor growth and metastasis in vivo. Journal of Clinical Oncology. 2004;22:2092-100.

[410] Palmieri G, Capone M, Ascierto ML, Gentilcore G, Stroncek DF, Casula M, et al. Main roads to melanoma. J Transl Med. 2009;7:76-86.